Aalto University
School of Chemical
Technology

School of Chemical Technology
Degree Programme of Chemical Technology

Tom Cameron

# PHASE EQUILIBRIUM OF POLYETHYLENE AND *n*-HEXANE SYSTEMS AT DIFFERENT OPERATING CONDITIONS

Master's thesis for the degree of Master of Science in Technology submitted for inspection, Espoo, 17 May, 2016.

Supervisor Professor Ville Alopaues

Instructors D.Sc. (Tech) Petri Uusi-Kyyny
PhD Mohammad Al-Haj Ali

Aalto University
School of Chemical
Technology

Aalto University, P.O. BOX 11000,
00076 AALTO
www.aalto.fi

**Abstract of master's thesis**

**Author** Tom Cameron

**Title of thesis** Phase equilibrium of polyethylene and *n*-hexane systems at different operating conditions

**Department** Chemical Engineering

**Professorship** Processes and products **Code of professorship** Kem-42

**Thesis supervisor** Prof. Ville Alopaeus

**Thesis advisor(s) / Thesis examiner(s)** D. Sc. (Tech) Petri Uusi-Kyyny and PhD Mohammad Al-Haj Ali

| **Date** | **Number of pages** | **Language** |
|---|---|---|
| 17.05.2016 | 110 + 9 | English |

**Abstract**

Phase equilibria knowledge of polymer – solvent systems is vital for the development of solution polymerization processes. When producing the polymer, the phase state of the reaction mixture can impact reaction rates and product properties. Also, when separating the polymer from the solvent, phase separation can be used.

The goal of this work is to investigate liquid-liquid phase boundaries in systems containing polyethylene and *n*-hexane by measuring points of liquid-liquid separation, also known as *cloud points*. Measurements were conducted for temperatures from 150 °C to 250 °C, for pressures up to 100 bar and for systems with 10-36 mass percentage (m-%) polymer concentration. Six different polymer types were used in the experiments. Cloud point measurements were conducted for binary systems containing polyethylene and *n*-hexane, as well as for multicomponent systems containing polyethylene, ethylene monomer, 1-butene or 1-octene comonomer, butane or iso-octane, and a hexane solvent. A pressure and temperature controlled variable volume cell was used for the measurements.

Lower critical solution temperature (LCST) behavior was observed in the investigated temperature range. Increasing polymer concentration was found to increase the solubility of the polymer, meaning the polymer concentrations investigated were larger than the critical polymer concentrations. Increasing differences between the properties of the polymer and solvent, such as molar mass and density, was found to decrease polymer solubility, meaning the system showed more tendency to separate into two liquid phases.

**Keywords** Cloud point, liquid-liquid separation, polyethylene, hexane

Aalto-yliopisto
Kemian tekniikan
korkeakoulu

Aalto-yliopisto, PL 11000, 00076
AALTO
www.aalto.fi

**Diplomityön tiivistelmä**

**Tekijä** Tom Cameron

**Työn nimi** Polyetyleeniä ja *n*-heksaania sisältävien systeemien faasitasapaino eri olosuhteissa

**Laitos** Kemian tekniikka

**Professuuri** Prosessit ja tuotteet **Professuurikoodi** Kem-42

**Työn valvoja** Prof. Ville Alopaeus

**Työn ohjaaja(t)/Työn tarkastaja(t)** TkT Petri Uusi-Kyyny ja FT Mohammad Al-Haj Ali

**Päivämäärä** 17.05.2016 **Sivumäärä** 110 + 9 **Kieli** Englanti

**Tiivistelmä**

Polymeeri – liuotinsysteemien faasitasapainon tunteminen on välttämätöntä kehitettäessä liuospolymerointiprosesseja. Polymeerejä tuotettaessa reaktioliuoksen faasitila voi vaikuttaa reaktionopeuksiin ja tuotteiden ominaisuuksiin. Myös, kun polymeeriä erotetaan liuottimesta, faasien erottuvuutta voidaan hyödyntää.

Tämän työn tavoite on tutkia polyetyleeniä ja *n*-heksaania sisältävien systeemien neste-neste faasitasapainoa mittaamalla kyseisten systeemien samepisteitä. Mittaukset suoritettiin lämpötilavälillä 150 – 200 °C paineen ollessa alle 100 bar, ja polymeerikonsentraation vaihdellessa välillä 10-36 massaprosenttia (m-%). Mittauksia tehtiin kuudella eri polymeerityypillä. Samepisteitä mitattiin vain polyetyleeniä ja *n*-heksaania sisältävistä binääriseoksista, sekä monikomponenttiseoksista, jotka sisälsivät polyetyleeniä, etyleenimonomeeriä, 1-buteeni- tai 1-okteenikomonomeeriä, butaania tai iso-oktaania, ja heksaaniliuotinta. Mittaukset suoritettiin tilavuussäädettävällä kennolla, jonka lämpötilaa ja painetta voitiin hallita.

Mitatulla lämpötilavälillä systeemeissä havaittiin alemman lämpötilarajan (LCST – lower critical solution temperature) tyyppistä neste-neste faasikäyttäytymistä. Polymeerikonsentraation noustessa polymeerin liukoisuus parani, tarkoittaen sitä, että käytetyt polymeerikonsentraatiot olivat suurempia kuin systeemien kriittiset polymeerikonsentraatiot. Polymeerin ja liuotinseoksen välisten ominaisuuksien, kuten moolimassojen ja tiheyksien erojen kasvaessa polymeerin liukoisuus huononi, ja systeemi erottui helpommin kahdeksi nestefaasiksi.

**Avainsanat** Samepiste, neste-neste faasitasapaino, polyetyleeni, heksaani

# Foreword

First and foremost I wish to thank my advisors D. Sc. (Tech) Petri Uusi-Kyyny and PhD Mohammad Al-Haj Ali for their invaluable help and guidance throughout the experiments and writing work. Their input cannot be overstated, and was greatly appreciated. I also wish to thank my supervisor Prof. Ville Alopaeus for his helpful guidance and comments during the work, and Prof. Dominique Richon for his help and expertise especially with the experimental equipment. In addition to this, I wish to thank Tommi Kivelä for his considerable help in carrying out many of the laboratory experiments, and Heikki Viianranta for his patient and frequent maintenance of the experimental equipment.

I also wish to express my heartfelt gratitude towards my family, girlfriend, and friends for their patient and unwavering support throughout the work.

Finally, I wish to thank Borealis Polymers for the resources and funding, which made this thesis possible.

# Table of Contents

# Abbreviations

EOS Equation of state

HDPE High-density polyethylene

LCSP Lower critical solution pressure

LCST Lower critical solution temperature

LDPE Low-density polyethylene

LLDPE Linear low-density polyethylene

LL Liquid-liquid

LLV Liquid-liquid-vapor

LST Lower solution temperature

MM Molar mass

MMD Molar mass distribution

MW Molecular weight

MWD Molecular weight distribution

PC-SAFT Perturbed chain statistical associating fluid theory

PE Polyethylene

PEP alternating poly(ethylene-propylene) copolymer

SAFT Statistical associating fluid theory

S-L Sanchez-Lacombe equation of state

UCEP Upper critical end point

UCSP Upper critical solution pressure

UCST Upper critical solution temperature

UST Upper solution temperature

# 1. Introduction

The phase equilibria of polymer systems plays a large part in the manufacturing and processing of polymers. Knowledge of the phase behavior of polymer systems is of the utmost importance, when investigating or designing polymer manufacturing and processing applications. The range of polymer systems used in polymer processing is countless from simple binary systems to complex multicomponent systems (Jeremic, 2004). Even polymers themselves are often comprised of different fractions, as commercial polymers tend to have broad molecular weight distributions, and non-uniform or unknown structure distributions (Folie et al., 1995). Some generalizations on the phase behavior of certain systems can be made, but ultimately the exact phase behavior is specific for each unique system.

Phase separation conditions of polymer systems are of special importance in polymer processing. Many polymers are manufactured by solution polymerization in multicomponent polymer – solvent systems. In addition to usual solid – liquid – vapor separations, polymer systems tend to separate into two liquid phases under certain conditions in so called liquid – liquid separation. In polymer manufacturing by solution polymerization, it is often advantageous to have the polymerization reaction carried out in a single phase system. Conversely separation steps in polymer processes may take advantage of phase separation phenomenon. Knowledge about the phase equilibrium of the system is important in both reaction and separation steps of polymer processes. (Jeremic, 2004; Krenz et al., 2005; Trumpi et al., 2003)

Polyethylene is one of the most common polymers in the world. This work focuses on the phase equilibria of linear low-density polyethylene (LLDPE) in different polymer – solvent systems. The goal of this work is to measure liquid – liquid separation temperatures and pressures, also known as *cloud points*, for these LLDPE – solvent systems. General information on polyethylene and its phase equilibrium will be covered, followed by example cases of experimental phase equilibrium measurements for different systems containing polyethylene found in literature. The phase behavior of these systems is often modeled with some type of thermodynamic

model. However, the modeling of phase equilibria in polymer systems is not covered in this work. Thermodynamic models and their names are mentioned in association with the experimental systems only as examples of which models can be used for the description of the phase behavior of these systems. Model accuracy is not discussed either, as it is not in the scope of this work, and often quantitative information on model accuracy is not provided in the literature examples covered in this work. Finally, the experiments conducted with the different LLDPE – solvent systems along with measurement results will be presented.

# 2. Polyethylene

## 2.1. General information

Polyethylene (PE) is one of the most widely used polymers in the world. Its basic structure is relatively simple (Figure 1), yet there are countless varieties of PE due to copolymerization potential, a wide range of possible density and molar mass (MM, also referred to in some literature as molecular weight MW), and the ability to vary molar mass distribution (MMD, also referred to in some literature as molecular weight distribution MWD). These characteristics make PE very versatile as properties can be engineered for a wide range of different application areas. Properties like high toughness, ductility, excellent chemical resistance, low water vapor permeability, and very low water absorption, along with easy processing, make PE an attractive choice for a wide range of applications, varying from medical applications to industrial energy and infrastructure materials, food packaging materials, and countless other consumer plastic products. However, PE does have its limits due to its relatively low yield stress, melting point, and modulus measuring deformation resistance. (Harper, 2000; Jeremic, 2014)

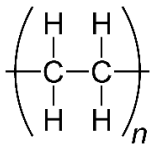

***Figure 1 Basic molecular structure of polyethylene***

PE is comprised of repeating ethylene monomer groups ( $-CH_2CH_2-$ ), and can be categorized into main groups according to the density of the polymer. These main PE groups according to the density and structure of the polymer are very-low-density PE (VLDPE), low-density PE (LDPE), linear low-density PE (LLDPE), medium-density polyethylene (MDPE), high-density PE (HDPE) and ultra-high molecular weight PE (UHMWPE). The density of the polymer is dependent on its molecular morphology, and different grades of PE can have significantly differing thermal and mechanical properties. Long linear polymer chains with few side branches can form a more compact and regular three-dimensional structure, and thus have higher density than polymers with more irregular structures and long side branches. Schematic molecular structures for LDPE, LLDPE and HDPE are presented in Figure 2. HDPE is comprised of linear polymer chains, whereas LDPE and LLDPE polymer chains are branched, which prevents the polymer from achieving a crystalline structure and high densities. LLDPE polymer chains are mainly linear with short-chain side branches, while LDPE is highly branched and partially cross linked. The chain branches and their distribution along the polymer chain influence the specific phase behavior of the polymer. The morphology of the polymer can be affected by processing conditions and co-monomers. (Harper, 2000; Jeremic, 2014)

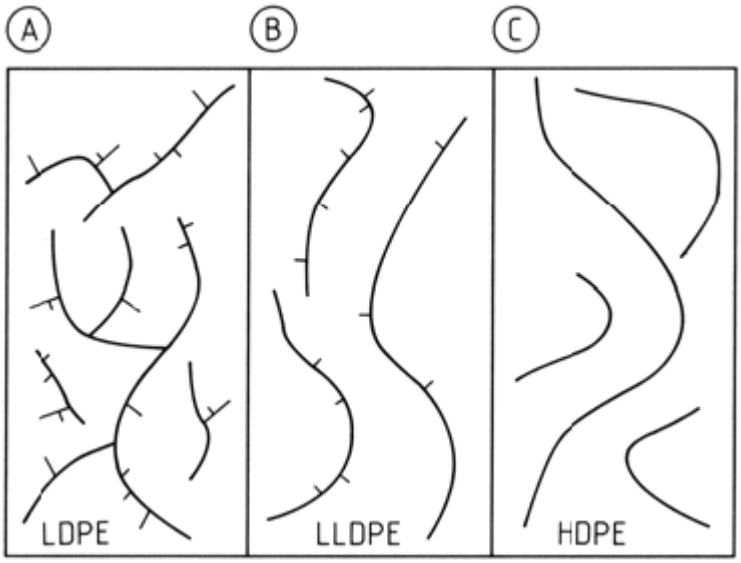


***Figure 2 Schematic molecular structures of LDPE (A), LLDPE (B), and HDPE (C) (Jeremic, 2014)***

## 2.2. Production of polyethylene

LDPE is commonly synthesized by free-radical bulk polymerization at relatively high temperatures (180-300 $^{o}$C) and pressures (1000-3000 bar) in a well-stirred single-stage or multistage autoclave or a tubular reactor; Folie et al. (1995) present an example of a high pressure process capable of producing LDPE and LLDPE. LLDPE is co-polymerized with alpha-olefins (usually 1-hexene or 1-octene), and the length of the branches depends on the co-monomer. The physical properties of the polymer are influenced by the length of the side chains and their distribution along the polymer, which is dependent on the catalyst used in the manufacturing process. Higher quality products tend to exhibit more evenly distributed side branches with equal distance between them. (Jeremic, 2014) LLDPE can be manufactured, for example, using a suitable metallocene catalyst in a high-pressure process (473–573 K, 150– 300MPa), a solution process (433–473 K, up to 30MPa), a slurry process (343–383 K, 4MPa) or a gas phase process (343–388 K, 2–4MPa) (Chen et al., 2004).

Polyethylene production in a gas phase process is relatively simpler than other production methods, as it has no need for solvents, solvent regeneration, and

product drying operations. Gas phase processes can use several different types of catalysts (Ziegler-Natta, chromium and metallocene), and copolymers (e.g. 1-butene, 1-hexene, and 1-octene) for production of polyethylene ranging from low-density polyethylene to high-density polyethylene. However, gas phase polymerization requires long residence times and product transition times. A single-reactor gas phase process for the production of polyethylene was developed by the US company Univation under the name Unipol. This process uses a simple fluidized bed gas phase reactor, which is operated at 11-85 $^{o}$C temperature and 2 MPa pressure. The process was further developed by the British company BP Amoco for gas-phase production of polyethylene with a wide range of possible densities (0.918-0.965 g/cm$^3$). (Bulkatov, 2008; Naidoo, 2013; Jeremic, 2004)

Polyethylene production by solution polymerization requires much shorter reactor residence times, and is thus able to produce polyethylene in a wide range of possible densities in a fairly short production cycle. However, the process requires more severe operating conditions than the gas-phase process, and separation along with possible regeneration and recirculation steps for the solvent. Polymer solution processes can face problems with higher polymer concentrations and molar masses, as the viscosity of the process solution increases with these properties. A single-reactor solution polymerization process for polyethylene production using hexane as a solvent was developed by the Dutch firm DSM. The reactor used in the process is a stirred tank reactor, and the process is operated at 170-200 $^{o}$C temperature and up to 9 MPa pressure. A Ziegler type catalyst is used in the process, and the catalyst contact time is only 10-12 min. (Bulkatov, 2008; Naidoo, 2013; Jeremic, 2004)

Polyethylene production in a slurry or suspension process does not require as harsh conditions as solution polymerization, and can still produce polyethylene with a relatively wide range of possible densities. Japanese company Mitsui Chemicals developed a two-reactor suspension process under the name CX for the production of bimodal medium-density and high density polyethylene, with a density range of 0.935-0.970 g/cm$^3$. The reactors in the process are vapor-phase sealed stirred tank reactors, which are operated at 75-85 $^{o}$C temperatures and 0.3-0.3 MPa pressures.

Titanium based Ziegler-Natta catalysts are used for the polymerization, and catalyst contact time is approximately 1.5-2 h. A similar two reactor slurry process is the Hostalen process developed by LyondellBasell. The reactors in the process are stirred autoclave reactors operated at 78-85 $^{o}$C temperatures and pressures under 1 MPa. Ziegler-Natta catalysts are used in the process, and catalyst contact time is approximately 1-3 h. Hexane is used as the solvent in both of these processes. The density range of polyethylene produced in the Hostalen process is approximately 0.938-0.970 g/cm$^3$. (Bulkatov, 2008; Naidoo, 2013; Jeremic, 2004)

A single reactor suspension process was developed by US firm Chevron Philips, and it uses a tubular loop-type reactor for production of polyethylene, with a density range of 0.915-0.970 g/cm$^3$. The tubular loop reactor provides better heat transfer capabilities, when compared to conventional stirred tank reactors. Isobutane is used as the solvent, and the type and density of the produced polyethylene depends on the catalyst used in the process: chromium oxide can be used for production of medium-density and high-density polyethylene (0.935-0.964 g/cm$^3$), titanium and chromium titanium can be used for producing molding types of polymers, and metallocene catalysts can be used for production of medium-density and low-density polyethylene. (Bulkatov, 2008)

A process combining gas phase and suspension polymerization is the Borstar process developed by the Austrian company Borealis. The process uses a loop reactor followed by a gas phase reactor in series. The loop reactor operates at 85-100 $^{o}$C temperature and 6.0-6.5 MPa pressure with a residence time of 1-2 h. The polymerization is completed in the gas phase reactor in operating conditions around 2.0 MPa pressure and 80-100 $^{o}$C temperature. Supercritical propane is used as the solvent in the loop reactor, and it is separated upon transfer to the gas phase reactor due to the pressure drop. Silica or alumina supported Ziegler catalysts can be used in the process, and comonomers can be fed to the gas phase reactor. The process is capable of producing bimodal polyethylene with a wide range of possible densities and molar masses. (Ahvenainen et al., 1992; Bulkatov, 2008; Naidoo, 2013; Jeremic, 2004)

# 3. Phase equilibrium of polymer-solvent systems

## 3.1. General information on phase equilibrium

The phase behavior knowledge of polymer solutions is of great importance for safe and efficient operation of polymer processes. However, there are several factors that make the prediction of phase boundaries and compositions for polymer-solvent systems difficult. Firstly, such systems are highly nonideal at high pressures, and the polymer and solvent often greatly differ in molecular size and critical conditions. Also commercial polymers are often composed of many molecules of different sizes, molecular masses and chemical compositions. (Folie et al., 1995)

Reaction kinetics in a polymerization reaction are controlled by the phase state of the reaction mixture, which affects the polymer structure and properties. Exothermic polymerization reactions are usually preferably carried out in a single phase to ensure sufficient control over reaction kinetics and temperature, and to avoid the forming of cross-linked materials and equipment fouling. Phase separation during the reaction can have a significant impact on the product properties leading to product quality issues. Forming of a highly viscous polymer-rich phase as a second liquid phase can cause accumulation of these heavier and more viscous components in the process resulting in flow problems and equipment fouling. This type of phase separation could also cause local hotspots in the reactor leading to runaway reactions via autoacceleration, also known as the Trommsdorff effect, in which termination reactions are slowed due to the increased viscosity in the polymer-rich phase. As a result the overall reaction rate, and thus temperature, in these high-viscosity droplets greatly increases resulting in increased polymer MW and highly cross-linked molecules, visible as films and gels. This can ultimately lead to serious reactor fouling, flow problems and in some instances even the decomposition reaction of ethylene. (Folie et al., 1995)

Alternately, in some cases phase separation can be used to achieve desired properties of the product polymer. For example, superior properties of LDPE

produced in a two-phase system due to narrower MMD and less long-chain branches when compared to LDPE similarly produced in a single-phase system have been reported in some instances (Folie et al., 1995). Phase separation can also be utilized in simple separation processes for product purification purposes. Phase separation of polymer mixtures can be brought about by lowering pressures or adding an inert antisolvent (such as $N_2$). However, undesirable phase separation can also occur in the reaction mixture. For example, unwanted cooling of the reaction mixture can lead to polymer precipitation and reactor fouling. These issues, among others, make it crucial to know the temperature and pressure of the demixing point of the reaction mixture at hand. The liquid-liquid demixing point, also known as the cloud point, is the temperature and pressure of a given mixture composition, where a second liquid phase begins to form. In polymer mixtures, cloud points largely depend on the size, structure, and chemical composition of the polymer. (Folie et al., 1995)

Polymer-solvent mixtures can be simplified and related to binary mixtures with two components of differing size, structure and polarity, even though in reality polymer-solvent systems are usually multicomponent systems due to polydispersity of the polymer. Folie et al. (1995) explain the phase behavior characteristics of mixtures with increasing degrees of molecular asymmetry, depicted in Figure 3. The behavior depicted in Figure 3 (a) represents binary components with a low degree of molecular asymmetry. The critical points of the components C1 and C2, at the ends of their respective vapor pressure curves, are joined by a continuous critical locus. A region of liquid-liquid immiscibility exists at lower temperatures, bounded by an upper critical solution temperature (UCST) line and the liquid-liquid-vapor (LLV) line meeting at an upper critical end point (UCEP). The UCST is defined as the temperature above which the components are completely miscible and only a single liquid phase exists for all compositions. In contrast, a lower critical solution temperature (LCST) is defined as the temperature below which the system is completely miscible for all compositions The liquid-liquid immiscibility region exists above the LCST, and temperature increase above the LCST induces a split into two liquid phases. For a given composition, these upper (UCST) and lower (LCST) boundaries for liquid-liquid

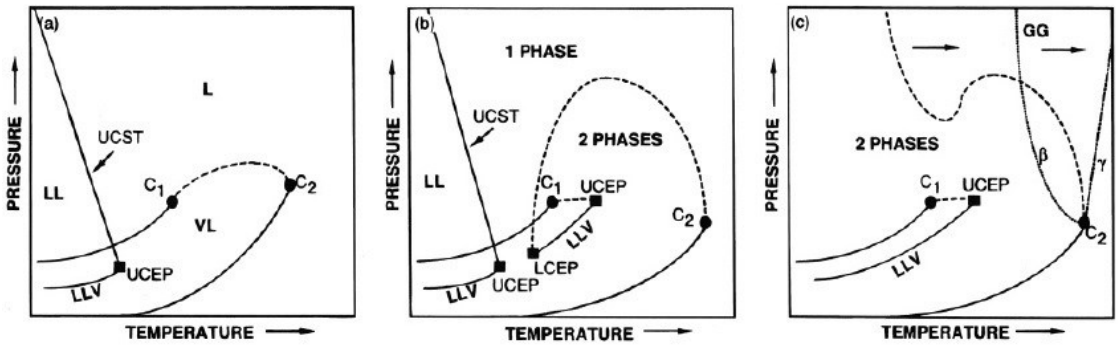


***Figure 3 P-T phase diagrams for binary mixtures of increasing degree of molecular asymmetry from (a) to (c). Dashed lines represent the critical loci of the mixtures. (Folie et al., 1995)***

immiscibility can be referred to as upper solution temperature (UST) and lower solution temperature (LST) respectively. (Folie et al., 1995)

The behavior depicted in Figure 3 (b) indicates a higher degree of molecular size asymmetry, for example between hydrocarbons. Here the critical locus is discontinuous, represented by dashed lines connecting the lower critical end point (LCEP) to the heavy component critical point C2, and the UCEP to the lighter component critical point C1. The behavior depicted in Figure 3 (c) indicates a very high degree of molecular asymmetry; the critical locus meets the LLV line only once, at the UCEP. The second part of the critical locus starting from the heavy component critical point C2 rises without meeting the LLV line or the light component critical point C1, and upon shift to higher temperatures gradually becomes smoother until it loses its pressure minimum and maximum. This type of critical loci are typically exhibited for example in gas-gas equilibria. (Folie et al., 1995)

Polymer-solvent systems generally tend to exhibit the types of phase behavior depicted in Figure 3. In P-T diagrams for polymer – solvent systems the vapor pressure curve for the polymer is usually not shown, because polymer vapor pressures are very low and polymers typically decompose before reaching their critical temperature. Figure 4 shows an example P-T phase diagram for a polymer-solvent mixture of an amorphous and monodisperse polymer. The mixture has high molecular asymmetry, and exhibits the type of behavior depicted in Figure 3 (b). Figure 4 shows the vapor pressure curve of the mixture along with liquid-liquid

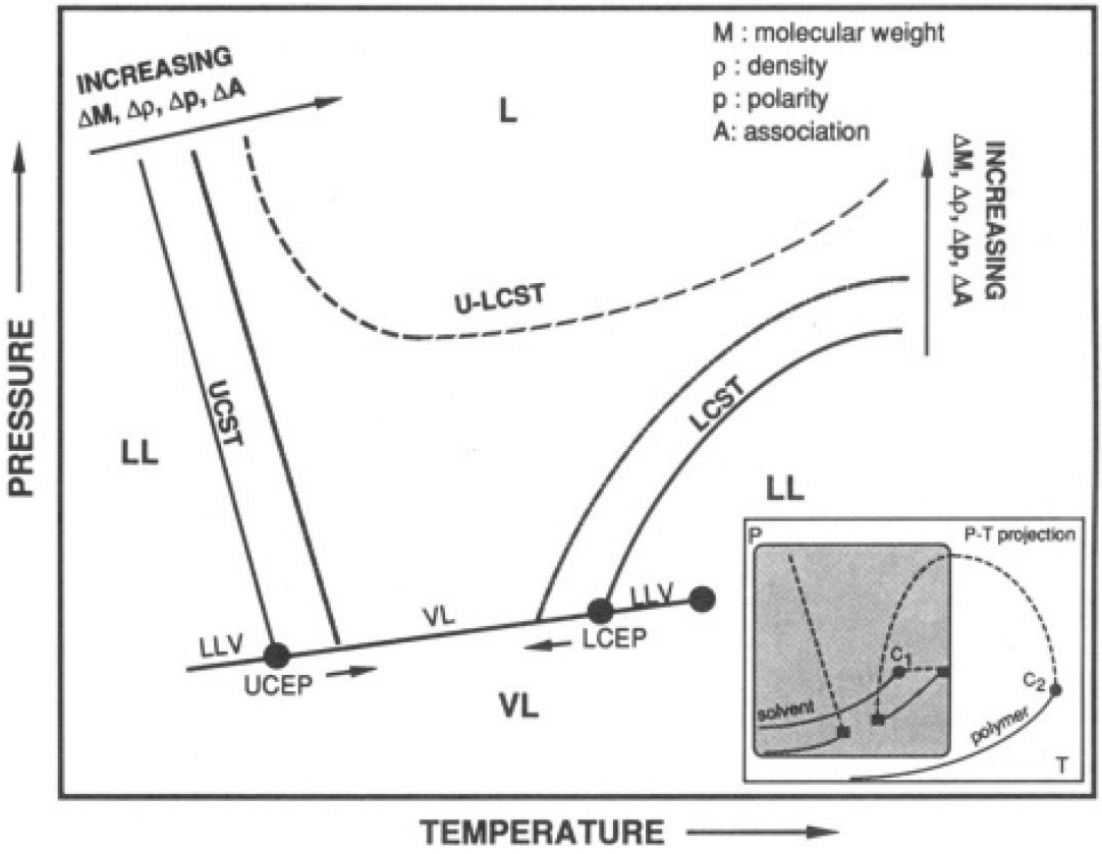


***Figure 4 P-T diagram of an amorphous and monodisperse polymer-solvent mixture showing the effect of increasing molecular asymmetry between the polymer and solvent. (Chen et al., 1992; Folie et al., 1995)***

boundary UCST and LCST curves intersecting the vapor pressure curve near the UCEP and LCEP respectively. However, these curves are not the critical loci. Two three – phase liquid-liquid-vapor (LLV) regions exist in temperatures above the LCEP and below the UCEP. Typically, the mixture vapor pressure curve is quite similar, but not identical, to the pure solvent vapor pressure curve extending some (3-5 K) above the solvent critical point. The LLV curve consequently extends toward higher temperatures with increasing solvent critical temperature. For polydisperse polymers, the LLV curve is not a single line but rather a LLV band (Radosz, 1987). Also depicted in Figure 4 is the effect of increasing molecular asymmetry between the polymer and solvent, which can be quantified by differences in molar mass ($\Delta M$) and density ($\Delta\rho$) for nonpolar systems, by a difference in polarity ($\Delta p$) for polar nonassociating systems, and by differences between self-association and cross-association ($\Delta A$) from specific chemical forces, such as hydrogen bonding, for polar

associating systems. Cloud point pressures increase with increasing molecular asymmetry, and UCST and LCST curves eventually merge into a single U-LCST curve (Chen et al., 1992). Only a single LLV curve exists in this case, extending to near the solvent critical point, similar to that depicted in Figure 3 (c). (Folie et al., 1995)

In reality, the number of phases in a binary or multicomponent system depends on three factors: the temperature, the pressure and the composition of the system. For all P-T diagrams, the composition of the system is constant. P-T diagrams are actually projections of a three dimensional P-T-X phase diagram, where two dimensional projections could alternately be made with respect to temperature and composition (T-X) in a fixed pressure, or pressure and composition (P-X) in a fixed temperature. Figure 5 depicts an example of a three dimensional P-T-X diagram for a polymer-solvent mixture exhibiting a U-LCST critical locus. In the case of polyethylene-solvent systems in this work, increasing pressure always induces mixing, due to negative excess volume of mixing ($\Delta V_m < 0$) (Folie et al., 1995). This effect can be illustrated with T-X projections from the P-T-X diagram in Figure 5. While P-X isotherms all have similar shapes and reach a maximum at the upper critical solution pressure (UCSP), T-X isobars change their shape with changing pressure, as depicted on the right hand side of Figure 5 by three T-X isobars with decreasing pressures from top to bottom. In high enough pressures (P1) the miscibility gap is continuous with a maximum at the UCST. Upon decreasing pressure (P2) the miscibility gap becomes discontinuous with a maximum at the UCST and minimum at the LCST, and eventually at pressures lower than the minimum critical pressure (P3) becomes an hourglass shape, in which case the system is immiscible in all temperatures for a certain concentration range. (Folie et al., 1995)

Phase diagrams of polymer-solvent systems can be distinguished from those of binary pairs with small similar sized molecules by a few characteristics. Cloud point curves for polymer-solvent mixtures are highly asymmetric and the maximum is shifted to the solvent rich side of P-X diagrams. The maximum moves towards higher polymer concentrations as size difference between the polymer and solvent decreases (Chen

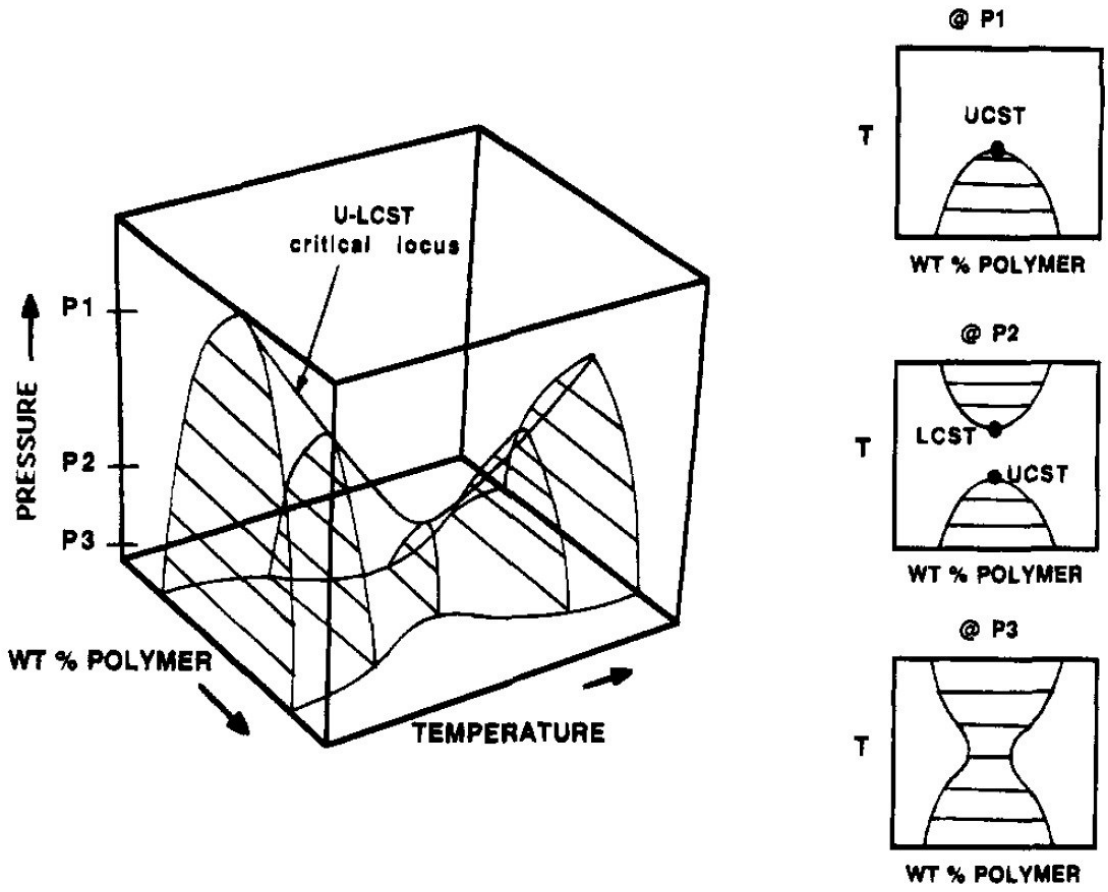


***Figure 5 P-T-X diagram for a monodisperse and amorphous polymer-solvent mixture exhibiting a U-LCST critical locus. T-X isobars at high pressure (P1), intermediate pressure (P2), and pressure lower than minimum critical pressure (P3). (Folie et al., 1995)***

et al., 1992). The critical point (UCSP) for polydisperse polymers does not coincide with the maximum of the phase boundary (also called the precipitation threshold), but is shifted towards higher polymer concentrations. The type of phase transition at the cloud point depends on the polymer concentration with respect to the polymer critical concentration. At polymer concentrations $X_i$ above the polymer critical concentration $X_{crt}$, a bubble point-type transition occurs (Figure 6 (a)), where a lower density (polymer lean) phase begins to form. Conversely, at polymer concentrations below the polymer critical concentration, a dew point-type transition occurs (Figure 6 (b)), where a higher density (polymer rich) phase starts to form. (Folie et al., 1995)

For small molecule binary pairs, the compositions of liquid phases in equilibrium at constant temperature, pressure and overall system composition coincide with the binodal compositions, and are given on the so-called coexistence curve by tie lines.

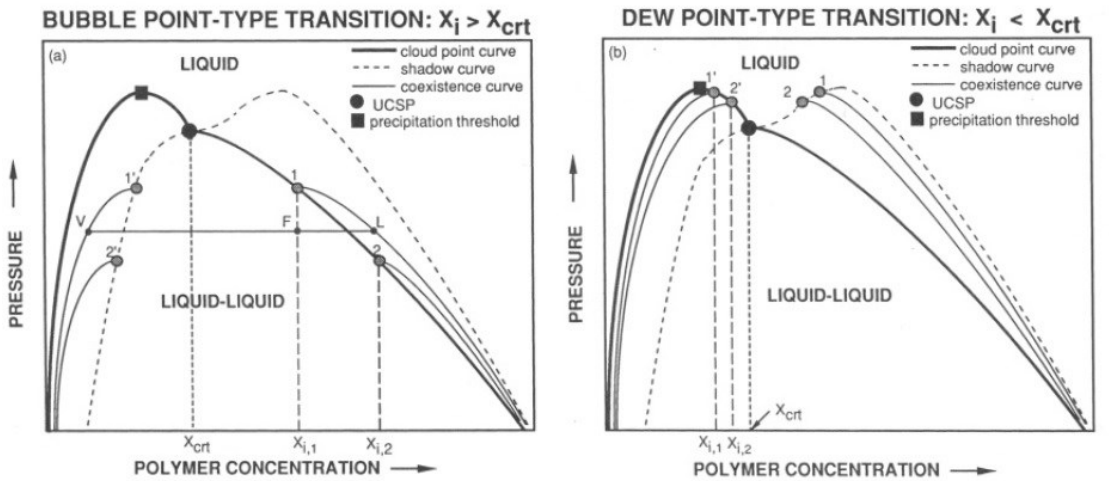


***Figure 6 P-X diagrams for polydisperse polymer-solvent systems exhibiting UCSP behavior. Bubble and dew point-type transitions occur at the cloud point depending on the critical polymer concentration of the system and the initial concentration of the polymer. (Folie et al., 1995)***

In comparison, cloud point (binodal) compositions of polydisperse polymer-solvent systems usually do not coincide with the phase compositions on the coexistence curves, which must be measured independently. The P-X dependence of the minor phase forming at the cloud point is represented by a so-called shadow curve, which differs from both the coexistence curve and the cloud point curve. The MMD of a polydisperse polymer is constant at the cloud point, while the MMD in the incipient phase can vary. The polymer concentration in this incipient phase can be quantified by neglecting MMD difference between the cloud point and incipient phase. These points projected onto the P-X (or T-X) diagram form the shadow curve. In a brief example, when a cloud point of a mixture is reached, the composition of the major phase exists on the cloud point curve, while the composition of the minor phase is formed on the shadow curve. After forming on these curves, compositions of both phases exist on their respective coexistence curves. These curves are qualitatively illustrated in Figure 6. For an initial polymer concentration of $X_{i,1}$ in Figure 6 (a), lowering pressure from a homogeneous state, the cloud point is reached at point 1 on the cloud point curve. At this pressure the major phase (the polymer rich phase in this case of bubble point-type phase transition) forms on the cloud point curve, while the minor phase forms on the shadow point curve at point 1'. Lowering the pressure

from this point, both phases exist on their respective coexistence curves. (Chen et al., 2004; Folie et al., 1995)

The weight fraction ratio of the two phases in equilibrium at a given pressure can be calculated using the lever rule, as illustrated in Figure 6 (a) for polymer concentration $X_{i,1}$. Points V and L represent the polymer rich phase (L) and polymer lean phase (V), and are located on the coexistence curves. Point F corresponds to the initial polymer concentration. The weight ratio of the polymer rich phase (L) to the polymer lean phase (V) in a given pressure is equal to the ratio of the distance between points F and V, and the distance between points F and L. (Folie et al., 1995)

## 3.2. Thermodynamics of UCST and LCST phase behavior

In a polymer – solvent system polymer and solvent molecules can interact amongst themselves and each other. The chemical and physical interactions between molecules along with the difference in free volume govern the phase behavior in the system. Physical forces, such as dispersion forces for nonpolar compounds and dipole moments for polar compounds, and chemical forces, such as hydrogen bonding and charge transfer complexing, can lead to self-association, which favors demixing, or cross association, which favors mixing. (Folie et al., 1995)

For a binary solution to be homogeneous it must meet the following two thermodynamic requirements:

$$\Delta G_m = \Delta H_m - T\Delta S_m < 0 \quad (1)$$

and

$$\left(\frac{\partial^2 \Delta G_m}{\partial X^2}\right)_{T,P} > 0 \quad (2)$$

Here $\Delta G_m$ is the difference in Gibbs free energy between the solution and the pure components, $\Delta H_m$ is the corresponding difference in enthalpy, and $\Delta S_m$ is the

corresponding difference in entropy. The change in entropy $\Delta S_m$ is inherently positive for all solutions, since disorder in a solution is greater than the original pure components. The change in enthalpy $\Delta H_m$ is dependent on the change in intermolecular energy, when a solution is formed. According to the "like-dissolves-like" –principle, $\Delta H_m$ is smaller the more similar the pure components of the mixture are, and the more they differ, the larger the $\Delta H_m$. Thus, for long chains $\Delta H_m$ is usually greater than $\Delta S_m$. UCST systems exhibit endothermic mixing ($\Delta H_m > 0$), so in order to achieve a homogeneous single phase mixture, the temperature has to be raised high enough so that the $-T\Delta S_m$ term compensates for the large positive $\Delta H_m$ term to give the required negative $\Delta G_m$. For a nonpolar polyethylene – *n*-alkane system, increasing the solvent size results in significantly decreased cloud point pressures. Dispersion forces between polymer and solvent molecules increase along with solvent polarizability with increasing solvent size (Hasch et al., 1992). This increases $\Delta H_m$, which would make $\Delta G_m$ more positive, and lead to increased cloud point pressures. However, the decrease in cloud point pressures in this case results from a comparatively larger increase in $\Delta S_m$. (Folie et al., 1995)

Temperature induced phase separation happens in polymer – solvent systems exhibiting LCST behavior when approaching the solvent critical temperature. Contrarily to UCST systems, mixing is exothermic ($\Delta H_m < 0$) in LCST systems favoring the single phase state. This means that in order for phase separation to happen ($\Delta G_m > 0$) with increasing temperature, $\Delta S_m$ must be negative. This is possible due to free-volume (density) dissimilarities between the polymer and solvent. As the system temperature approaches the solvent critical temperature in a constant pressure, the solvent molecules begin to slowly expand towards a more-gas like state decreasing in density. The polymer molecules meanwhile are far from their theoretical critical state, and do not experience such expanding, resulting in an increase in free volume (density) difference between the polymer and solvent. The increasing difference between the polymer density and solvent density is what causes the phase separation with increasing temperature. Thus, in order to stay in a single homogeneous phase, higher pressures are required to compensate for this effect. This can also be seen in Figure 4, where the LCEP temperature decreases with

increasing difference in density ($\Delta\rho$) between the polymer and solvent. In the case depicted in Figure 4, the polymer has a containing effect on the expanding solvent molecules causing a negative change in $\Delta S_m$ as the solvent molecules are confined to a more rigid matrix, and the degree of spatial disorder in this space is less than in a fully expanded state. (Folie et al., 1995)

## 3.3. Phase separation mechanisms

Knowledge of the phase separation mechanism is important in the design of efficient process equipment, especially for continuous separation processes. Liquid-liquid phase separation in polymer-solvent systems takes place by two main mechanisms: dew point-type transition and bubble point-type transition. A dew point type transition is characterized by the formation and growth of a higher density minor phase, while in a bubble point type transition the forming minor phase is of lower density than the original single phase mixture. The naming of these transitions come from comparison to phase transitions in vapor liquid equilibrium (VLE), where a higher density liquid phase starts forming in vapor at the dew point, while a lower density vapor phase starts forming in liquid at the bubble point. These transitions are illustrated schematically in Figure 7. (Chen et al., 1992; Folie et al., 1995)

The type of transition is dependent on the polymer concentration in the system and the critical concentration of polymer, as described before for Figure 6. If the concentration of the polymer in the system is below its critical concentration, the phase separation happens by the dew point type transition, and if the polymer

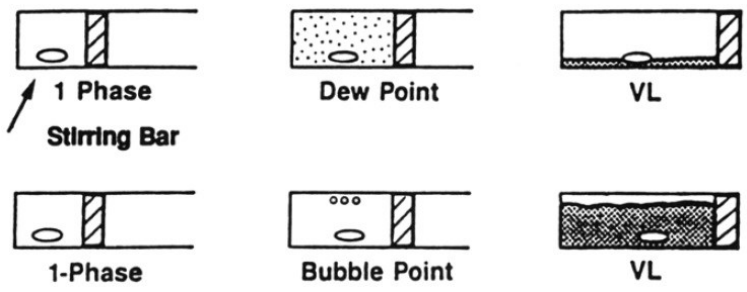


***Figure 7 Dew point and bubble point type transitions. (Chen et al., 1992)***

concentration is above its critical concentration, the phase separation happens by the bubble point type transition. As the critical concentration of the polymer is known to decrease with increasing polymer MW, higher MW polymers and systems with larger polymer concentrations tend to separate by the bubble point type-transitions, while dilute solutions and lower MW polymers tend to separate dew point-type transitions. (Folie et al., 1995)

The phase state and microscopic demixing mechanism of a system can be determined from the shape and curvature of its Gibbs free energy of mixing ($\Delta G_m$) as a function of concentration at a given T and P. As equilibrium systems always minimize their Gibbs free energy, the phase state of the system, whether it's single phase or demixes into two liquid phases, can be seen from the shape of the $\Delta G_m$ curve. An illustrative example of a system exhibiting LCST behavior is given in Figure 8 and Figure 9. At lower temperatures ($T=T_0$, Figure 8) the system is homogeneous, but separates into two liquid phases above the LCST ($T=T_1$, Figure 9). For a completely convex curve (Figure 8) with positive curvature ($d^2G_m/dx^2 > 0$) across the whole concentration range and a single minimum, the Gibbs free energy of mixing for the mixture is always lower than an unmixed state. Thus a completely convex curve of $\Delta G_m$ indicates a single phase system at that T and P, since the system cannot lower its $\Delta G_m$ at any composition by demixing. A $\Delta G_m$ curve with a concave section (i.e. locally negative curvature $d^2G_m/dx^2 < 0$) and two minimums, illustrated in the top part of Figure 9, indicates demixing of the system into two liquid phases, since the $\Delta G_m$ of the system can be lowered by demixing in the concentration range in the concave section between the two minimums. (Folie et al., 1995)

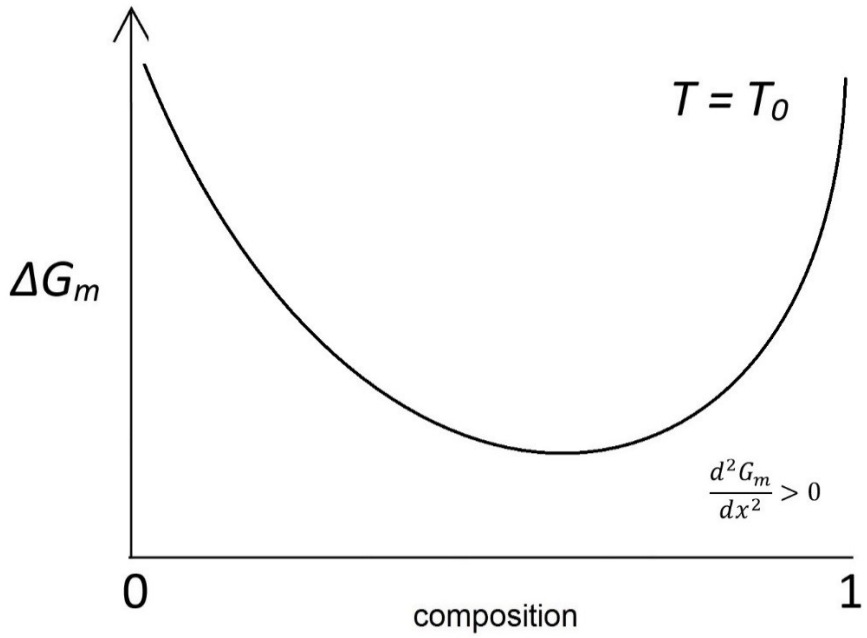


***Figure 8 Gibbs free energy of mixing as a function of composition for a single phase system at constant T and P.***

The phase stability and microscopic phase separation mechanism of demixing systems can be determined from the curvature of the $\Delta G_m$ curve. Constructing a *T-X* phase diagram with binodal and spinodal curves from the shape and curvature of $\Delta G_m$ as a function of composition is illustrated in Figure 9 for a system exhibiting LCST behavior. The compositions of the two phases in equilibrium are given by the double tangent to the minimums (points $B_1$ and $B_2$ in Figure 9) of the $\Delta G_m$ curve, as the chemical potential of each species is the same in both phases. These equilibrium compositions correspond to the binodal compositions at that *T* and *P*, as shown in Figure 9 by points $B_1$' and $B_2$' on the binodal curve. The inflection points where the $\Delta G_m$ curve changes curvature from concave to convex and vice versa ($d^2G_m/dx^2 = 0$, points $S_1$ and $S_2$ in Figure 9) correspond to spinodal compositions at that *T* and *P*, shown in Figure 9 as points $S_1$' and $S_2$' on the spinodal curve. Between the inflection points $S_1$ and $S_2$, the $\Delta G_m$ curve has locally negative curvature ($d^2G_m/dx^2 < 0$). Since the $\Delta G_m$ curve as a function of composition is always at constant *T* and *P*, and changes shape with changing *T* and *P*, the *T* (and *P*) and composition at which the inflection points and equilibrium points (the binodal and spinodal points) merge into a single point, which is the crtitical point of the system. (Folie et al., 1995; Higgins et al., 2010)

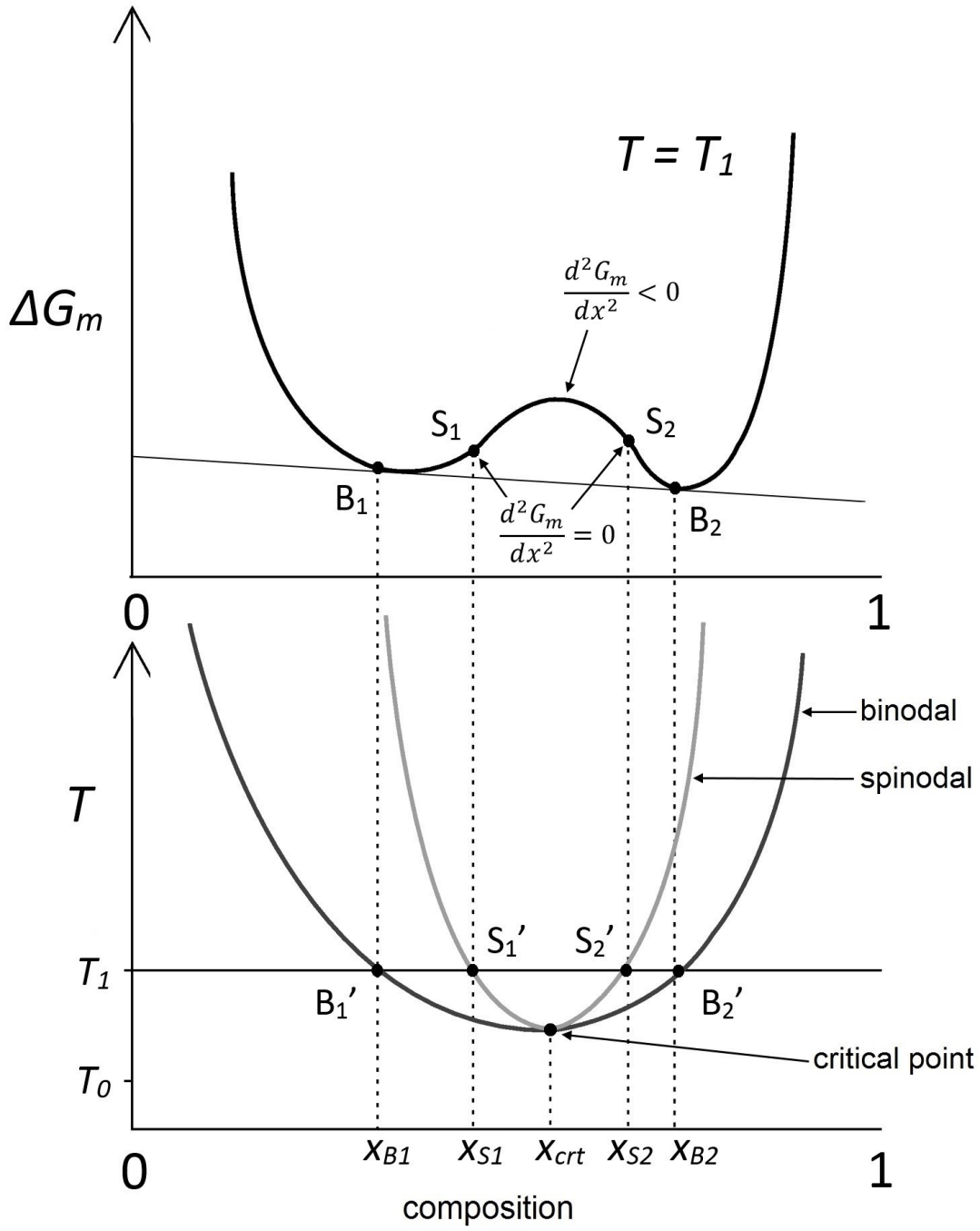


***Figure 9 Constructing a T-X phase diagram from the shape and curvature of Gibbs free energy of mixing as a function of composition for a system exhibiting LCST behavior. (Higgins et al., 2010)***

The *T-X* phase diagram is divided into three distinct regions by the binodal and spinodal curves, as illustrated in Figure 10 for a system exhibiting UCST behavior. Outside the binodal curve is the stable region, where the system is in a single

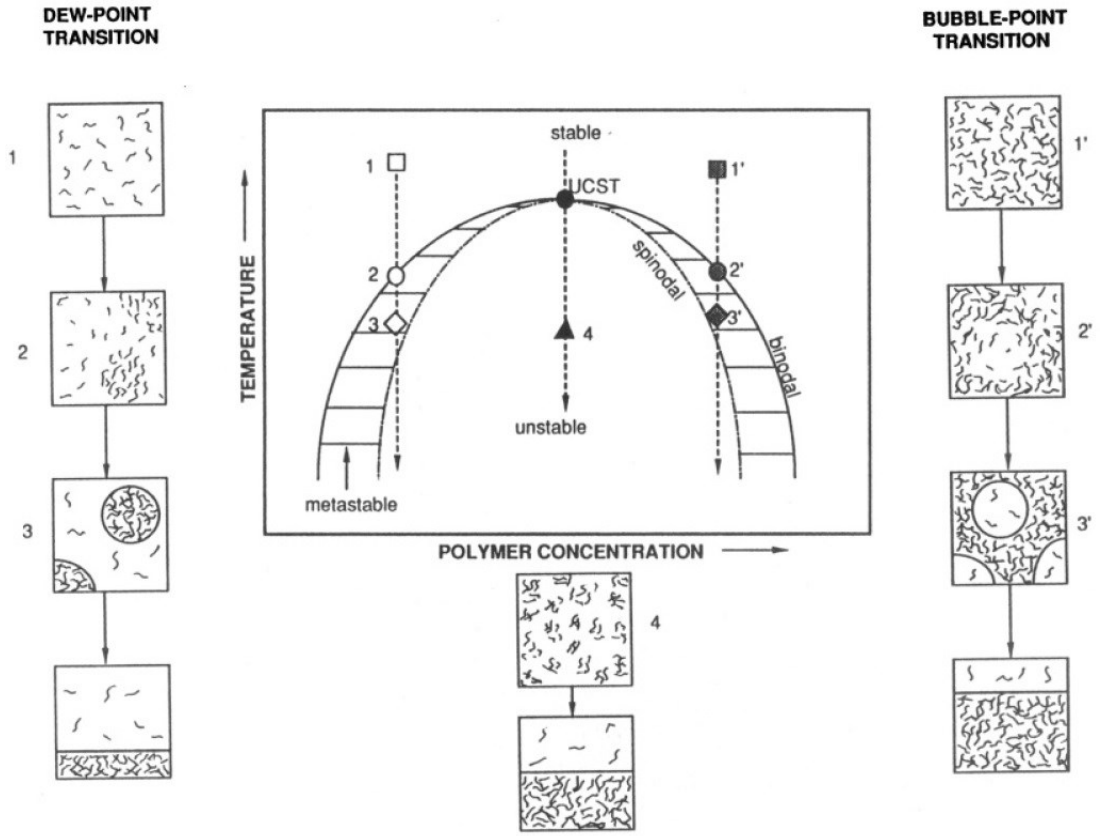


***Figure 10 Regions and phase separation mechanisms in a T-X phase diagram for a system exhibiting UCST behavior. (Folie et al., 1995)***

homogeneous phase. The binodal curve is the boundary inside which two phases can coexist and phase separation can happen, whereas the spinodal curve is the absolute boundary inside which spontaneous phase separation will happen. Between the binodal and spinodal curves is the metastable region, in which nuclei of the new phase can start forming and growing in dispersed droplets inside the continuous phase. This phase separation mechanism is called nucleation and growth. Inside the spinodal curve is the unstable region, where the system separates spontaneously into two distinct continuous phases. This phase separation mechanism is called spinodal decomposition. Pictures 1-3 and 1'-3' in Figure 10 illustrate the nucleation and growth mechanism moving from the stable region to the unstable region for the dew-point and bubble-point type transitions discussed earlier, while picture 4 in Figure 10 shows a depiction of the spinodal decomposition mechanism. Both mechanisms lead to two separate phases with enough settling time at equilibrium, but at differing rates of phase formation. (Folie et al., 1995)

# 4. Experimental polyethylene-solvent systems

Phase equilibrium measurements for polyethylene can be found in literature for a wide range of solutions with different solvents and co-polymers. In this section some examples of experimental polyethylene-solvent systems are presented in order to better understand the theory and real world behavior of such systems. The studies presented as examples here have been selected to share at least some sort of relevant interest with the experiments conducted in this work.

## 4.1. Polyethylene + ethylene mixtures

The phase behavior of polyethylene and ethylene mixtures draws great interest, resulting from the commercial importance of polyethylene, and its production from ethylene in high pressure processes. de Loos et al. (1983) investigated the phase behavior of linear polyethylene and ethylene mixtures with differing weight fractions of polymer. Cloud point pressures were found to increase with decreasing polymer weight fraction (or increasing ethylene weight fraction). Cloud point pressures were also found to increase with increasing polymer molar mass. Critical points and the type of phase transition were determined by the position of the phase boundary. For bubble point-type transitions, where $T < T_c$, lowering pressure at a constant temperature causes the phase boundary to initially form at the top of the vessel and move downward with decreasing pressure. Contrarily, for dew point-type transitions, where $T > T_c$, the phase boundary initially forms at the bottom of the vessel and moves upward with decreasing pressure at a constant temperature. Critical temperatures were determined between two temperature points where the type of phase transition shifts from one type to the other. Critical temperatures were found to slightly increase with increasing polymer weight fraction. However, the change in critical weight fraction was found to be very small in the studied temperature range 403.15 – 443.15 K. Critical points and cloud point curves were also found to be

affected by polydispersity, as already described before for Figure 6. Increasing polydispersity causes the critical point to be shifted to higher polymer concentrations from the maximum of the T-X (or P-X) cloud point curve. Polydispersity also causes a noticeable break point in T-X (and P-X) cloud point curves, which is an equilibrium point for three fluid phases. The acquired measurement results were modeled by de Loos et al. (1983) by fitting the data to the Flory-Huggins theory (Flory, 1941; Huggins, 1941) extended by Koningsveld and Kleintjens (Konigsveld et al., 1971) with parameters for empirical pressure dependence and molar mass distribution.

The polyethylene + ethylene data obtained by de Loos et al. (1983), along with newly acquired experimental data for a polybutene + 1-butene system, were modeled by Koak et al. (1999) using the SAFT and Sanchez-Lacombe models. The effect of polydispersity was investigated by first treating the polymers as monodisperse, and comparing the results to a second case, where the polydispersity of the polymer was taken into account by characterizing the polymer as a number of pseudo-monodisperse polymer fractions (pseudocomponents) based on the MMD. The modeling results for the polyethylene + ethylene system were deemed satisfactory, while estimation of polymer parameters had to be strongly adjusted to get a reasonable fit for the polybutene + 1-butene system. Polydispersity was concluded to have a significant effect on both systems, shifting the maximum of the P-X cloud point curves to lower polymer concentrations and higher pressure. The critical point of the polydisperse cases does not coincide with the maximum of the P-X curve, but is located at slightly higher polymer concentrations.

de Loos et al., (1995) investigated the effect of branching on the phase behavior of polyethylene-ethylene systems in the pressure range 90-200 MPa and temperature range 380-445 K. Samples of branched polyethylene were prepared and investigated, and results were compared to previous measurement results with systems of linear polyethylene and ethylene**.** The degree of branching was described with the number of end groups ($CH_3$-groups) per 100 C-atoms. Measurements were carried out for varying polymer molar mass, weight fractions, and degrees of branching. Exact direct comparison between linear and branched polyethylene samples was deemed

extremely difficult due to the fact that samples of linear and branched polyethylene with exactly the same MM and MMD are virtually impossible to manufacture. However, indirect comparison of such systems could be made on the basis of experimentally determined critical pressures of branched polyethylene + ethylene systems compared with predicted critical pressures of linear polyethylene + ethylene systems. The behavior of the critical point of branched polyethylene systems was found to be similar to earlier measurements with linear polyethylene (de Loos et al., 1983), with the critical points being located at slightly higher polymer concentrations from the maximum of the cloud point curves. Increased degrees of branching were concluded to noticeably decrease cloud point pressures of polyethylene samples with similar MM and MMD for all weight fractions, and thus increase the solubility of polyethylene in ethylene.

Chan et al. (2000) investigated the phase equilibria of systems containing ethylene copolymerized with 1-octene, poly(ethylene-co-octene-1), and ethylene for effects of polymer concentration, polymer MM, and branch density for polymer concentrations up to 15 m-%, and temperatures up to 180 $^{o}$C. Branch density was described as branches per 100 ethyl units in the polymer backbone, which simultaneously describes the measure of copolymer incorporation. The cloud point pressures were found to increase with increasing polymer MM and decreasing branch density, due to increasing free-volume difference between the polymer and solvent. The polymer concentration was found to have little impact on cloud point pressures in the concentration range studied. U-LCST type behavior was observed for all the systems studied, and results were correlated with the SAFT EOS.

Trumpi et al. (2003) measured cloud points for nearly monodisperse LLDPE + ethylene systems in the temperature range 395-440 K and pressures up to 175 MPa. Polymer concentrations from 0.5-18.5 m-% were considered, and critical points were measured similarly as described in the study be de Loos et al. (1983). The observed cloud points were of the UST type, seen in Figure 11, and the critical polymer concentration was nearly constant in the studied temperature and pressure range, as can be observed from Figure 12. The obtained data was modeled with the

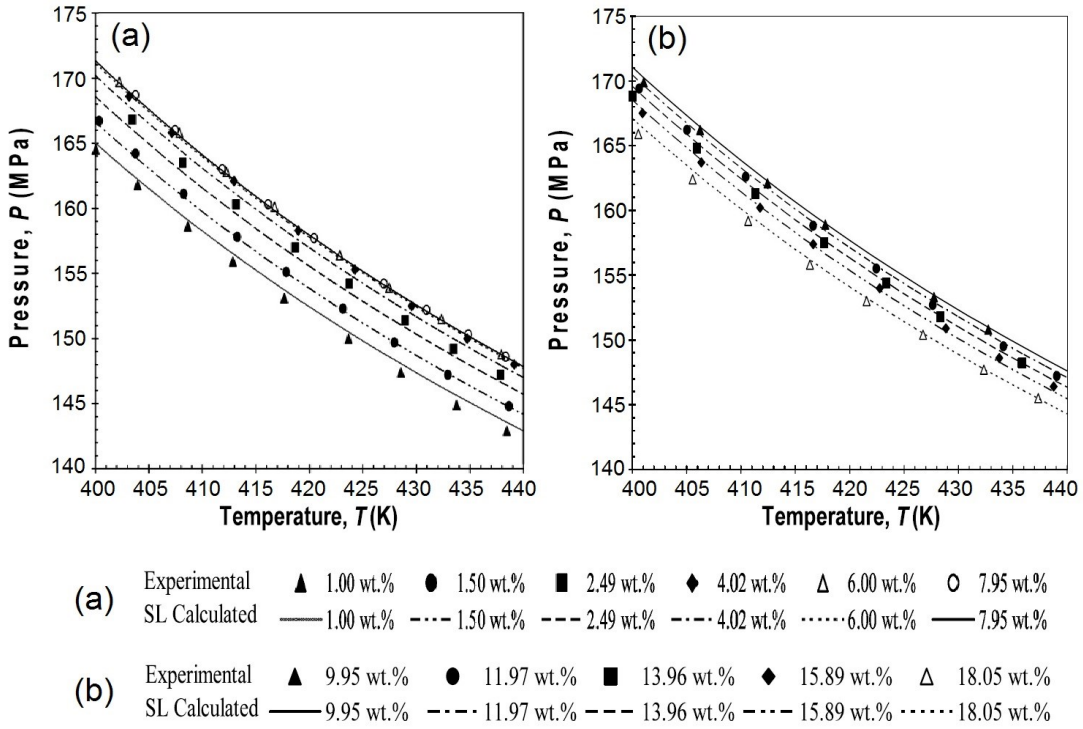


***Figure 11 Cloud point isopleths for LLDPE + ethylene systems, modeled with the Sanchez-Lacombe equation of state. (Trumpi et al., 2003)***

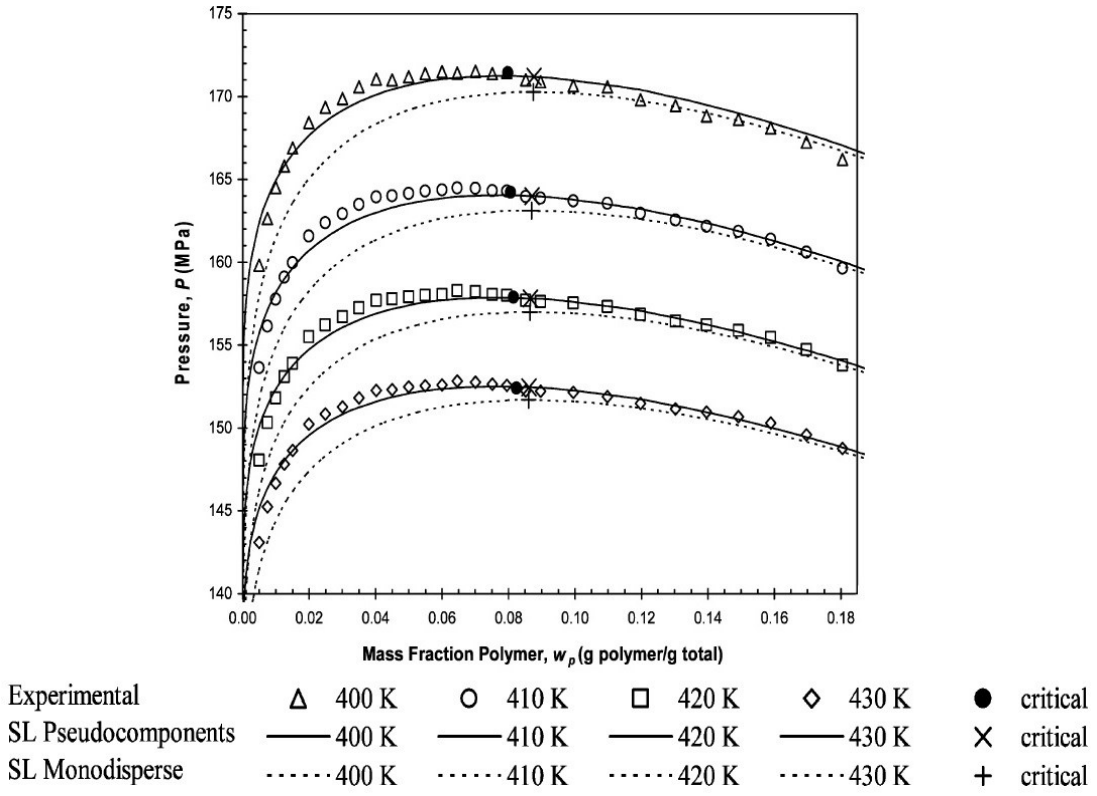


***Figure 12 Isothermal cloud point curves for LLDPE + ethylene systems, modeled with the Sanchez-Lacombe equation of state for a monodisperse polymer and taking polydispersity into consideration. (Trumpi et al., 2003)***

Sanchez-Lacombe equation of state in two ways: (i) assuming the polymer to be monodisperse, and (ii) taking polydispersity into account by characterizing the polymer by a number of pseudocomponents. Taking the polydispersity of the polymer into consideration produced more accurate modeling especially at low polymer concentrations, as can be seen from Figure 12, even though the polymer samples were characterized as nearly monodisperse.

## 4.2. Polyethylene – solvent systems

The manufacturing of ethylene polymers like LLDPE by solution polymerization brings attention to the phase behavior of polyethylene – solvent systems. As LLDPE is a copolymer of ethylene and an alkene comonomer, it is usually produced by solution polymerization of ethylene and an alkene comonomer in a light alkane or mixture of light alkanes with a suitable catalyst. Knowledge of the phase behavior of such systems is of utmost importance when designing manufacturing processes. As described before, it is usually advantageous to carry out the polymerization in a homogeneous solution, while phase separation could be utilized in separating the solvent from the polymer product.

The type of solvent or solvent mixture has great influence on the phase behavior of polyethylene – solvent systems. Studies of polyethylene solutions with varying *n*-alkane solvents show a change from UCST to LCST behavior with increasing *n*-alkane chain length, with UCST behavior being observed for smaller solvents like ethane and pentane, and LCST behavior being observed for butane and larger solvents (pentane, hexane etc.). Additionally, supercritical components (such as supercritical ethylene) in the solvent mixture have been found to act as antisolvents shifting LST behavior of systems to lower temperatures and higher pressures.(de Loos et al., 1996)

de Loos et al. (1996) investigated the influence of pressure, solvent type, and polymer structure on the phase behavior of LLDPE – solvent systems in the temperature range 400-600 K, and pressures up to 13 MPa. The different solvents investigated in the

study were *n*-hexane, *n*-heptane, *n*-octane, isohexane(2-methyl- pentane), and cyclohexane. Observed LST temperatures were found to increase with increasing solvent chain length, as can be seen in Figure 13 (a). This indicates longer chained alkanes are better solvents for LLDPE, which is in agreement with the concept of better polymer solubility with increasing similarity between the polymer and solvent. Similarly isohexane was found dissolve less polymer than *n*-hexane, as isohexane has a shorter chain length due to chain branching when compared to straight chained *n*-hexane. Cyclohexane was found to be a better solvent than *n*-hexane due to higher critical density. Cloud points for LLDPE in these different C6 solvents are presented in Figure 13 (b).

The influence of the molecular structure of LLDPE on the phase behavior of LLDPE + *n*-heptane systems was studied by de Loos et al. (1996) using LLDPE samples with differing molar mass, different comonomers, and differing degrees of chain branching. Density was used as a measure for the degree of chain branching, where increasing density corresponds to decreasing chain branching, meaning decreasing comonomer content. LST cloud point temperatures were found to decrease slightly with both increasing MM and density, as can be seen in Figure 14. However, the influence of the structure of the polymer on the phase behavior of the studied LLDPE + *n*-alkane systems was concluded to be minor compared to the influence of the solvent used. This can also be observed by comparing Figure 13 and Figure 14. The different comonomers studied in the LLDPE + *n*-alkane systems were propene, 1-butene, 1-hexene, 1-octene and 4-methyl-1-pentene. Even though the samples compared in these results did not have exactly the same MM and density, the type of comonomer was concluded to have no actual systematic influence on the phase behavior of the studied LLDPE + *n*-alkane systems, as can be seen in Figure 15 (a). The influence of ethylene was studied in 10 m-% LLDPE + *n*-heptane systems with ethylene concentrations up to 3 m-%. Ethylene was found to act as an antisolvent, as increasing ethylene concentration significantly lowered LST cloud point temperatures (Figure 15 (b)). The type of phase behavior, influence of solvent type and influence of polymer MM on the phase behavior of LLDPE – alkane systems were also correctly predicted using the Perturbed Hard Chain Theory. (de Loos et al., 1996)

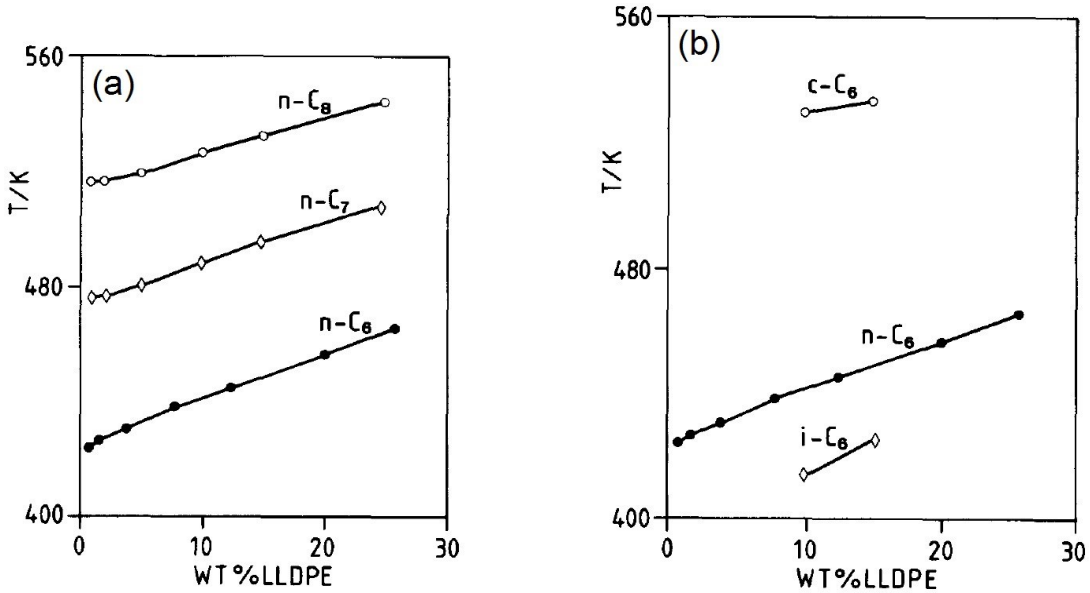


***Figure 13 Isobaric cloud point curves for LLDPE with different n-alkane solvents (a) and different C6 solvents (b) at a pressure of 3 MPa. (de Loos et al., 1996)***

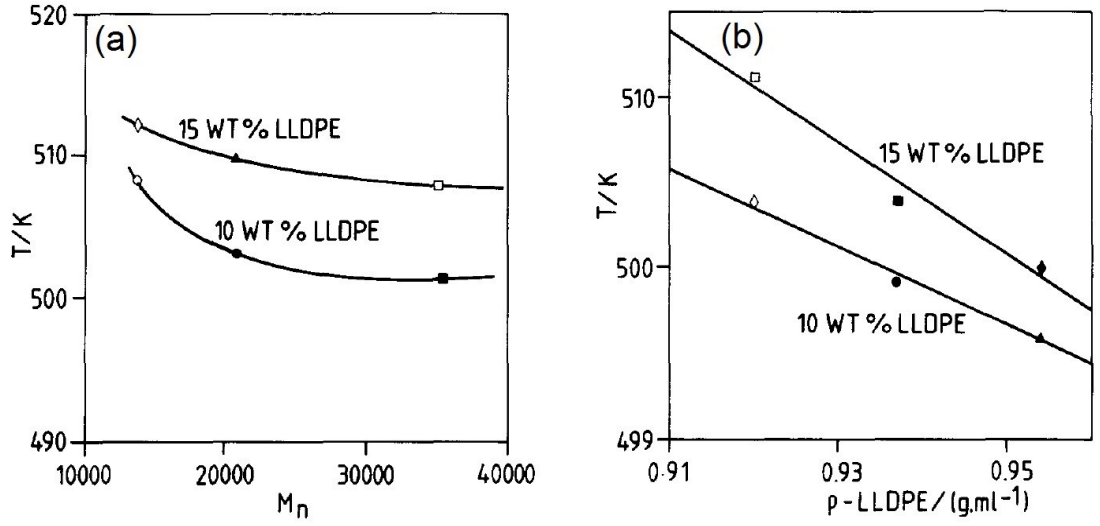


***Figure 14 Influence of MM (a) and density (b) on cloud points of LLDPE + n-heptane at a pressure of 5 MPa. (de Loos et al., 1996)***

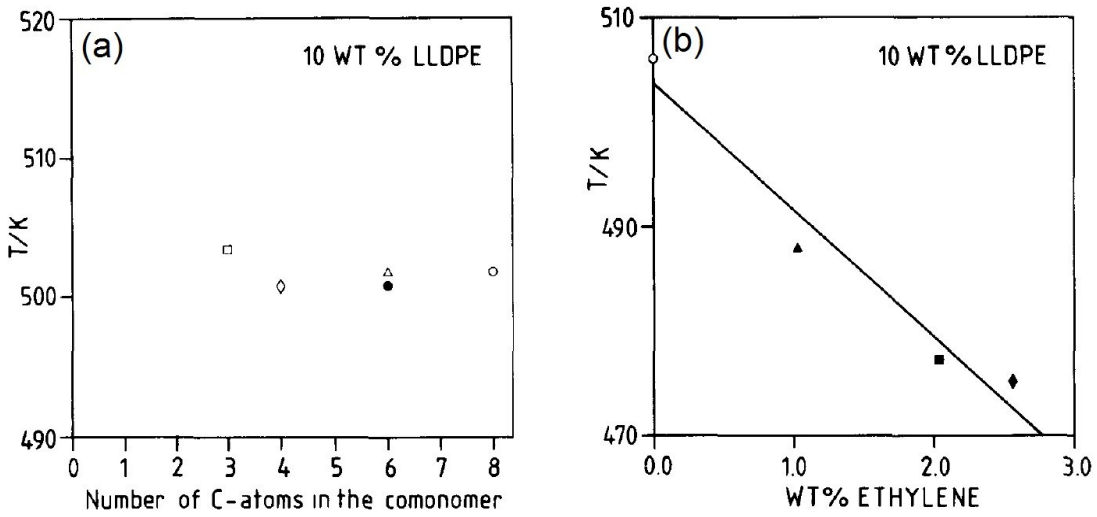


***Figure 15 Influence of the comonomer used (a) and concentration of ethylene (b) on cloud points of LLDPE + n-heptane at a pressure of 5 MPa. (de Loos et al., 1996)***

Chen et al. (2004) investigated influences of ethylene concentration, polymer MM and MMD on the phase equilibrium in mixtures of polydisperse LLDPE, *n*-hexane, and ethylene in temperatures from 373 K to 473 K, and pressures up to 20 MPa. The LLDPE used in the measurements was industrially manufactured with a metallocene catalyst, and measurement results were compared to similar measurements done with two nearly monodisperse PE grades (PE15k and PE108k, named by their respective MM). LCST behavior was observed, as the solvent *n*-hexane expands much more rapidly than the polymer with increasing temperature. The increasing free-volume (density) difference between the polymer and solvent causes phase separation. Increasing PE molar mass was found to increase cloud point pressures, as free-volume generally decreases with increasing molecular size causing an increase in free-volume difference between the polymer and solvent, and thus making higher MW polymers less soluble. The maximum (pressure) of cloud point isotherms were found to shift to lower polymer concentration with increasing polymer MM and polydispersity.

Chen et al. (2004) also conducted experiments with combinations of the two nearly monodisperse PE grades and *n*-hexane. Addition of higher molar mass components was found to significantly increase cloud point pressures, as with a mixture with 50 m-% of both, the cloud point pressures were higher than the average between the

cloud point pressures of both singular PE grades. This can be seen in Figure 16 (a). The combined (bimodal) mixture of monodisperse polymers was taken as a simplification of the LLDPE, as average MM was nearly the same. However, when measurement results of the different polymer + *n*-hexane systems were compared, the cloud point pressures of the bimodal system were notably higher than cloud point pressures of the LLDPE system (Figure 16 (a)), despite the nearly equal average MM of the polymers. This was concluded to be due to the polydispersity of the LLDPE. Ethylene was again found to act as an antisolvent increasing cloud point pressures, which were found to be nearly directly proportional to the weight fraction of ethylene (seen in Figure 16 (b)). Results were modeled with the Sanchez-Lacombe (S-L) equation of state, and polydispersity of the LLDPE was taken into account using pseudocomponents. While the amount of deviation between the S-L modeled and experimental results was dependent on several factors, the S-L EOS was concluded to provide qualitative agreement with the phase equilibrium data.

In a following study Haruki et al. (2008) measured cloud point pressures for the same polymers as done previously by Chen et al. (2004), in order to expand on the previous study, and investigate reproducibility of the data. Measurements were done for two PE samples (PE15k and PE108k, named by MM) in systems of PE + hexane and PE + hexane + ethylene in temperatures ranging from 373 K to 473 K, and pressures up to 21 MPa. Polymer weight fractions up to 0.13, and ethylene weight fractions up to 0.10 were considered. LCST behavior was observed for all binary and ternary systems, and cloud point pressures were found to increase with increasing polymer MM. The critical weight fraction was found to decrease with increasing polymer MM, due to stronger intermolecular interaction in larger MW polymers. For ternary systems of PE + hexane + ethylene, polymer weight fractions at maximum phase separation pressures were found to be slightly larger than their respective binary systems. The addition of ethylene also flattens the shape of the cloud point isotherms, as the decrease in hexane concentration with increasing PE weight fraction and constant overall ethylene concentration may enhance the effect of ethylene addition. In comparison with the previous study (Chen et al., 2004), the data was within uncertainty limits and was concluded reproducible. Cloud point

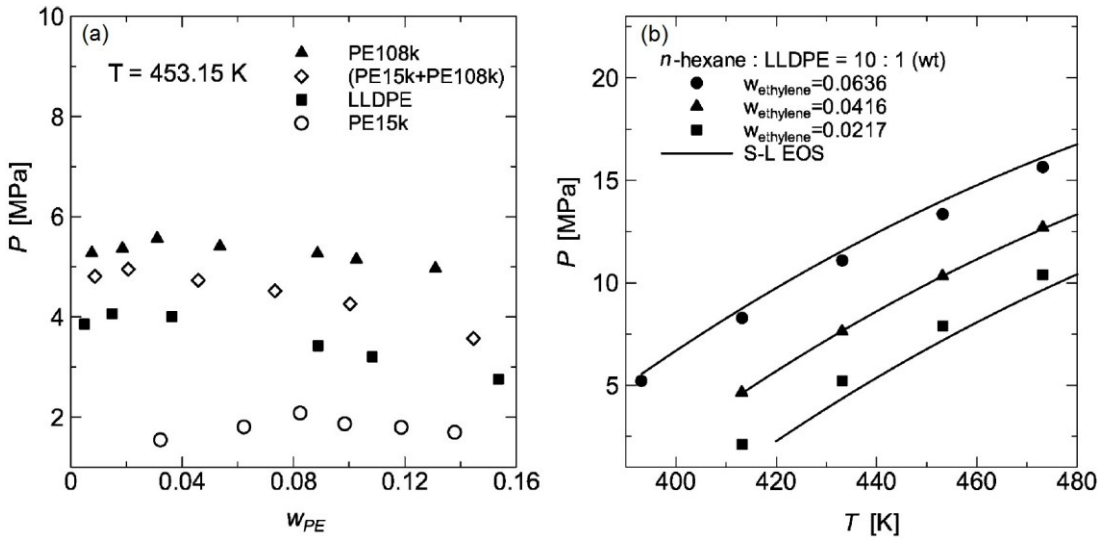


***Figure 16 (a) cloud point pressures for the monodisperse PE + n-hexane systems and the LLDPE + n-hexane system. (b) effect of ethylene on the cloud point pressure of 10 m-% LLDPE + n-hexane system. (Chen et al., 2004)***

isotherms for binary PE + hexane systems from both studies, along with ternary PE + hexane + ethylene cloud point isotherms for the same polymer can be seen in Figure 17. Measured phase boundaries along with binary data for LLDPE + hexane measured by Nagy et al. (2006), were satisfactorily predicted with the Sanchez-Lacombe EOS by adjusting the binary interaction parameters.

Expanding on previous studies (Chen et al., 2004; Haruki et al., 2008) done with binary PE + hexane and ternary PE + hexane + ethylene systems, Haruki et al. (2009) investigated binary, ternary, and quaternary systems containing PE, hexane, cyclohexane, and ethylene, especially for the addition of cyclohexane to the system, and its effect on the liquid-liquid phase behavior. The same polymers (PE15k and PE108k, named by MM) were used, and polymer mass fractions from 0.017 to 0.152, and ethylene mass fractions up to 0.10 were studied in temperatures from 373 K to 488 K, and pressures up to 14 MPa. No liquid-liquid phase separation was observed for binary PE + cyclohexane systems in the studied conditions, even though liquid-liquid separation was observed for binary PE + hexane mixtures in the previous study (Haruki et al., 2008). Cyclohexane was found to be a better solvent for PE than hexane, as also noted by de Loos et al. (1996). The addition of ethylene dramatically raised the vapor pressure, as ethylene is much more volatile than cyclohexane. Increasing ethylene concentration also reduced the solubility of PE, and induced a

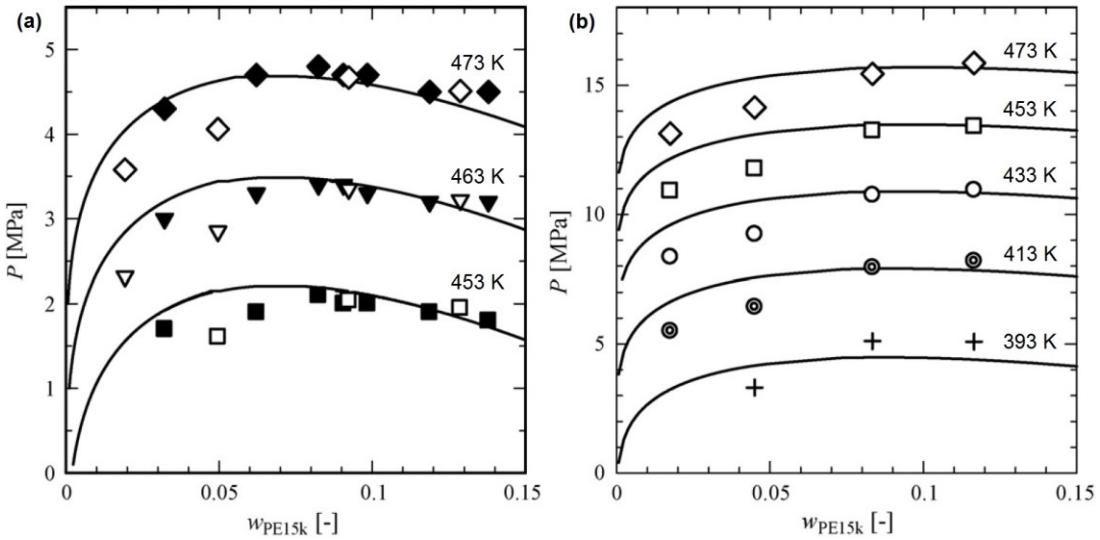


***Figure 17 (a) Cloud point isotherms for binary PE + hexane. Filled (black) points are experimental data from (Chen et al., 2004), and non-filled (white) points are data measured by (Haruki et al., 2008). (b) Cloud point isotherms for ternary PE + hexane + ethylene with an ethylene fraction of 0.1. Solid lines were calculated with the S-L EOS. (Haruki et al., 2008)***

LCST liquid-liquid split for the PE + cyclohexane + ethylene system. It was noted that in the studied range, the liquid-liquid separation pressures increased with increasing PE weight fraction for the PE + cyclohexane + ethylene system. This was explained by a decrease in cyclohexane concentration, when the PE weight fraction increases and ethylene concentration is kept constant, thus enhancing the effect of the ethylene addition.

For ternary PE + *n*-hexane + cyclohexane systems, cloud points were shifted to higher temperatures and lower pressures with the addition of cyclohexane, as the solubility of PE increased with increasing cyclohexane concentrations. The observed effects with binary and ternary systems also held true for the quaternary PE + *n*-hexane + cyclohexane + ethylene system; increasing ethylene concentration decreased polymer solubility and moved cloud points to lower temperatures and higher pressures (Figure 18 (a)), while increasing cyclohexane concentration enhanced polymer solubility and moved cloud points to higher temperatures and lower pressures (Figure 18 (b)). The data for all the systems were correlated and satisfactorily reproduced using the same procedure as in the previous study (Haruki et al., 2008) with the S-L EOS. Liquid-liquid phase boundaries were predicted for the quaternary system increasing the cyclohexane to total solvent ratio at constant

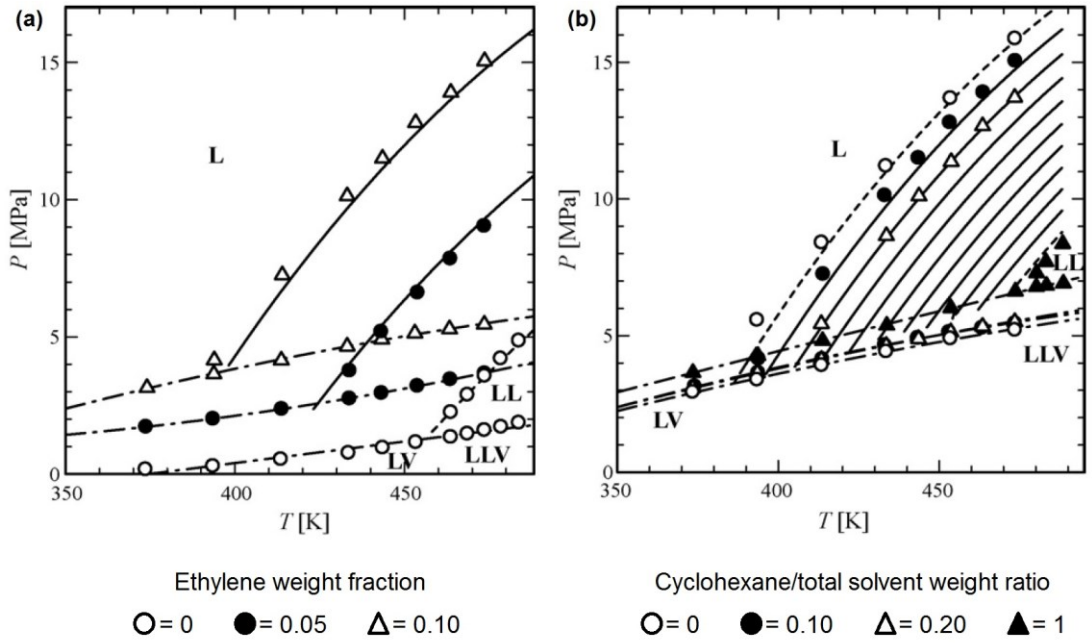


***Figure 18 (a) The effect of ethylene on the phase boundaries of the quaternary PE + n-hexane + cyclohexane + ethylene system. Cyclohexane/hexane ratio was kept constant at 1/9 and PE weight fraction was 0.10. (b) The effect of cyclohexane on the phase boundaries of the quaternary PE + n-hexane + cyclohexane + ethylene system. PE weight fraction was 0.10 and ethylene weight fraction was 0.10. Lines are predictions calculated with the S-L EOS. Dotted lines represent LV and LLV phase boundaries. Dashed lines in (b) represent LL phase boundaries for ternary PE + n-hexane + ethylene (upper line) and PE + cyclohexane + ethylene (lower line) systems. Predictions in (b) for cyclohexane/total solvent ratio were done from 0 to 1 at intervals of 0.1. (Haruki et al., 2009)***

intervals. As can be seen from Figure 18 (b), the location of the liquid-liquid phase boundary is nearly directly proportional to the amount of cyclohexane in the quaternary system. (Haruki et al., 2009)

In order to develop solution polymerization processes for PE colopolymers, Haruki et al. (2010) studied phase behavior in binary, ternary, and quaternary systems containing PE, hexane, 1-hexene, and ethylene, where 1-hexene was used as the comonomer, and hexane the solvent. Experiments were done in temperatures up to 473 K, pressures up to 19 MPa, ethylene weight fractions up to 0.102, and polymer weight fractions up to 0.123 using the same polymers (PE15k and PE108k, named by MM) as previous works (Haruki et al., 2008; Haruki et al., 2009). Measurement results were compared to the systems studied in these previous works. LCST type behavior was observed for all the studied systems, and phase behavior along with the effect of differing polymer MM was found to be similar to the previously studied systems. Liquid-liquid phase boundaries for the binary PE + 1-hexene systems were at slightly

higher pressures and lower temperatures than LL boundaries for the corresponding PE + hexane systems, as seen in Figure 19. Differences between the systems, however, were observed to be very small, and phase behavior was very similar, which was attributed to the similarities in characteristic properties, such as vapor pressure and critical temperature, between 1-hexene and hexane. For ternary systems of PE + 1-hexene + hexane with equal weight amounts of 1-hexene and hexane, cloud point pressures were found to be located approximately halfway in between the corresponding pressures for the binary systems (Figure 19). For ternary systems of PE + 1-hexene + ethylene, increasing ethylene amounts decreased the polymer solubility, and shifted cloud points to higher pressures and lower temperatures when compared to the respective binary PE + 1-hexene systems. The behavior of these systems was once again found to be very similar to the previously studied PE + hexane + ethylene systems.

The effects observed in the ternary systems held true for the quaternary system of PE + 1-hexene + hexane + ethylene; increasing ethylene concentrations shifted cloud points to higher pressures and lower temperatures. The magnitudes of these boundary shifts were similar to those of ethylene addition to the binary PE + 1-hexene and PE + hexane systems. The phase boundary behavior of the quaternary systems was not found to have any significant dependence on the mixture ratio of 1-hexene and hexane, due to the large similarity between 1-hexene and hexane. The difference in MM of PE was also found to have an insignificant effect on the phase boundary behavior of the quaternary system. Thus it was concluded that quaternary systems of PE + 1-hexene + hexane + ethylene at varying ratios of 1-hexene to hexane could be handled the same as both PE + 1-hexene + ethylene and PE + hexane + ethylene systems. The experimental results were correlated using the same procedure with the S-L EOS as in the previous works. The LL phase boundaries were satisfactorily predicted for all systems, and experimental results were reproduced especially well for systems containing the higher MM polymer (PE108k). (Haruki et al., 2010)

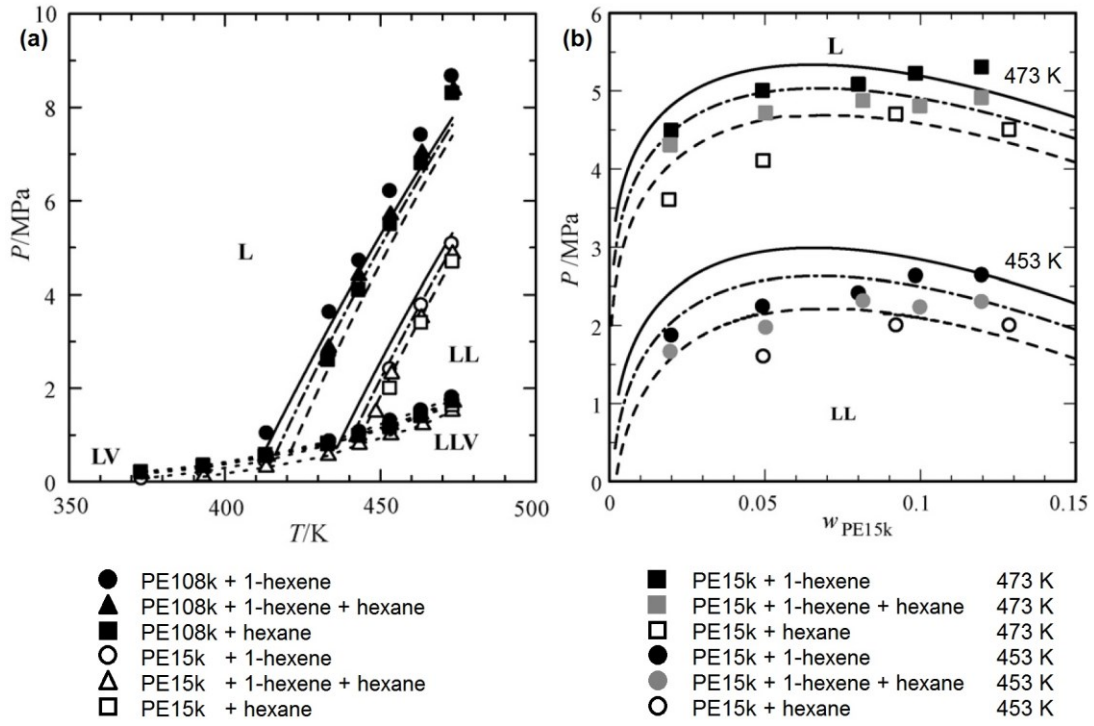


***Figure 19 (a) Phase boundaries for PE + 1-hexene + hexane systems. 1-hexene/hexane weight ratio was 1/1, and polymer weight fraction was 0.08. (b) Cloud point isotherms for PE + 1-hexene + hexane systems. 1-hexene/hexane weight ratio was 1/1. Lines are predictions calculated with S-L EOS. (Haruki et al., 2010)***

de Loos et al. (2004) reported phase equilibrium data for binary systems of nearly monodisperse LLDPE + *n*-hexane, and ternary systems of LLDPE + *n*-hexane + ethylene in a temperatures between 400 K and 500 K, and pressures up to 14 MPa. P-X isotherms can be seen in Figure 20 (a) and ternary isopleths along with the effect of ethylene can be seen in Figure 20 (b). The critical weight fraction of the polymer was found to be nearly constant in the studied range. Critical points were found to be slightly shifted towards higher polymer concentrations from the pressure maxima of the cloud point isotherms (Figure 20 (a)). This was concluded to be due to the polydispersity of the polymer, even though the polymer was nearly monodisperse. Increasing ethylene concentration was found to shift cloud points of the system to lower temperatures and higher pressures (Figure 20 (b)). Addition of ethylene also increased the pressures for liquid-vapor and liquid-liquid-vapor bubble-points. The acquired data was modeled in the studied range with a modified Sanchez-Lacombe EOS, as seen in Figure 20.

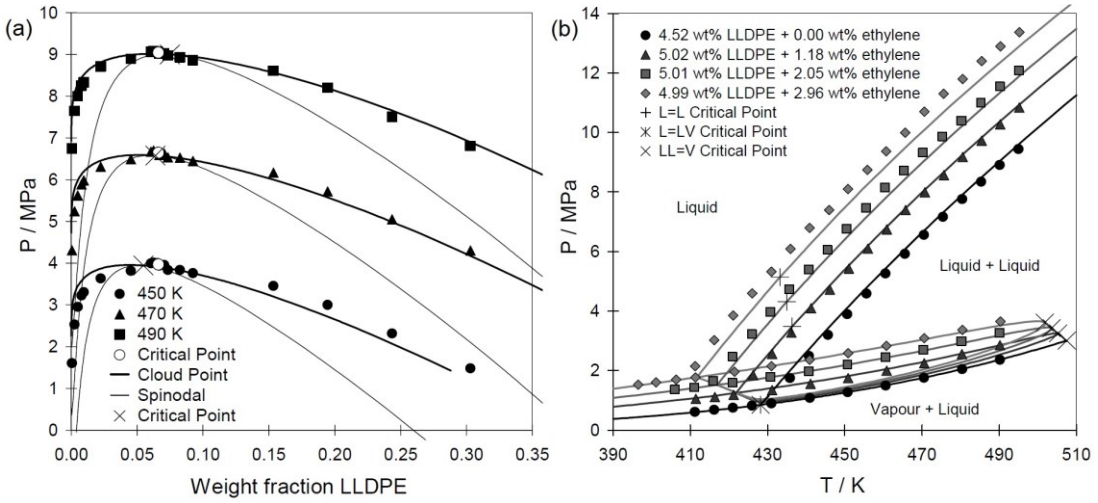


***Figure 20 Cloud point isotherms for binary LLDPE + n-hexane systems (a) and isopleths for ternary LLDPE + n-hexane + ethylene systems (b). Curves calculated with a modified S-L EOS. (de Loos et al., 2004)***

Nagy et al. (2006) reported phase equilibrium data for systems of LLDPE + *n*-hexane and LLDPE + *n*-hexane + ethylene systems. Vapor pressure and cloud point data were measured for polymer mass fractions from up to 0.30 for binary systems and polymer mass fractions up to 0.15 for ternary systems in the temperature range 400-500 K and pressures up to 14 MPa. The system was found to have liquid-liquid phase separation characterized by lower critical solution temperatures and upper critical solution pressures. The critical weight fraction for the systems stayed nearly the same for the systems regardless of temperature, which can be seen in Figure 21 (a) for a LLDPE + *n*-hexane system. The same figure also shows critical points shifted slightly towards larger polymer concentrations from the pressure maxima of cloud point isotherms due to polydispersity. Figure 21 (b) presents vapor pressure and cloud point curves for 10 m-% LLDPE + *n*-hexane + ethylene systems with varying amounts of ethylene. Increasing the concentration of ethylene was found to increase cloud point and vapor pressures. The system was modeled with a modified Sanchez-Lacombe EOS using pseudocomponents to characterize the polydispersity of the polymers. The S-L EOS fitted to the binary and ternary data was concluded to provide a good fit.

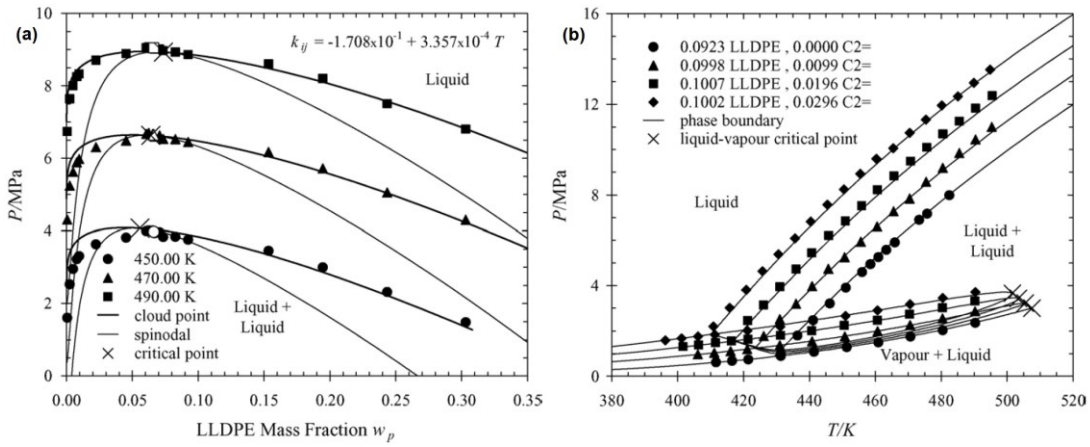


***Figure 21 Cloud point isotherms for binary LLDPE + n-hexane systems (a) and isopleths for ternary LLDPE + n-hexane + ethylene systems (b). Curves calculated with a modified S-L EOS. (Nagy et al., 2006)***

In a following study, Nagy et al. (2007) reported cloud point and vapor pressure data for LLDPE + isohexane systems, and compared the obtained results to LLDPE + n-hexane systems investigated in the previous study (Nagy et al., 2006). Measurements were done with polymer mass fractions varying from 0 to 0.25 in the temperature range 380-500 K, and pressures up to 12 MPa. The cloud point and liquid-liquid critical point behavior with isohexane as the solvent is very similar to *n*-hexane, with critical polymer mass fraction being nearly constant and slightly shifted to higher polymer concentrations from the cloud point isotherm pressure maxima. This can be observed in Figure 22 (a). *n*-hexane was found to be a better solvent than isohexane for the studied LLDPE in the investigated range, as cloud points in *n*-hexane systems were observed at lower pressures than corresponding isohexane systems. The vapor pressures of the systems were very close to vapor pressures of the pure solvents, and were only slightly higher for the isohexane systems. Comparison between cloud points and vapor pressures for the two solvents in systems of equaling polymer concentration can be seen in Figure 22 (b). The results were modeled with a modified Sanchez-Lacombe EOS, and polydispersity was characterized with a number of pseudocomponents. When fitted to the data, the S-L EOS was able to represent both systems with similar accuracy. Slightly more inaccuracy was experienced with small polymer concentrations, which was attributed to the uncertainty in MWD measurements of small MW components along with model limitations.

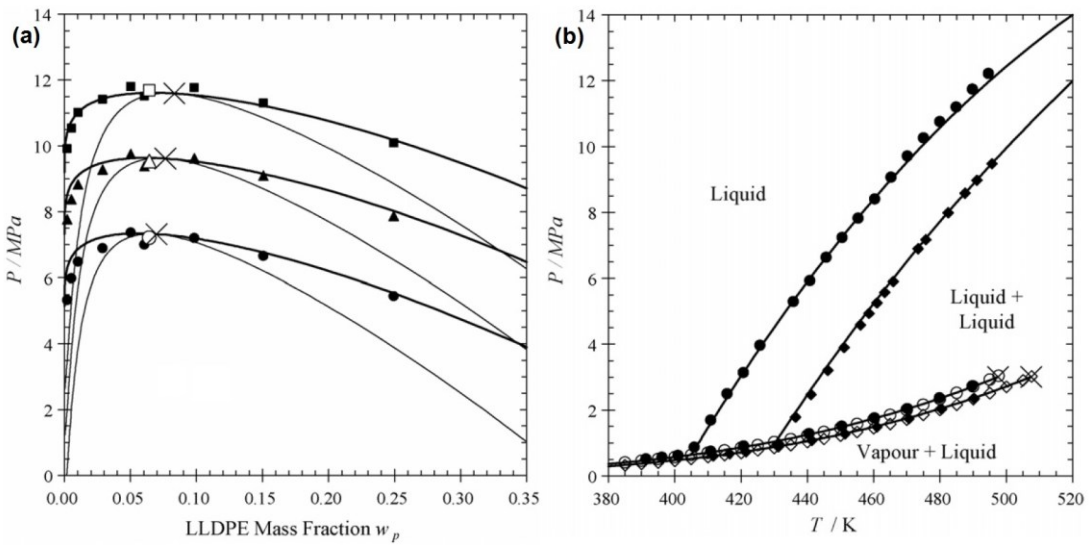


***Figure 22 (a) Cloud point isotherms for the LLDPE + isohexane system and (b) comparison of phase diagrams for LLDPE + isohexane (circles, higher curve) and LLDPE + n-hexane (squares, lower curve) systems. Symbols represent experimental points, and curves were calculated with a modified S-L EOS. (Nagy et al., 2007)***

Schnell et al. (2004) measured cloud points for systems of nearly monodisperse linear PE + *n*-hexane in temperatures up to 500 K and pressures up to 15 MPa. Three samples of PE with varying MM and slightly varying MMD were used in the experiments. The systems exhibited LCST-type behavior, and cloud point pressures were observed to increase with increasing molar mass. The aim of the study was to extrapolate a critical line for infinite molar mass from the data collected. This critical line specifies a P-T dependence area of homogeneity, wherein the system remains in a single phase regardless of the polymer MM, MMD or concentration. Such a diagram for the linear PE used in the experiments can be seen in Figure 23 along with predictions calculated with Sanchez-Lacombe and Flory-Huggins theories. The lower "triangle" part of the diagram represents the area of complete miscibility, while two liquid phases can coexist in the upper "triangle" depending on the system composition and MW of the polymer.

Chen et al. (1999) studied phase behavior in dilute systems of polyethylene co-polymerized with 1-butene in solutions of 1-butene and ethylene. PE concentrations in the measurements ranged from 0.01 m-% to 1 m-% in temperatures up to 180 $^{o}$C and pressures up to 1500 bar. Measurement results were modeled with a copolymer SAFT EOS. Polymer branch density was described by the number of ethyl branches

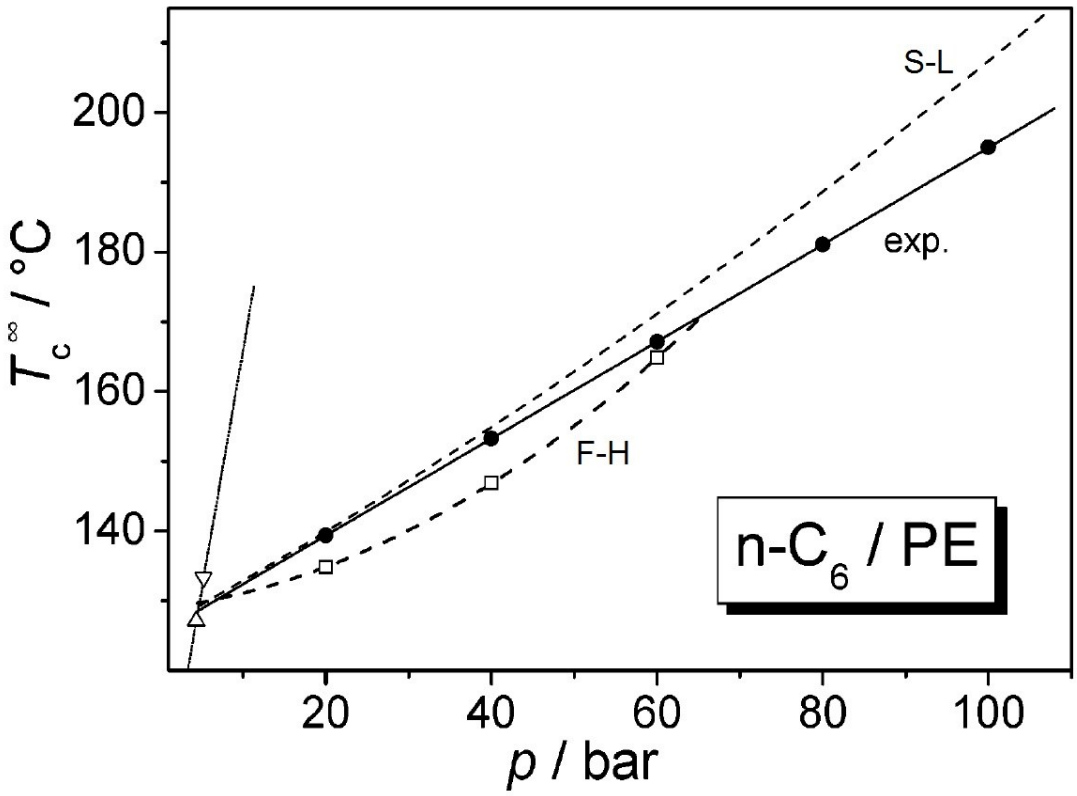


***Figure 23 Pressure dependence of the critical demixing temperature for infinitely long PE molecules in n-hexane. Points on the exp-curve are extrapolated from experimental data, while S-L and F-H curves represent predictions made with Sanchez-Lacombe and Flory-Huggins theories respectively. The steep line on left represents the vapor pressure curve of the pure solvent. (Schnell et al., 2004)***

per 100 ethyl units in the polymer backbone. Amorphous PE with a branch density number of 100 exhibited LCST behavior in binary PE + ethylene systems, while other studied samples with lower branch densities exhibited UCST behavior in binary PE + ethylene systems. Binary PE + 1-butene systems exhibited a (UCST-type) solid-liquid transition at very low temperatures (below 5 $^{o}$C), and LCST liquid-liquid transitions above 90 $^{o}$C. Cloud point pressures for binary PE + 1-butene systems were found to be significantly lower than for corresponding binary PE + ethylene systems. Increasing ethylene concentrations shifted cloud point curves to lower temperatures and higher pressures, while increasing branch density was found to decrease cloud point pressures for all systems.

Pan et al. (1999) investigated the influences of polymer concentration, polymer density, and melt index on solid-liquid and liquid-liquid phase equilibria in poly(ethylene-co-1-hexene) solutions in isobutene and propane in temperatures up

to 150 °C, and pressures up to 1000 bar. Polymer concentration was varied between 4-11 m-%, and was found to have little effect in such a small concentration range for the studied systems. Isobutane was found to be a better solvent for the polymer than propane due to smaller size difference between the polymer and solvent. Increasing comonomer 1-hexene concentration was found to increase the overall solvent density, which lead to improved polymer solubility as a result of decreased density difference between the polymer and solvent. Increasing polymer density, i.e. decreasing the degree of branching in the polymer, was found to increase cloud point pressures, as density difference between the solvent and polymer increases. As melt index is a function of the polymer MM, it decreases with increasing polymer MM. This increases the difference in MM between the polymer and solvent, which decreases polymer solubility and increases cloud point pressures.

Lee (Lee, 2005) reported phase behavior measurements for polyethylene co-polymerized with 15.3 mol-% 1-octene ($PEO_{15}$) in binary systems using *n*-pentane, *n*-hexane, *n*-heptane, and *n*-octane as solvents in temperatures up to 170 °C. A ternary system containing PE, 1-octene(co-monomer) and ethylene(monomer) was also investigated. Liquid-liquid phase separation was observed for only the PE + *n*-pentane system, and bubble point and cloud point curves for the system with varying PE concentrations are presented in Figure 24 (a). Systems with higher molar mass alkane solvents did not exhibit liquid-liquid phase separation in temperatures below 170 °C, as solubility of PE increases with increasing alkane solvent size. Cloud point pressures for the binary PE + *n*-pentane system were observed to reach a maximum between polymer concentrations of 2 to 11 m-% (around 5 m-%), which was concluded to be near the polymer critical concentration for the system. Cloud points were also notably shifted to higher temperatures with polymer concentrations below 2 m-% or above 11 m-%, as can be seen in Figure 24 (a). Cloud point curves for the ternary PE + 1-octene + ethylene system are presented in Figure 24 (b), where PE concentration was kept at approximately 5 m-% and ethylene content was varied. The addition of ethylene decreased the solubility of the polymer and significantly increased cloud point pressures. Figure 24 (b) also shows that the phase separation behavior shifts

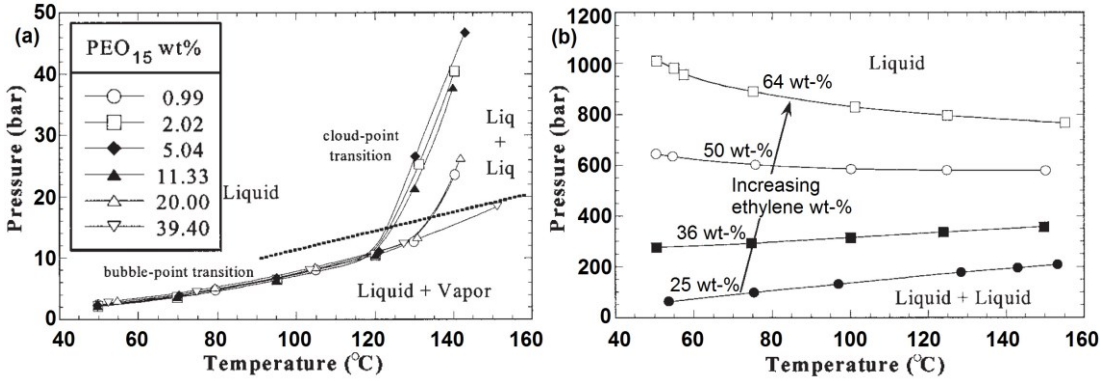


***Figure 24 (a) Bubble point and cloud point isopleths for binary PE + n-pentane systems with varying PE concentrations. Cloud points were observed above the dashed line. (b) Cloud point isopleths for ternary PE + 1-octene + ethylene systems with 5 m-% PE concentration and varying ethylene concentration. Liquid-liquid phase separation shifts from the LCST type to the UCST type between 36 m-% and 50 m-% ethylene. (Lee, 2005)***

from the LCST type to the UCST type (between 36 m-% and 50 m-% ethylene), when ethylene concentrations are sufficiently increased.

The influence of inert gases on the phase equilibria of systems containing polyethylene, ethylene, and 1-hexene was investigated by Dörr et al. (2001). The polymer used in the experiments was a copolymer of ethylene and 1-hexene, poly(ethylene-co-1-hexene). Several inert compounds (helium, nitrogen, $CO_2$, methane, ethane, propane, *n*-butane) were studied in PE + ethylene systems, and nitrogen was studied in a system containing PE, ethylene and 1-hexene. Cloud points measurements were reported for the systems in temperatures ranging from 393 K to 493 K, and pressures up to 215 MPa. Increasing 1-hexene concentrations in systems of 15 m-% PE + ethylene significantly decreased cloud point pressures, i.e. increasing ethylene concentrations were found to increase cloud point pressures. UCST type behavior was observed for the PE + 1-hexene + ethylene system at pressures higher than 60 MPa, as increasing temperature was found to improve polymer solubility. The opposite (LCST type behavior) was observed for the same system at pressures lower than 60 MPa. The addition of helium, nitrogen, methane, and $CO_2$ was found to increase cloud point pressures in PE + ethylene systems, while ethane, propane and *n*-butane improved the polymer solubility. Increasing temperature was found to improve polymer solubility in all cases. The magnitude of cloud point pressure increase was greatest with helium and declined in the order helium > nitrogen >

methane > $CO_2$ with decreasing critical temperature. For the PE + 1-hexene + ethylene system nitrogen was found to similarly increase cloud point pressures with increasing nitrogen concentration. Ethane, propane and *n*-butane were found to be soluble in the copolymer as well as the solvent mixture of 1-hexene + ethylene, and thus act as cosolvents similarly as the comonomer 1-hexene, decreasing cloud point pressures with increasing concentration. By comparison, the solubility of helium, nitrogen, methane, and $CO_2$ in the copolymer is much lower. The magnitude of decrease in cloud point pressure was found to be greatest for *n*-butane and decreased in the order *n*-butane > propane > ethane with decreasing critical temperature and molar mass, i.e. increasing difference in MM (and density) between the polymer and solvent. The influence of all the inert compounds on the cloud point pressure of 15 m-% PE + ethylene systems can be seen in Figure 25.

Similar observations were made for supercritical ethane, propane, and nitrogen gases added to systems of polystyrene + cyclohexane and polyethylene + cyclohexane in temperatures up to 516 K, and pressures up to 160 bar by ter Horst et al. (2002). Observed LCST cloud points were shifted to lower temperatures and cloud point pressures increased with increasing concentrations of supercritical gas for all systems. The magnitudes of shift in order from greatest to smallest were nitrogen > ethane > propane. However, nitrogen was also found to significantly increase bubble point pressures of the systems due to its high volatility and low solubility in cyclohexane, thus requiring high pressures for dissolving it. Ethane and propane have comparatively much higher solubility in cyclohexane, and do not dramatically increase bubble point pressures of the system, while still shifting cloud points to lower temperatures and higher pressures providing a higher effect in actual liquid-liquid separation at moderate pressures. Ethane was thus concluded to be the most effective among the studied gases for liquid-liquid separation using a supercritical gas as an antisolvent. Cloud point shifts to higher pressures along with the magnitude of the shifts with the addition of supercritical gases in the studied systems can be explained with increasing free-volume (density) difference between the polymer and solvent system.

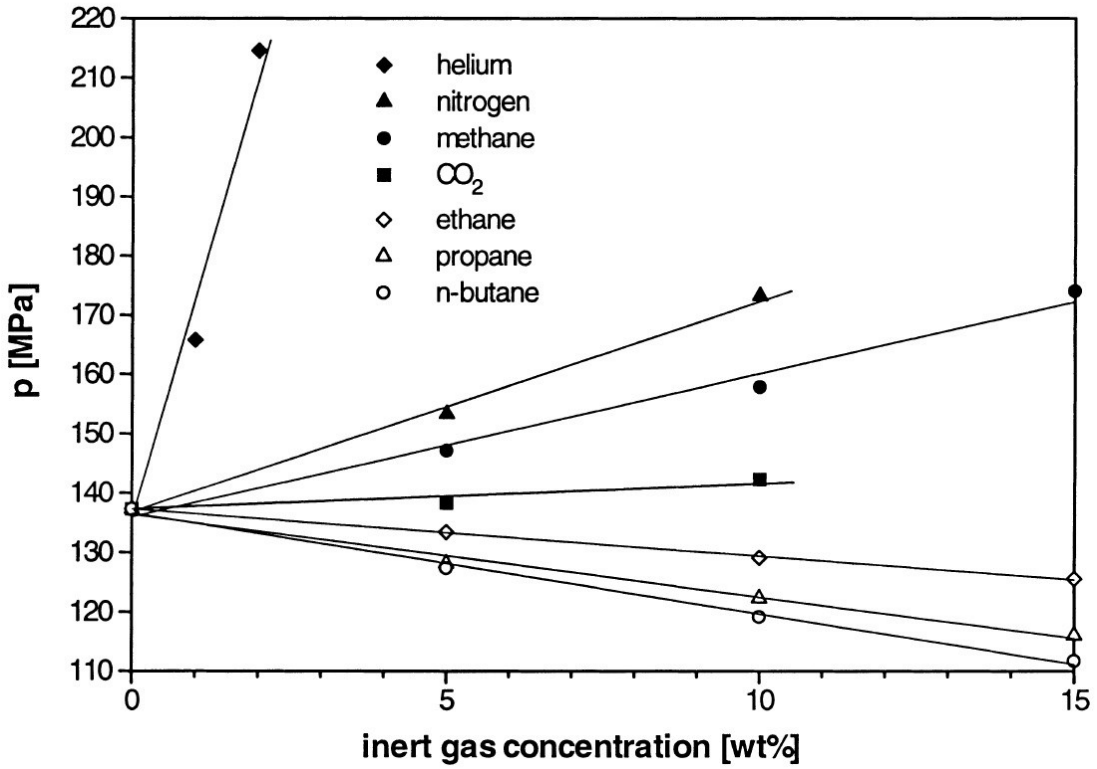


***Figure 25 The influence of inert gases on the cloud point pressures of 15 m-% PE + ethylene systems at T = 433 K. (Dörr et al., 2001)***

As already mentioned before, polydispersity in a polymer can produce an abrupt change in slope in its cloud point isotherm, as described for Figure 6, signifying a possible equilibrium point for three fluid phases (de Loos et al., 1983). Moreover, calculations correlated to reproduce this effect can result in cloud point curves that fold over themselves, forming phase boundaries for three-fluid-phase or even four-fluid-phase regions. Hypothetical three and four-fluid-phase regions were proposed by Krenz et al. (2005) near this cusp point, when the liquid-liquid critical point is on the metastable part of the two-phase boundary. Calculations of phase boundaries for LDPE + ethylene and LLDPE + *n*-hexane systems were carried out on the basis of experimental data using a modified Sanchez-Lacombe EOS. Polydispersity of the polymers was taken into account using a large number of pseudocomponents to gain good resolution for the calculations, as the proposed three-phase and four-phase areas are very small. An example of a calculated phase boundary curve folding on itself is presented in Figure 26 for LDPE + ethylene at 383 K. Flash calculations in the three phase area revealed one of the phases to contain mainly the heaviest MW

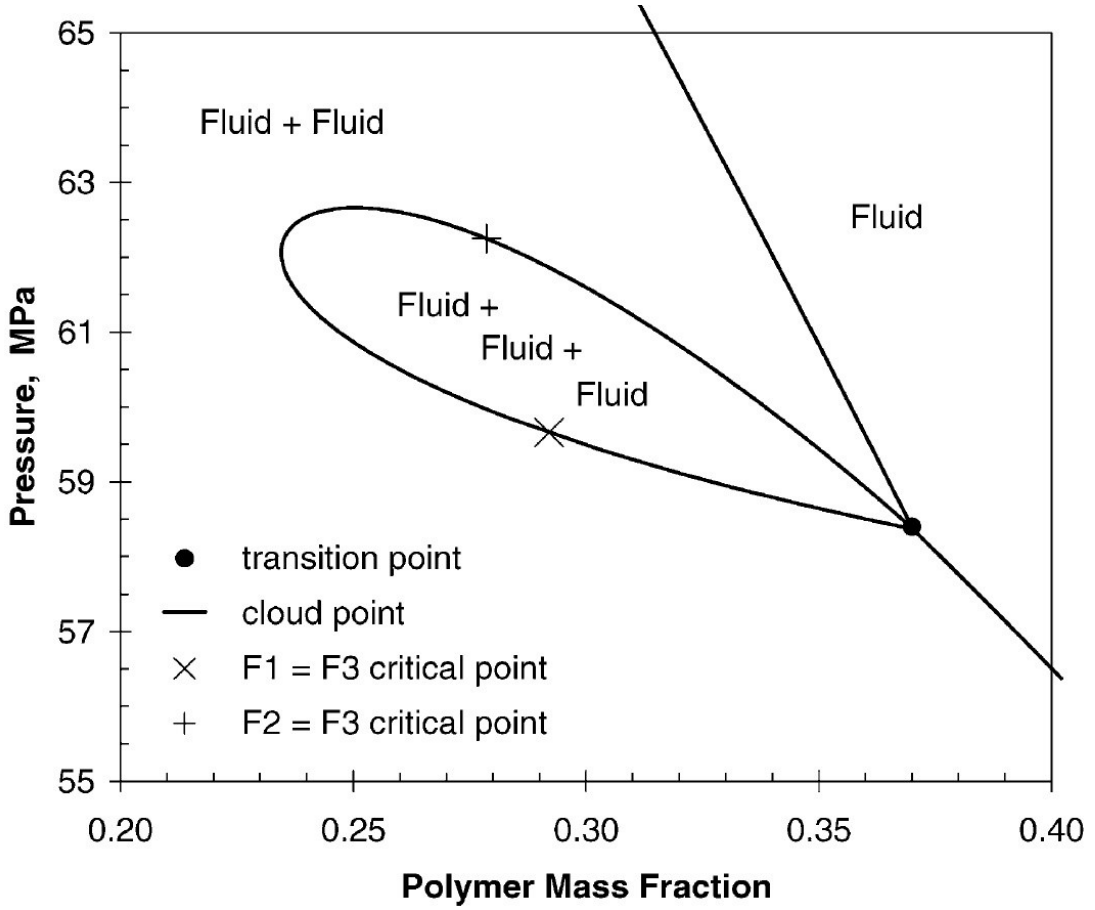


***Figure 26 Two-fluid-phase and three-fluid-phase boundaries calculated by the modified S-L EOS at the cusp of a cloud point isotherm for a polydisperse LDPE + ethylene system at 383 K. Critical points on the three-phase boundary represent points, where compositions of two of the phases are identical. (Krenz et al., 2005)***

components in the system, and the amount of this phase was found to be very small compared to the other two.

For the LLDPE + *n*-hexane system the MWD was extended to include higher MW components to investigate their effect on the model behavior. The heavier MW components were found to increase the tendency for multiphase behavior in the modeled isotherms, producing the proposed three-phase area, and even a twice folding isotherm containing a very small four-fluid-phase area inside the three-phase area. Flash calculations revealed the system to be comprised mainly of two phases in all cases, with additional phases being comparatively very small and containing heavier MW components. The heaviest MW components were concluded to destabilize the incipient phase, and produce the observed multiphase behavior. However, it was strongly emphasized, that the three- and four-phase calculations

were highly hypothetical, and extending the MWD of a polymer to include higher MW components is far removed from the most probable cases of actual MWD. The work served as a demonstration, that characterization of the polymer, and especially the heavy end of the polymer MWD, can have a large impact in the prediction of the phase behavior of a polymer-solvent system. Experimental observation of the proposed three-phase and four-phase regions was concluded to be very difficult, due to very small differences in densities between phases and thus extremely slow phase separation. Additionally, MWD would need to be adjusted very accurately in these experiments, as the calculations were very sensitive to changes in the heaviest components. (Krenz et al., 2005)

## 4.3. Ethylene-propylene copolymer (PEP) systems

Phase equilibria measurements by Chen et al. (1992) and Gregg et al. (1993) in temperatures up to 200 $^{o}$C, and pressures up to 550 bar for a nearly-monodisperse, amorphous, and alternating ethylene-propylene copolymer (PEP) demonstrated that higher size difference between polymer and solvent leads to higher cloud point pressures, and higher tendency towards type B and C behavior from Figure 3. This is exemplified in Figure 27 for low MM (790 g/mol) PEP at 15 m-% in three different solvents, namely ethylene, propylene and 1-butene. In this case the PEP – 1-butene system shows type A behavior from Figure 3 with no liquid-liquid phase separation, while the PEP – propylene system exhibits type B LCST behavior. The PEP – ethylene systems exhibits type C behavior, for which part of the U-LCST curve can be seen in Figure 27. Similarly, increasing MM of the polymer results in increased cloud point pressure in a fixed temperature, as can be seen in Figure 28 for a PEP – propylene system. (Chen et al., 1992; Gregg et al., 1993)

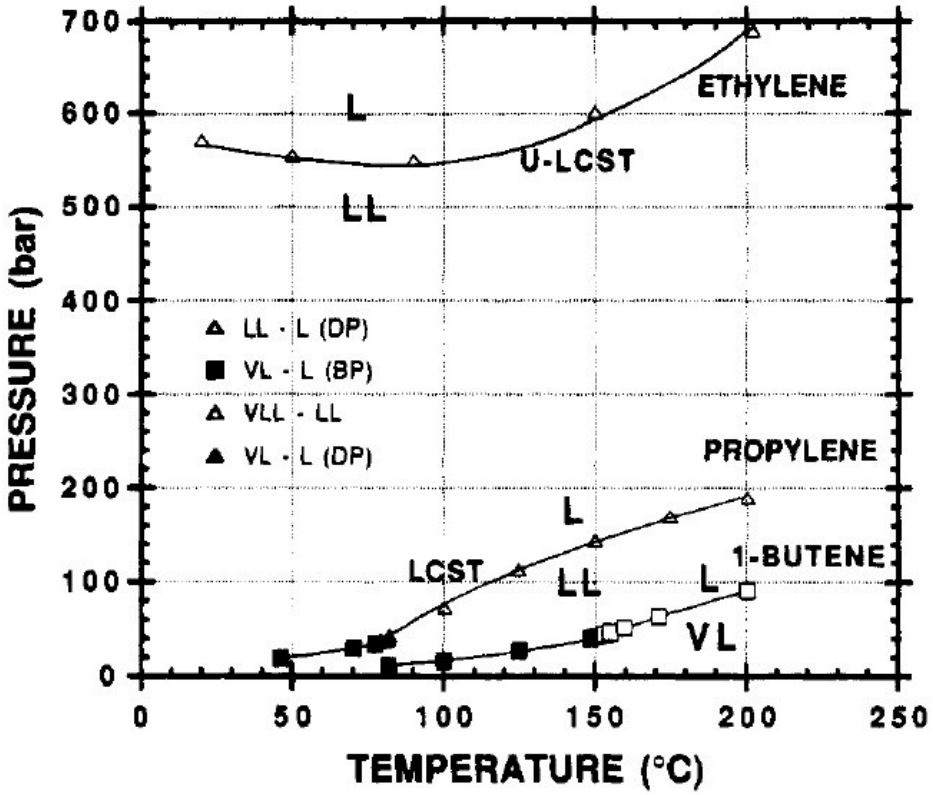


***Figure 27 P-T isopleths for 15 m-% PEP (790 g/mol) in 1-butene, propylene and ethylene exhibiting type A, B and C behavior respectively with decreasing solvent size and density. Data from Chen et al. (1992) and Gregg et al. (1993). (Folie et al., 1995)***

Both LCST and U-LCST transitions were observed for PEP – propylene systems, while only U-LCST transitions were observed for PEP – ethylene systems in the MM range (790 – 96000 g/mol) investigated by Gregg et al. (1993). The slope of the cloud point curve was shown to change sign with decreasing polymer MM. High MM polymers exhibited UCST behavior while lower MM polymers exhibited LCST behavior in the studied temperature range. It was concluded that the LCST curves were the LCST branches of U-LCST curves, while the UCST curves may or may not be branches of the U-LCST curve depending on whether or not the critical locus of the system has a minimum(such as in Figure 3 (c)).

Effects of changing both polymer and solvent size were studied by Chen et al. (1992). Decreasing solvent size for a given polymer was found to shift the LCST curves to lower temperatures and higher pressures. Similarly, the cloud point pressure at a fixed temperature is shown to increase with increasing MM in a given solvent, so

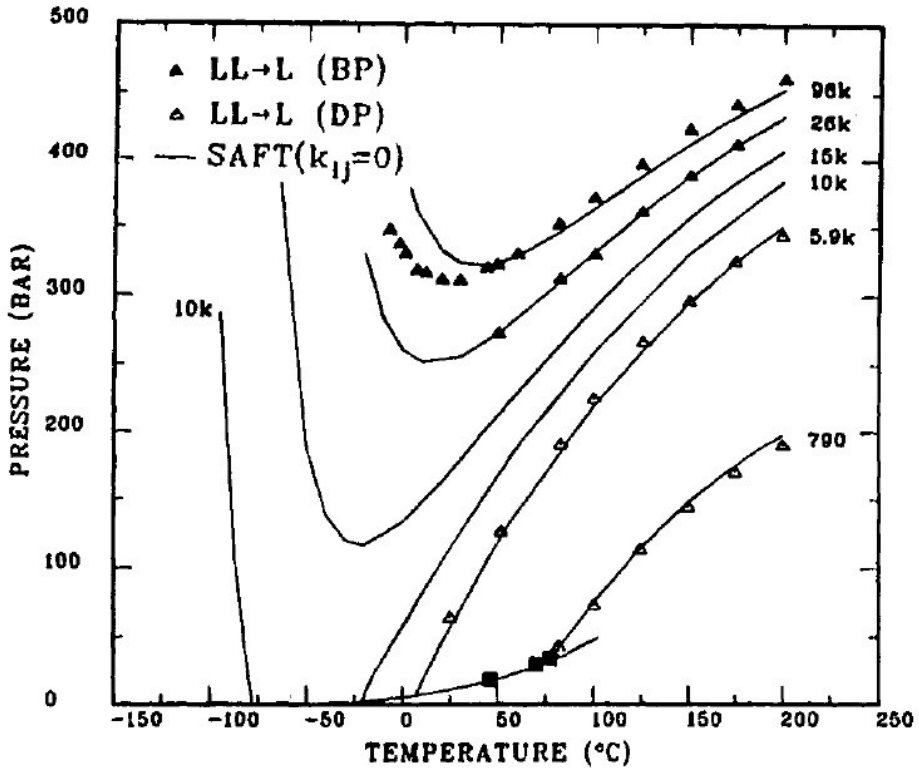


***Figure 28 P-T isopleths for 15 m-% PEP – propylene systems with different PEP MM. Filled points indicate bubble-point type transition, while open points indicate dew-point type transition. (Chen et al., 1992)***

increasing size difference results in increased cloud point pressures. The effect of MM on the cloud point curve is illustrated in Figure 28 for PEP – propylene systems. Increasing polymer MM also shifted the phase transition behavior from LCST to U-LCST (from type (b) to type (c) in Figure 3), and additionally resulted in a qualitative change in the phase disengagement mechanism from a dew-point type transition for lower MM polymers (790 and 5,9k in Figure 28, the numbers signifying the MM of the polymer in g/mol) to a bubble-point type transition for higher MM polymers (26k and 96k in Figure 28). This indicates that the 15 m-% of polymer used in the work was below critical concentration for the lower MM polymers separating by dew-point type transitions, and above critical concentration for the higher MM polymers separating by bubble-point type transitions. Further studies by cooling the solutions down to -70 $^{o}$C indicated a U-LCST boundary for the higher MM polymers separating by bubble-point-type transitions, while no such boundary was found for the lower MM polymers separating by dew-point type transitions. The data in Figure 28 was

also modelled with the statistical associating fluid theory (SAFT) model, which is able to predict the transition from LCST to U-LCST as well as the increase in temperature and pressure of the U-LCST minimum with increasing polymer MM. However, predictions of the UCST branch of the U-LCST curve along with critical points of the solvents are slightly less accurate. (Chen et al., 1992)

In typical ternary polymer reaction mixtures the polymer is mixed with its monomer and a higher α-olefin. Following studies of binary PEP mixtures, Chen et al. (1992) investigated ternary mixtures of PEP and ethylene mixed with 1-butene and 1-hexene. It was found that ethylene acted as an antisolvent for the systems, as it increased the difference in densities between the polymer and solvent. Isothermally increasing ethylene concentration was found to result in increased cloud point pressure, as depicted in Figure 29 for PEP (26 000 g/mol) + 1-butene + ethylene mixtures with differing ethylene concentrations. Similar results were obtained for the mixtures with 1-hexene instead of 1-butene. Higher α-olefins than the primary solvent were found to behave like co-solvents for the binary PEP – solvent mixtures, as they reduce the difference in densities. Larger and denser α-olefins were found to be better solvents, due to smaller size/density difference between the polymer and solvent. The solvation power for α-olefin solvents depend on their molecular structure. (Folie et al., 1995) Difference in solvation power between straight and branched olefins (for example *n*-hexane and methyl-pentane) is relatively small, while cyclic compounds (in this case methyl-cyclopentane for example) act as better solvents due to higher critical density. As the difference in density between the polymer and solvent increases, the LCST curve is shifted to lower temperatures increasing the size of the two phase region.

LDPE and LLDPE differ somewhat from the PEP used as the example cases above in crystallinity, polydispersity (or molar mass distribution, MMD), and chain branch distribution. LDPE and LLDPE are commonly semicrystalline in structure, whereas the example PEP is amorphous. PEP was assumed nearly monodisperse while LLDPE and especially LDPE are usually polydisperse with varying degrees of molar mass distribution. The effects of chain branches and their distribution in LDPE and LLDPE

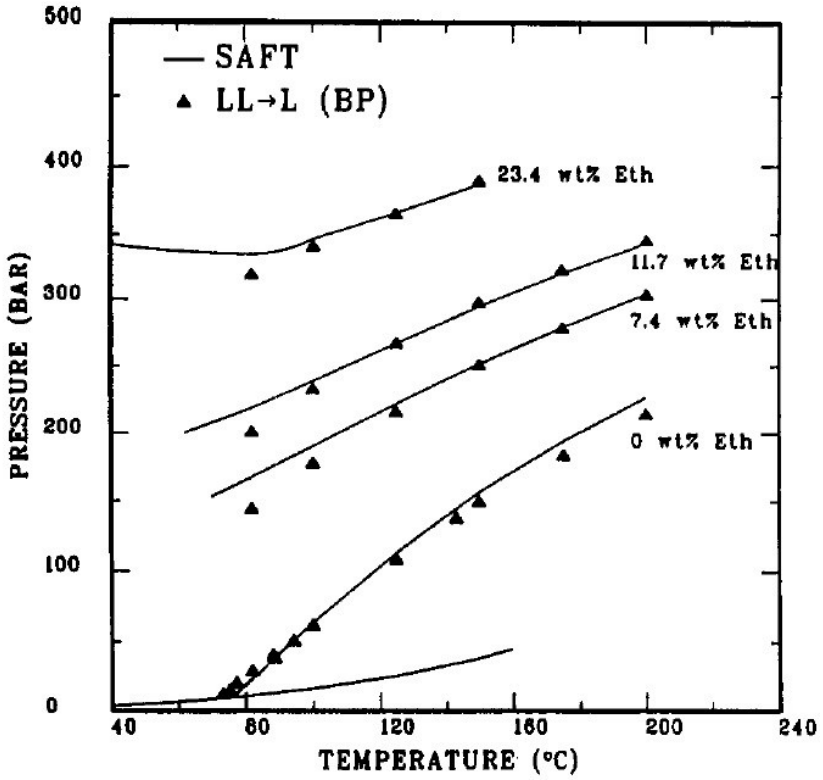


***Figure 29 P-T isopleths of 15 m-% PEP (2600 g/mol) + 1-butene + ethylene mixture at different ethylene concentrations.***

are also important aspects of understanding their phase behavior. The presence of long chain branches in LDPE has been shown to increase polymer solubility and decrease cloud point pressures, when compared with HDPE of the same MM and MMD (Folie et al., 1995). Increasing short chain branch density has also been shown to decrease cloud point pressures (Folie et al., 1995), which is consistent with higher density polymers being less soluble, and thus requiring higher pressures to be complete soluble.

## 4.4. Conclusions on experimental polymer systems

A variety of studies exist for polyethylene in a number of different systems, as can be observed from the presented example studies. The research topics for the studies vary widely. Some build upon earlier studies and share similarities, while other studies examine more unconventional aspects of polymer systems. Despite the

multitude of experimental work on the phase behavior of polyethylene systems, some rough general conclusions regarding these systems can be made based on the example studies presented above. It must be remembered, however, that the actual phase behavior is always system specific, and depends on the composition and operating conditions of the system.

A general phenomenon in liquid-liquid phase behavior of polyethylene – solvent systems can be concluded as increasing molecular asymmetry between the polymer and solvent decreases the polymer solubility. This means that increasing differences between the polymer and solvent in properties such as molar mass or density decrease the solubility of the polymer, and increase the tendency of the mixture to separate into two (or hypothetically more) distinct liquid phases. This phenomenon was also presented in chapter 3 for Figure 4. Many of the more specific conclusions made for the phase behavior of polyethylene – solvent systems can be attributed to this main phenomenon.

Several aspects were found in many of the studies to have an impact on the phase equilibrium of polyethylene – solvent systems. All the aspects handled here have to do with the LCST type phase behavior. Increasing the concentration of the polymer in a constant temperature obviously causes a change in the cloud point pressures, which increase to a maximum near the polymer critical concentration, and then decrease with increasing polymer concentration. This can be seen from P-X cloud point isotherms. The polydispersity of the polymer affects the location of the pressure maximum and the critical concentration. With increasing polydispersity pressure maxima are shifted to smaller polymer concentrations, while critical polymer concentrations are shifted to larger polymer concentrations from the pressure maxima (Chen et al., 2004; de Loos et al., 1983). The critical polymer concentration was usually found to change very little with regard to pressure and temperature changes in the system, and was often handled as constant in appropriate temperature and pressure ranges (de Loos et al., 1983, 2004; Nagy et al.,2006; Trumpi et al, 2003). Critical polymer concentrations were found to decrease with increasing polymer molar mass (Haruki et al., 2008). Increasing polymer molar

mass was found to decrease polymer solubility, as differences in MM between the polymer and solvent increase (Chan et al., 2000; Chen et al., 1992; Chen et al., 2004; de Loos et al., 1983, 1996; Haruki et al., 2008; Pan et al., 1999; Schnell et al., 2004). Increased degrees of branching in polymers were found to improve solubility (Chan et al., 2000; Chen et al., 1999; de Loos et al., 1995; Pan et al., 1999), as this decreases the polymer density and consequently the density difference between the polymer and solvent.

The type of solvent mixture in a polymer – solvent system has a significant impact on the phase behavior of the system, usually more so than the polymer structure. Alkane solvents are often used for polymers, and increasing alkane solvent size was found to improve polyethylene solubility, as this increases the molar mass and density of the solvent consequently decreasing respective differences between the polymer and solvent. Straight chained alkanes were found to be better solvents than branched alkanes, and cyclic alkane were found to be better solvents than straight chained alkanes due to increasing density, and thus decreasing density difference with respect to the polymer, from branched to straight chained to cyclic alkanes (Chen et al., 1992; de Loos et al., 1996; Haruki et al., 2009, 2010; Lee et al., 2005; Nagy et al., 2007; Pan et al., 1999). For solvent mixtures, increasing or decreasing the concentration of a compound will have an effect on the phase equilibrium of the system dependent on the change in overall density and/or molar mass of the solvent mixture. Components lighter than the main solvent will act as antisolvents decreasing polymer solubility, while denser and heavier compounds will act as cosolvents improving polymer solubility. For example, ethylene was handled in many of the studies, and was found to act as an antisolvent, as increasing ethylene concentrations in heavier alkane solvent systems decreased polymer solubility, and shifted cloud points to lower temperatures and higher pressures (Chen et al., 1992; Chen et al., 1999; Chen et al., 2004; de Loos et al., 1996, 2004; Dörr et al., 2001; Haruki et al., 2008, 2009, 2010; Lee et al., 2005; Nagy et al., 2006). The same effects were also observed for addition of inert compounds, such as nitrogen, to polymer – solvent systems, depending on their impact on the overall solvent density and/or molar mass (Dörr et al., 2001; ter Horst et al., 2002). However, inert compounds that were not

soluble in the solvent mixture were observed to increase vapor pressures relative to their concentration in the system, while inert compounds that were soluble in the solvent mixture did not have this effect.

## 4.5. Challenges in experimental cloud point measurements

The procedures and interpretations in cloud point measurements are far from simple and unambiguous. Klenin et al. (2013) discuss aspects of cloud point measurements in systems containing polymer and solvent, which is also referred to as a low molecular weight liquid. Forming of a second liquid phase in polymer – solvent systems is often evident as incipient and increasing turbidity in the system. The premise of the discussed cloud point measurement technique is based on assigning a preset turbidity level from an initial cloud point measurement to determine cloud points in subsequent measurements, i.e. the system is moved from a homogeneous single phase state towards a two-phase state, and the point (temperature/pressure) where the preset turbidity level is reached is accepted as the binodal point.

With decreasing temperature in systems with an UCST, or conversely with decreasing pressure in systems with a LCST (as is the case for the systems investigated in this work), the turbidity in polymer – solvent systems owing to concentration fluctuations increases to a maximum at the spinodal temperature (or pressure). However, as the concentration of the polymer gets more distant from its critical concentration, which is the point shared by the binodal and spinodal, the temperature or pressure range between the binodal and spinodal increases. According to the Klenin et al. (2013), increasing range between the binodal and spinodal also results in a reduction in the initial turbidity level at the binodal point, as the polymer concentration moves farther from its critical concentration, meaning the initial tubidity level of the system at the binodal temperature/pressure is dependent on the concentration of the polymer. Because of this phenomenon, fixing a preset turbidity level to determine binodal temperatures/pressures for a system leads to inconsistent measurement results.

The turbidity of a polymer – solvent system is told to consist of two main causes, namely molecular scattering and colloidal scattering. Colloidal scattering here means the formation of new particles, which was concluded to be dependent on many parameters beyond account and analysis. Aside from the usual turbidity dependencies, such as polymer morphology and concentration, turbidity formation due to colloidal scattering also depends on possible impurities in the system, the volume and shape of the vessel, possible shakings of the system, and influence of the vessel walls amongst others, which make this aspect impossible to estimate. This formation of new particles in the metastable region takes place after an induction period of unknown length, which depends on the location of the system state in the metastable region with respect to the binodal and spinodal; the closer to the spinodal the system is, the shorter the induction period. Near the binodal the induction period becomes theoretically infinitely long, and oppositely near the spinodal it approaches zero. Thus the implications of a sudden increase in turbidity cannot be ascertained, as it could be a result of molecular scattering when approaching the spinodal or the formation of new particles after the induction period at some unknown point in the metastable region between the binodal and spinodal. (Klenin et al., 2013)

Similarly as with the initial turbidity, the rate of turbidity formation is also believed to change with polymer concentration, decreasing when the polymer concentration moves farther away from its critical concentration, and the metastable gap between the binodal and spinodal becomes larger. This further complicates the procedure of defining a set level of turbidity as the binodal point, as this preset level could be well inside the metastable region as the polymer concentration moves further from its critical concentration. Additionally, as turbidity in the system caused by concentration fluctuations may at any time be supplemented by formation of particles of a new phase, it is impossible to know exactly what is being fixed when determining a preset turbidity level for cloud point measurements. (Klenin et al., 2013)

Turbidity levels of solutions containing high molecular weight compounds, such as polymers, exceed turbidity levels of lower molecular weight solutions. According to

Klenin et al. (2013) a preset turbidity level may be observed in a range of critical opalescence, a somewhat different phenomenon, even before the phase separation range. This also suggests that the initial turbidity of polymer – solvent systems at the binodal, or even before the binodal in a single phase state, may depend on the molecular weight along with concentration of the polymer.

Measurement difficulties due to polymer concentration were also reported for some experimental systems. de Loos et al. (1983) reported bad reproducibility in systems of polyethylene + ethylene with very low and very high weight fractions of polymer. Similar effects were also encountered by Trumpi et al. (2003) for polymer concentrations over 9.95 m-% and below 2.5 m-%. At high polymer concentrations mixing becomes less effective due to increased viscosity of the mixture resulting in slowing of mass transfer and phase separation along with possible concentration gradients in the system. In dilute systems so little of the second phase is initially formed at the cloud point that it is hard to detect. Additionally, cloud point pressures for dilute systems start rapidly dropping below polymer concentrations of 1 m-%, which further increases measurement uncertainty. Increasing uncertainty was also encountered by de Loos et al. (1983) in critical point measurements with increasing concentration and molar mass of the polymer, because determining the phase boundary position takes much longer in higher viscosity systems. Schnell et al. (2004) reported increased measurement uncertainties with lower molar mass polymers in polyethylene + *n*-hexane systems due to increased difficulty in determination of the cloud point.

Another issue in this type of cloud point measurements pointed out by Klenin et al (2013) is the actual visual observation of the cloud point, which is also a significant part of this work. The visual observation of the cloud point with certainty can be challenging, as observations can depend on the volume and shape of the vessel, the background color behind this vessel, room illumination, not to mention the psychological and ophthalmologic state of the observer himself. This leads to technical and procedural uncertanities in measurements, as observations can differ depending on the measurement procedure and equipment setup.

# 5. Equipment for phase equilibria measurements

In this section, examples will be presented of experimental equipment, which have been used for phase equilibria measurements of polymer containing systems. Experimental phase equilibria measurements are usually conducted with batch systems, where the polymer is measured into a high pressure chamber of some sort, and known amounts of solvent liquids and/or gases are added for a known total overall composition of the sample mixture. For reliable phase equilibria measurements for a certain mixture, the high pressure chamber must be completely sealed for a totally isolated system. Temperature of the chamber is then set and controlled with a temperature controlling device, such as an oven, an air/liquid bath, or a heating jacket for example. Pressure in the chamber is controlled with a pump and pressure transmitting medium (usually some type of liquid suitable for the experimental temperatures), and applied to the system for example by using some type of piston or metal bellows. The pressure system must also be sealed off from the chamber to avoid contaminants, and keep the composition inside the sample chamber constant and known.

Characteristics of the system being measured should be taken into account when planning experiments, and many of the experimental setups presented in this section have been specifically designed with a certain system in mind. For polymer – solvent systems required temperatures and pressures for phase change may be quite high depending on the system composition. Other characteristics include high viscosity or large viscosity difference between phases, especially at higher polymer concentrations, which could lead to slow mass transfer and present challenges with complete mixing of the system and achieving thermodynamic equilibrium. Many types of equipment have been designed and used for phase equilibria measurements of polymer – solvent systems, such as high pressure autoclaves and different types of variable volume cells. Phase changes in the systems have been observed visually or through the use of light transmission and scattering detectors. Most of the examples introduced here are equipment used in the studies presented before.

de Loos et al. (1983) conducted phase equilibria measurements for a PE + ethylene system in an optical high pressure cell, presented in Figure 30. The cell was designed for pressures up to 4000 bar and temperatures up to 450 K. The pressure cell J, equipped with a magnetic stirrer and temperature probe, is housed in a thermostated air bath L, and heated by external heating mantles $K_1$ and $K_2$. The investigated mixture is contained in a glass vessel, and separated from the pressure transmitting medium water by mercury. A pressure balance A is used to measure the pressure, and pressure is controlled either with a hand pump M or a high-pressure bench C, which is connected to the cell through a hydraulic oil-water separator H. The high-pressure bench C can be operated by hand or by the pressure balance A through switches $B_1$ and $B_2$, and small pressure changes can be applied with rotating pump G. Phase changes can be observed visually through a sapphire window.

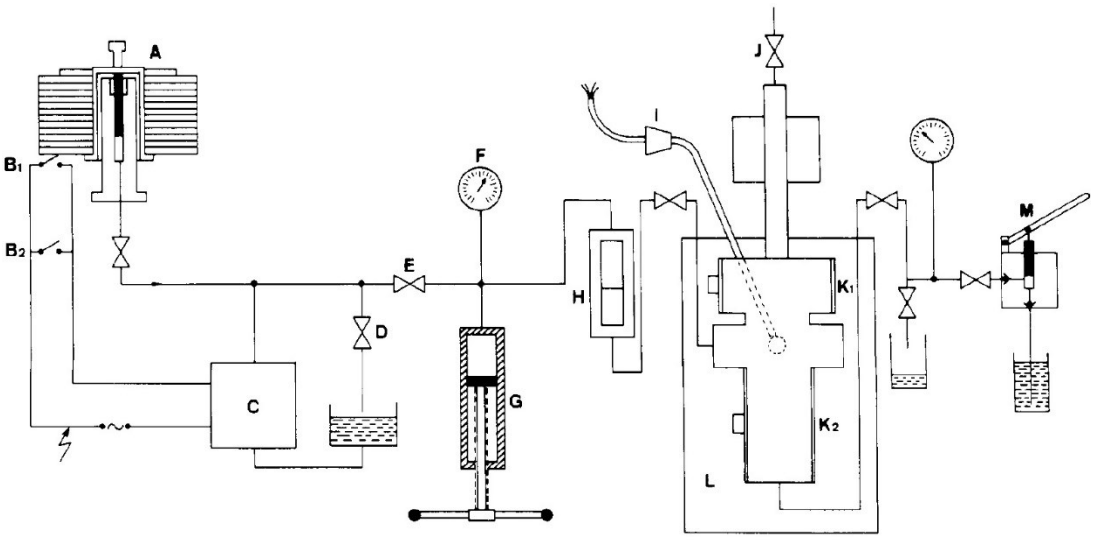


***Figure 30 Experimental setup used by de Loos et al. (1983). A, pressure balance; $B_i$, switches for high pressure bench control; C, high-pressure bench; D, pressure safety valve; E, hydraulic oil valve; F, manometer; G, rotating pump; H, oil-water separator; I, thermometer; J, pressure cell (inlet); $K_i$, heating mantles; L thermostated air bath; M, hand pump.***

A so-called Cailletet apparatus, presented in Figure 31, designed for pressures up to 20 MPa and temperature up to 473 K was used for phase equilibria measurements by de Loos et al. (1983). A sample of the mixture to measured M is confined over mercury in the sealed end of a thick walled capillary glass tube C, which is fitted to plug P of a stainless steel autoclave A at approximately 1/3 of its length, and the glass to steel interface is sealed with O-rings (Viton) R. The autoclave is filled with mercury, in which the open end of the capillary is immersed. The mercury serves as a pressure intermediate between the sample and hydraulic oil. A soft-iron rod sealed in glass, with a diameter slightly smaller than the capillary, is used as a stirrer by moving button magnets B up and down. Temperature is controlled by circulating thermostat liquid (e.g. oil) in the glass thermostat Th. Pressure is controlled with a screw pump H, and measured with a dead-weight pressure gauge L. Phase changes in the system can be observed visually. This type of setup was used in the measurements conducted by de Loos et al. (1996) and Nagy et al. (2006; 2007) for systems of LLDPE and alkane solvents.

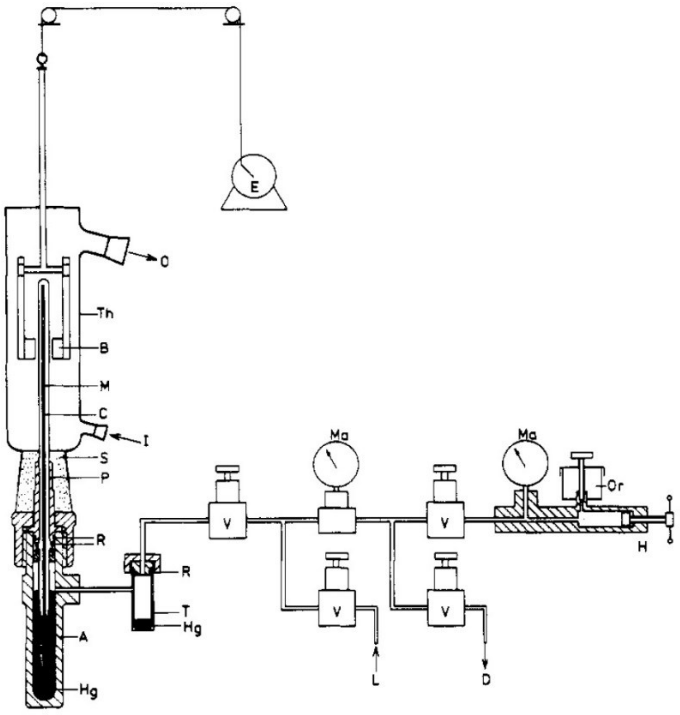


***Figure 31 The Cailletet apparatus used by de Loos et al. (1986). A, autoclave; B, button magnets; C, capillary glass tube; D, drain: H, rotating hand pump: Hg, mercury: I, thermostat liquid in; L, Yne to dead weight presswe gauge: M, mixture being investigated: Ma, manometers: 0, thermostat liquid out; Or, hydraulic oil reservoir; P, closing plug; R, Viton O-rings; S, silicone rubber stopper; T, mercury trap; Th, glass thermostat; V, valve.***

A thermo-optical apparatus, presented in Figure 32, was used for phase equilibria measurements by Bae et al. (1991). The apparatus consists of a polarizing microscope, a heating-cooling stage beneath the microscope lens, a photodiode to measure luminosity, and a microprocessor connected to a computer used for data acquisition. A small amount (around 0.02 ml) of sample is placed in a sealed cell inside the internal housing of the heating-cooling stage, and illuminated for the microscope by a light source. A temperature program is given to the microprocessor to apply a heating/cooling medium through the external housing of the heating-cooling stage for a controlled heating/cooling rate, and temperature is measured with a platinum resistance thermometer. The photodiode quantitatively measures the intensity of transmitted light as a function of temperature, which is recorded on the computer, and used to determine phase changes (cloud points) in the sample.

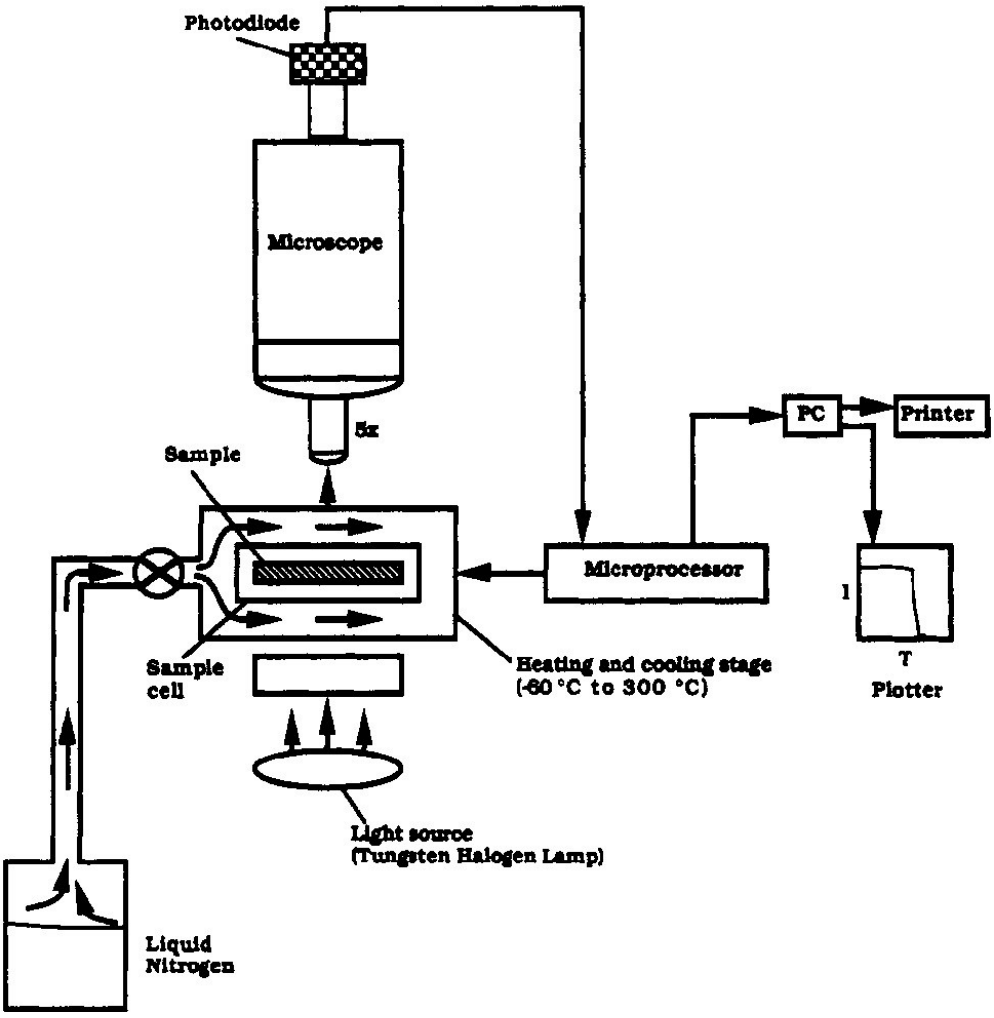


***Figure 32 The experimental setup used by Bae et al. (1991).***

Chen et al. (1992) used a batch optical cell, presented in Figure 33, for phase equilibria measurements of PEP – solvent systems. The investigated mixture is contained in a stainless steel cell (max. V ≈ 17 ml) sealed by two O-rings and designed for temperatures up to 200 $^{o}$C and pressures up to 550 bar. Temperature is set and controlled by an oven, and pressure is controlled with a movable piston inside the cell, variating volume and thus pressure. Pressure is measured with a pressure transducer and checked against a dial gauge calibrated against a dead weight. Three sampling lines are connected from the cell via a chromatographic valve and a polymer collection trap to a gas chromatograph (UTI) for gas composition analysis. Phase transitions (cloud points) can be observed visually through a sapphire window displayed on a screen by a borescope and a video camera.

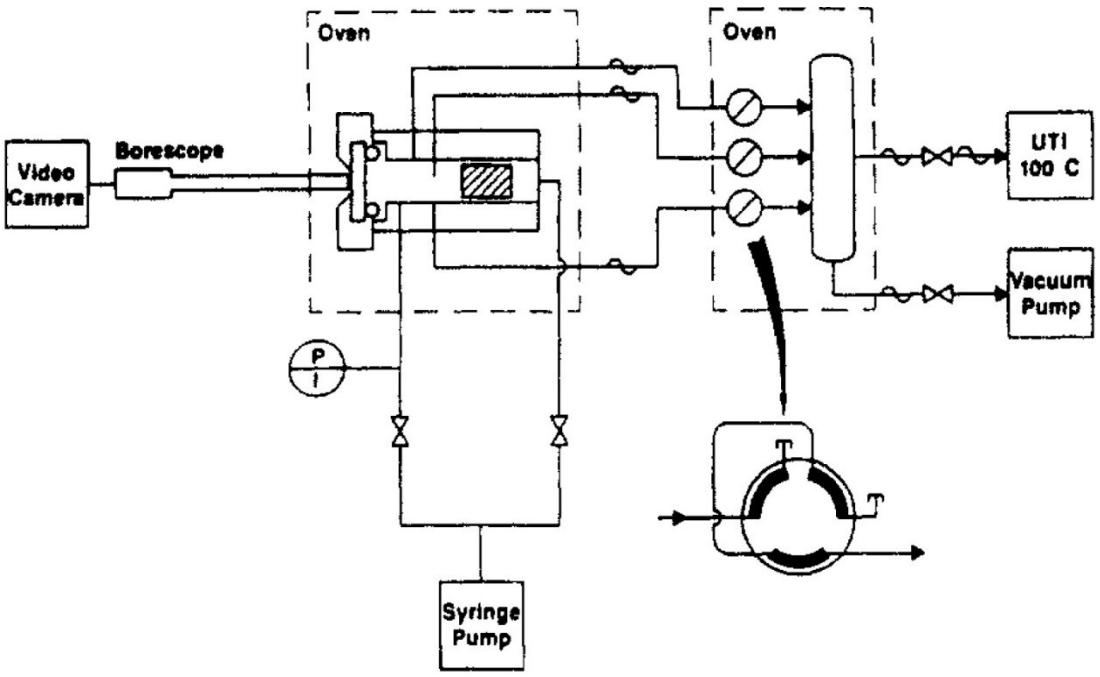


***Figure 33 The experimental setup used by Chen et al. (1992)***

A variable volume cell setup, presented in Figure 34, used for phase equilibria measurements of polymer containing systems is described in detail by Gregg et al. (1994). The cell itself, presented in Figure 35, was designed for pressures up to 2000 bar (hydrostatically tested up to 4000 bar). The cell was constructed mainly out of stainless steel, and equipped with a movable piston for pressure/volume control, inserts for pressure and temperature sensors, a sampling line, and a sapphire window for observation. Movement of the piston is controlled by a computerized pump, and the position of the piston can be tracked with a linear variable differential transformer (LVDT) positioned on the axle rod connected to the piston. Gas and solvent are loaded into the cell with a hand pump, and heating is provided by a heating jacket. Supercritical components are added from a gas cylinder contained in a hot box. Pressure measurements are checked with a dial gauge calibrated against a dead-weight tester. The sampling line leads to a sample trap, a sampling device and a wet test meter. Phase changes (cloud points) can be observed through the sapphire window and projected onto a monitor with a borescope and camera. A similar setup was used for the experiments conducted by Pan et al. (1999) for PE in solutions of isobutene and propane.

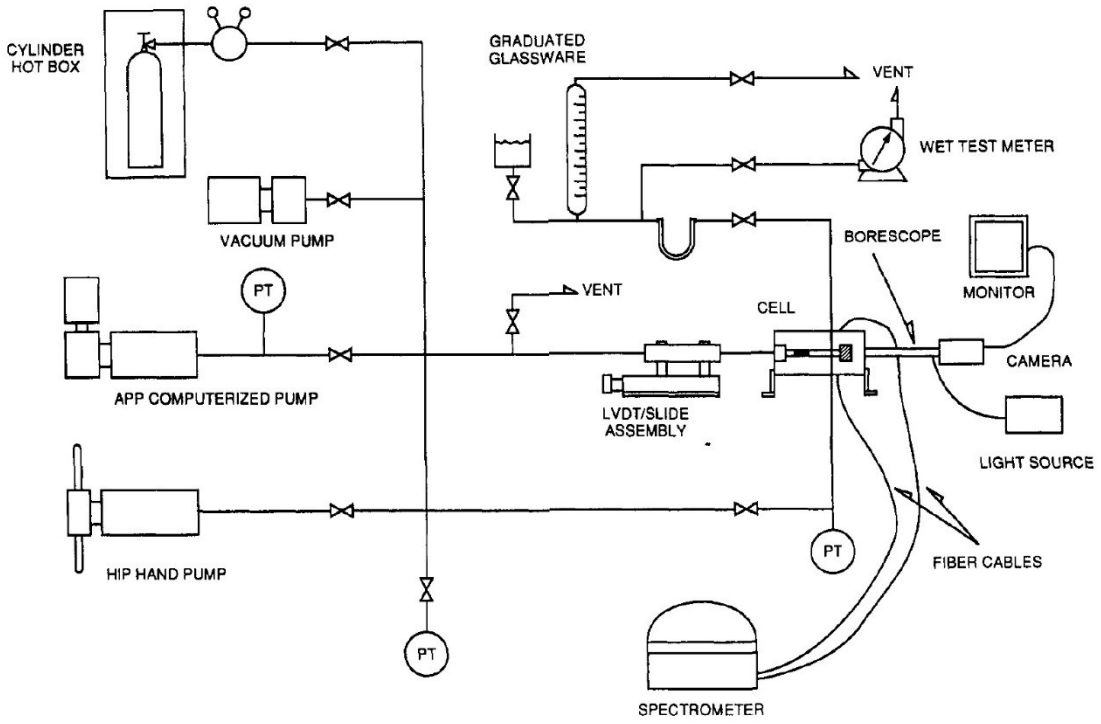


***Figure 34 The experimental setup used by Gregg et al. (1994)***

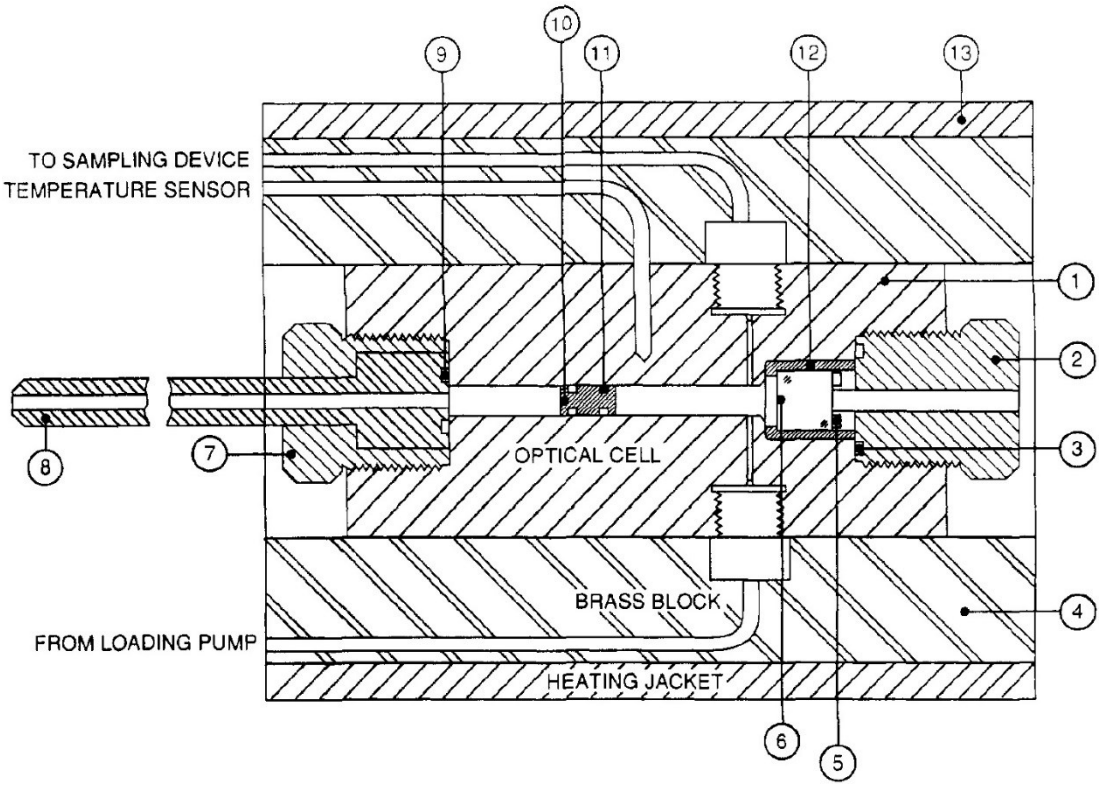


***Figure 35 Detailed schematic of the cell used by Gregg et al. (1994). (1) main body, (2) front gland nut, (3) Viton O-ring, (4) brass heating block, (5) Viton O-ring, (6) sapphire window, (7) rear gland nut, (8) tube gland, (9) Viton O-ring, (10) movable piston, (11) Viton O-ring, (12) brass window cap, (13) heating jacket.***

A high-pressure light scattering apparatus for phase equilibria measurements in polymer – solvent systems is described in detail by Xiong et al. (1998). The equipment, depicted in Figure 36, consists of a polymer loading chamber, a solvent charge line, a variable-volume scattering cell with a movable piston, and a recirculation pump. The equipment is housed in a temperature controlled oven, and pressure is controlled by either the moveable piston connected to a pressure generator, or an air-actuated moveable expansion rod assembly. A He-Ne laser beam is guided through the cell, and the transmitted and scattered light intensities at different angles are recorded with a computerized data acquisition system. Phase changes are observed by monitoring the recorded light intensities with respect to temperature and pressure. The system was designed for pressures up to 70 MPa and temperatures up to 473 K, and was used in the experiments conducted by Liu et al. (2001) for PE + *n*-pentane systems.

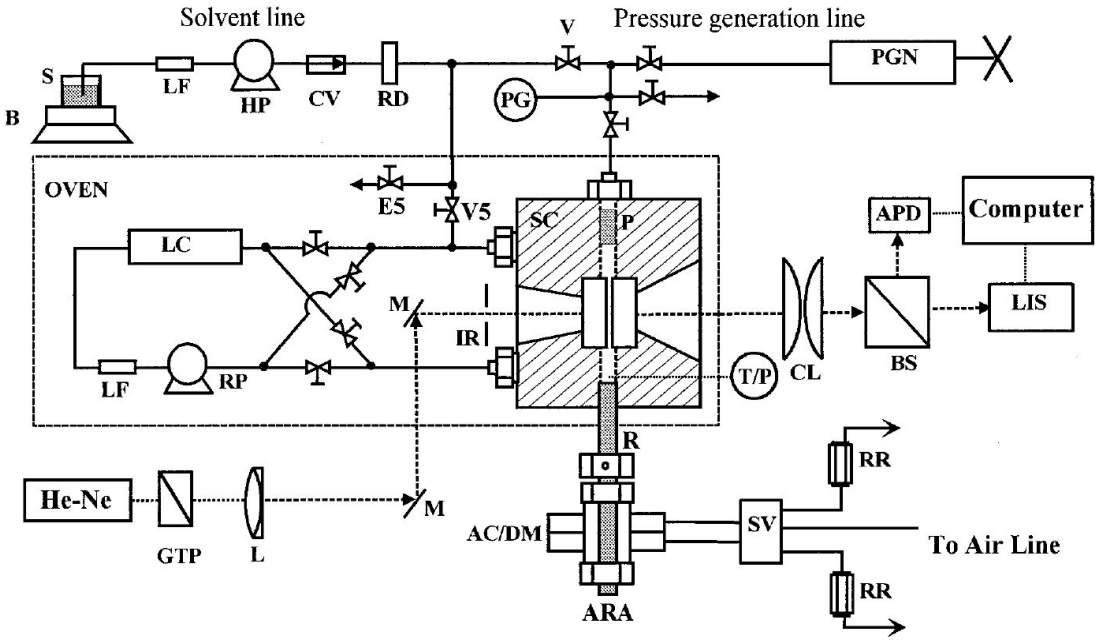


***Figure 36 Equipment setup of the high-pressure light scattering apparatus used by Xiong et al. (1998) AC/DM, air cylinder/diaphragm; ARA, air-actuated rod assembly; APD, avalanche photodiode; B, balance; BS, beam splitter; CL, condensing lens; CV, check valve; GTP, Glan–Thompson polarizer; HP, high pressure pump; IR, iris; L, focusing lens; LF, line filter; LIS, linear image sensor; M, mirror; LC, loading chamber; P, piston; PG, pressure gauge; PGN, pressure generator; R, movable rod; RR, release regulator; RD, rupture disk; RP, recirculation pump; S, solvent; SC, scattering cell; SV, solenoid valve; T/P, thermocouple/pressure transducer; V,V5, E5, valves; W, sapphire window.***

A temperature controlled high pressure autoclave used for phase equilibria measurements, shown in Figure 37, is described by Kinzl et al. (2001). Volume and pressure in the autoclave was varied with metal bellows connected to a pump for hydraulic oil, and tracked by a position transducer. The maximum volume of the inner chamber is approximately 19 ml. Phase changes in the system can be observed optically through sapphire windows. The equipment was designed for a maximum pressure of 250 MPa at a temperature of 513 K, and was used in the experiments conducted by Dörr et al. (2001) for the influence of inert gases in PE + 1-hexene + ethylene systems. A very similar autoclave setup, as described by Horst et al. (1998), was used by Schnell et al (2004) for phase equilibria measurements in PE + *n*-hexane systems.

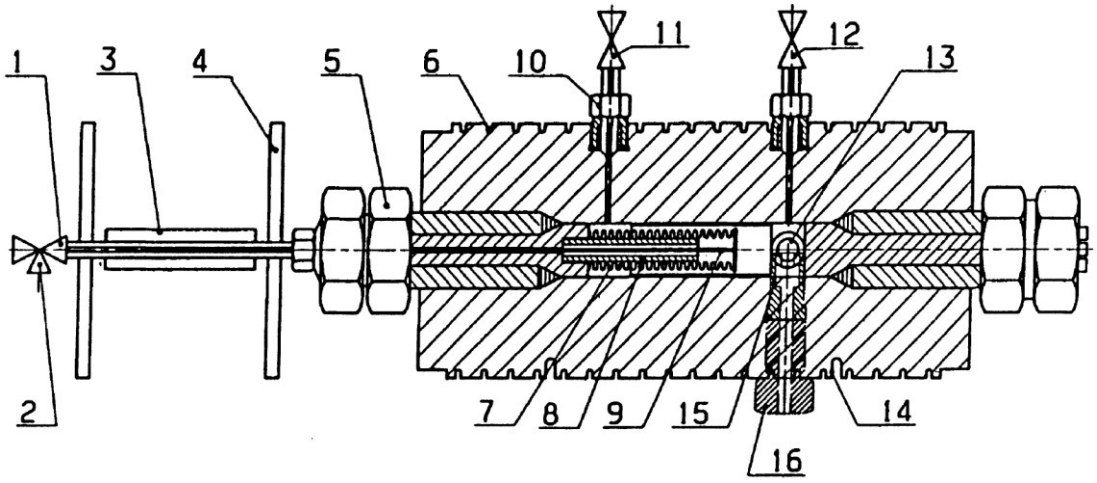


***Figure 37 The high pressure autoclave used by Kinzl et al. (2001). (1) Needle valve; (2) hydraulic oil inlet; (3) position transducer; (4) heat shield; (5) nut; (6) rabbet; (7,8) metal bellows; (9) metal stick; (10) high-pressure screwing; (11) ethylene inlet; (12) inert compound inlet; (13,15) sapphire window; (14) rabbet for thermocouple; (16) high-pressure screwing.***

Chan et al. (2000) used a high pressure cell with a moveable piston and a light scattering probe, presented in Figure 38, to measure phase equilibria in systems containing polyethylene. A hand pump and computer controlled pump are used to load the solvent as well as control the pressure of the cell by movement of the piston. Heating is provided by heating tape wrapped around a brass block and connected to a controller. The light-scattering probe consist of a He-Ne laser and two photodiode detectors to measure the intensity of transmitted and scattered light. Mass transfer inside the cell is promoted using a magnetic stirrer, and phase transitions can be detected with the light-scattering probe, or visually using a borescope.

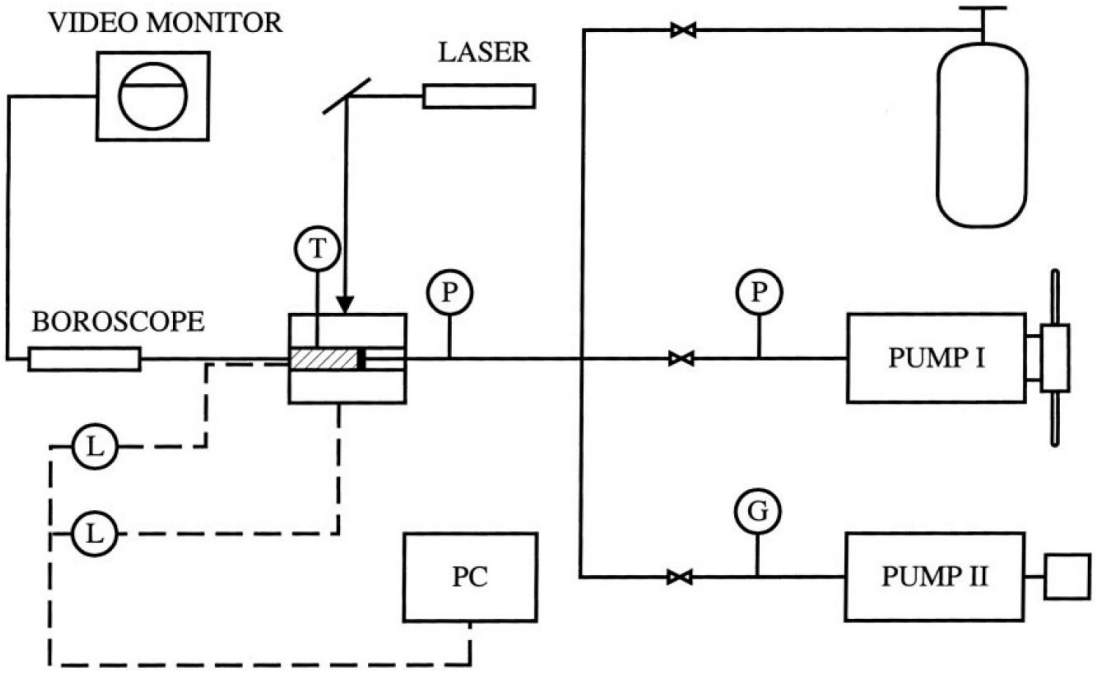


***Figure 38 The high pressure cell setup used by Chan et al. (2000). G, Pressure gauge; L, Photodiode; P, Pressure transducer; T, Temperature controller.***

An optical variable volume cell, shown in Figure 39, was used by Chen et al. (2004) for phase equilibria measurements in PE + *n*-hexane + ethylene systems. The cell was designed for pressures up to 20 MPa, and temperatures up to 473 K. Heating to the cell is provided with a heater jacket connected to a temperature controller, and pressure along with volume inside the cell is varied with a moveable piston. The cell has a maximum volume of approximately 20 ml, and the location of the piston is tracked using a linear variable differential transformer (LVDT) connected to the piston with a stainless steel rod. A Teflon-coated magnetic stirrer is used to promote mass transfer in the cell, and phase transitions can be observed with a charge-coupled device (CCD) camera. A very similar setup was used in all experiments by Haruki's group (Haruki et al., 2008; 2009; 2010) for phase equilibria measurements concerning the various polyethylene systems described before in the part referring to their work.

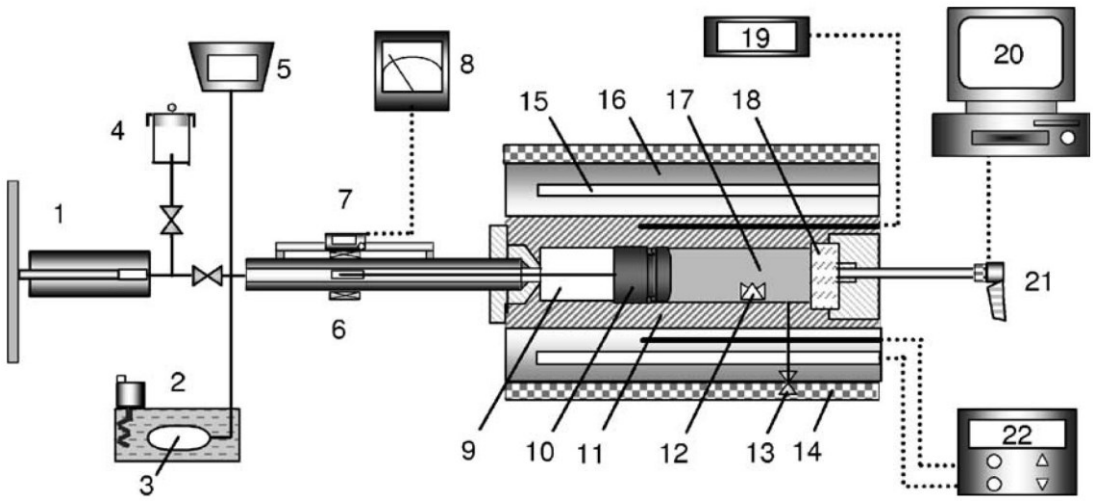


***Figure 39 Schematic of the optical cell used by Chen et al. (2004). (1) pressure generator; (2) thermostatic water bath; (3) pressure damper; (4) silicone oil reservoir; (5) pressure indicator; (6) LVDT; (7) linear scale; (8) displacement meter; (9) silicone oil; (10) piston; (11) view cell; (12) stirring bar; (13) injection port; (14) insulations; (15) heater; (16) aluminum block; (17) sample; (18) quartz window; (19) temperature indicator; (20) computer monitor; (21) CCD camera; (22) temperature controller.***

A high pressure variable volume cell was used by Lee et al. (2005) for phase equilibria measurements in mixtures of PE and hydrocarbons. The stainless steel cell is housed in a temperature controlled air bath, and pressure along with volume in the cell is varied with a moveable piston. A magnetic stirrer is used inside the cell to promote mass transfer, and phase transitions can be observed optically through a sapphire window with a camera. A schematic of the cell along with the equipment setup is presented in Figure 40.

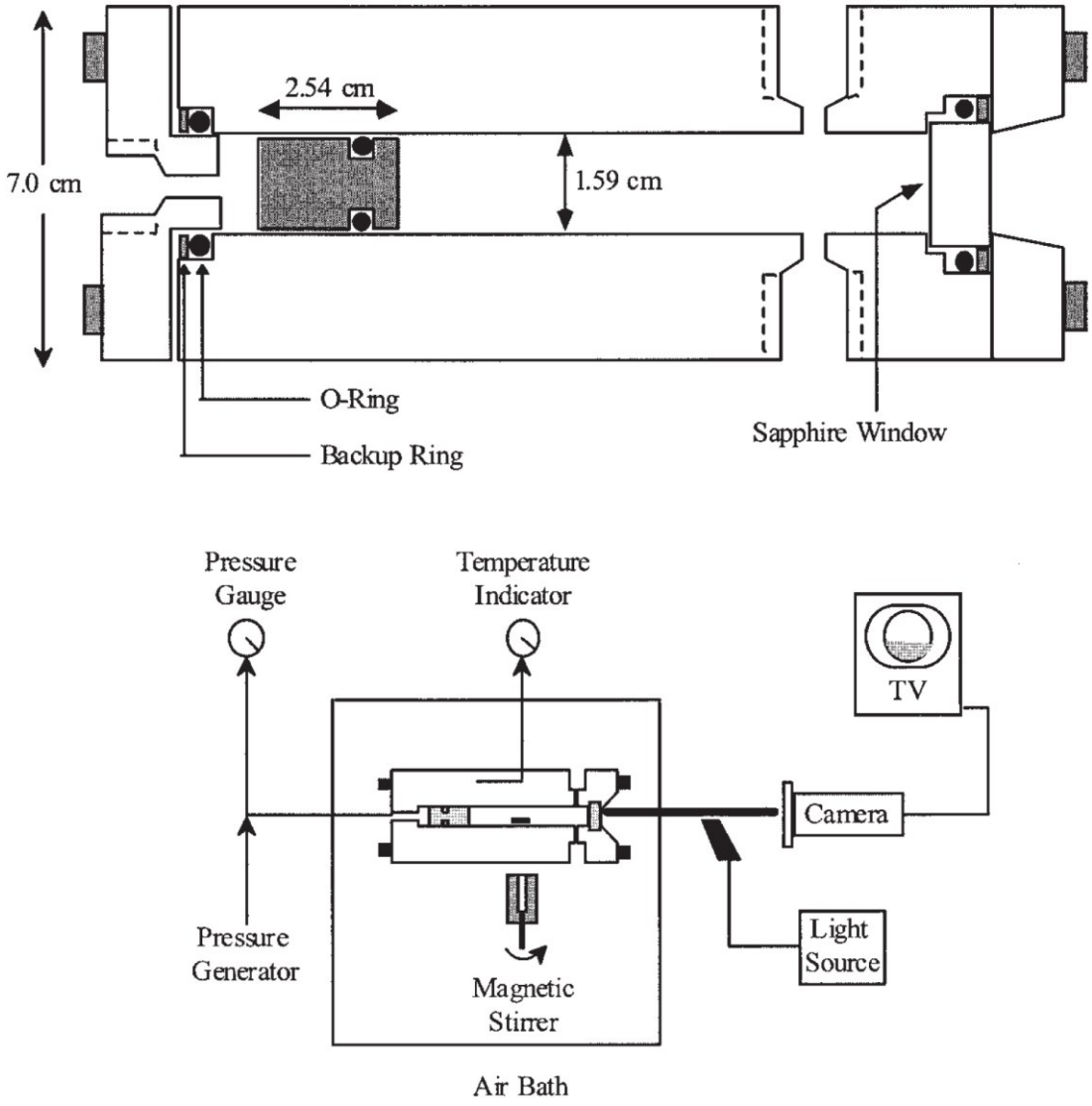


***Figure 40 Schematic of the high pressure variable volume cell and equipment setup used by Lee et al. (2005).***

A high pressures variable volume cell for phase equilibria measurements is described by Richon (2009). The cell, presented in Figure 41, has a moveable piston to control volume and pressure inside the cell. Movement of the piston is controlled with a pump and pressurizing liquid. A schematic of the equipment setup is presented in Figure 42. The cell is housed in a thermostated air bath, and equipped with a magnetic stirring device. The cell is connected to external piston position measurement and interface level measurement devices, as well as a vacuum pump and a pump for the pressurizing liquid.

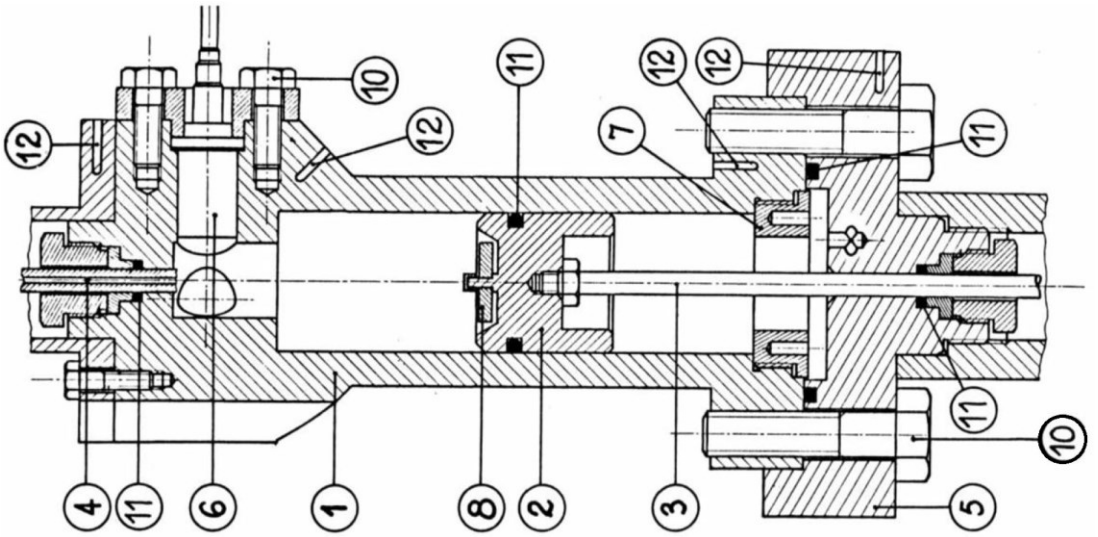


***Figure 41 Schematic of the variable volume cell described by Richon (2009). (1) cell body; (2) piston; (3) probe for piston level measurements; (4) thermistor probe for vapor–liquid interface level measurements; (5) pressurizing assembly; (6) membrane pressure transducer; (7) stop screw; (8) magnetic rod; (10) bolts; (11) viton O-ring; (12): thermocouple well.***

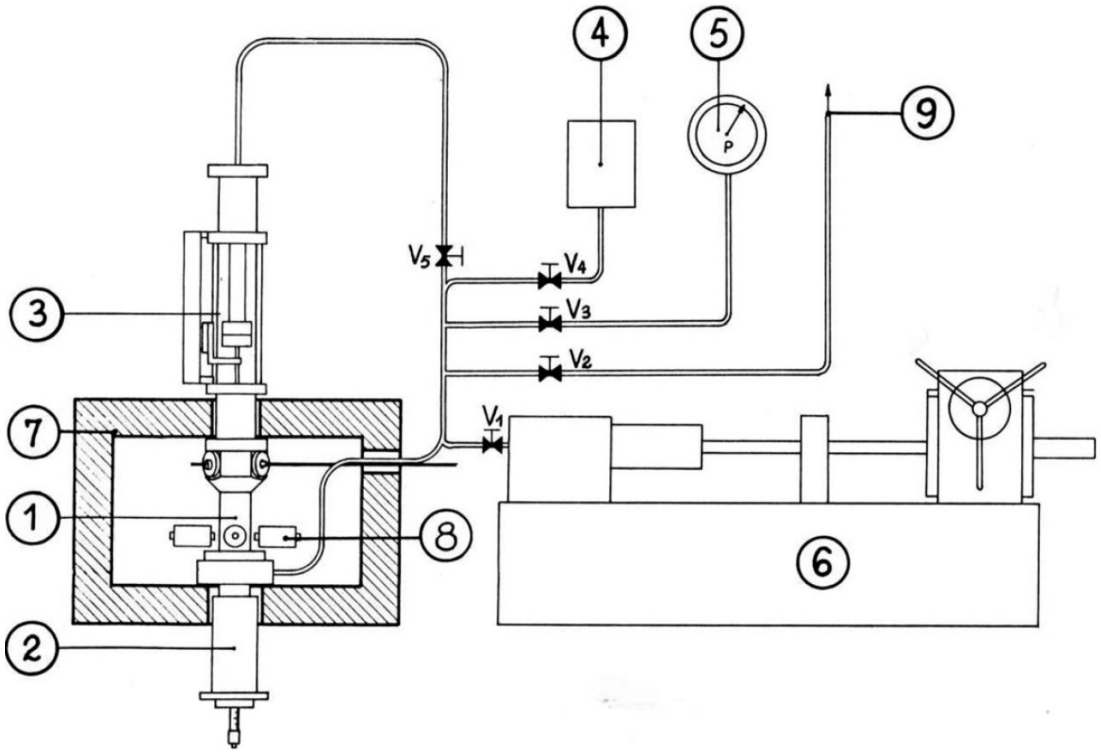


***Figure 42 Schematic of the variable volume cell equipment setup described by Richon (2009). (1) equilibrium cell; (2) assembly for piston-level measurements; (3) assembly for interface-level measurements; (4) pressurizing liquid reservoir; (5) manometer; (6) high-pressure pump; (7) air thermostat; (8) solenoids to create a rotating magnetic field; (9) fitting to vacuum pump; (vi) shut-off valves.***

# 6. Experimental

The goal of the experiments was to observe and record cloud points in systems containing linear low-density polyethylene (LLDPE) mixed with a solvent. The experiments were conducted for varying system compositions in a pressure and temperature controlled variable volume cell. This section will cover the materials, equipment, and procedures used in the experiments.

## 6.1. Materials

All chemicals that could be obtained in liquid form at room temperature and atmospheric pressure (*n*-hexane, iso-hexane, 1-octene, iso-octane) were acquired from Sigma-Aldrich Co. at greater than 99 % purity. Gas pressure cylinders of chemicals that are gaseous at room temperature and normal pressure (ethylene, *n*-butane, 1-butene, nitrogen) were acquired from AGA AB at greater than 99 % purity. LLDPE for the experiments was provided by an industrial source.

## 6.2. Experimental apparatus

The experiments in this work were conducted with a variable volume cell, which is schematically presented in Figure 43. The cell consists of a thick walled sapphire tube with specifically crafted titanium blocks at either end, referred to as “ends” of the cell from here on out. Titanium was selected due to its very similar thermal expansion as the sapphire tube. The sapphire tube is sealed at both ends with O-rings in O-ring grooves. The volume, and thus pressure of the cell is controlled with a moveable piston, and the piston also houses a magnet for operation of a magnetic

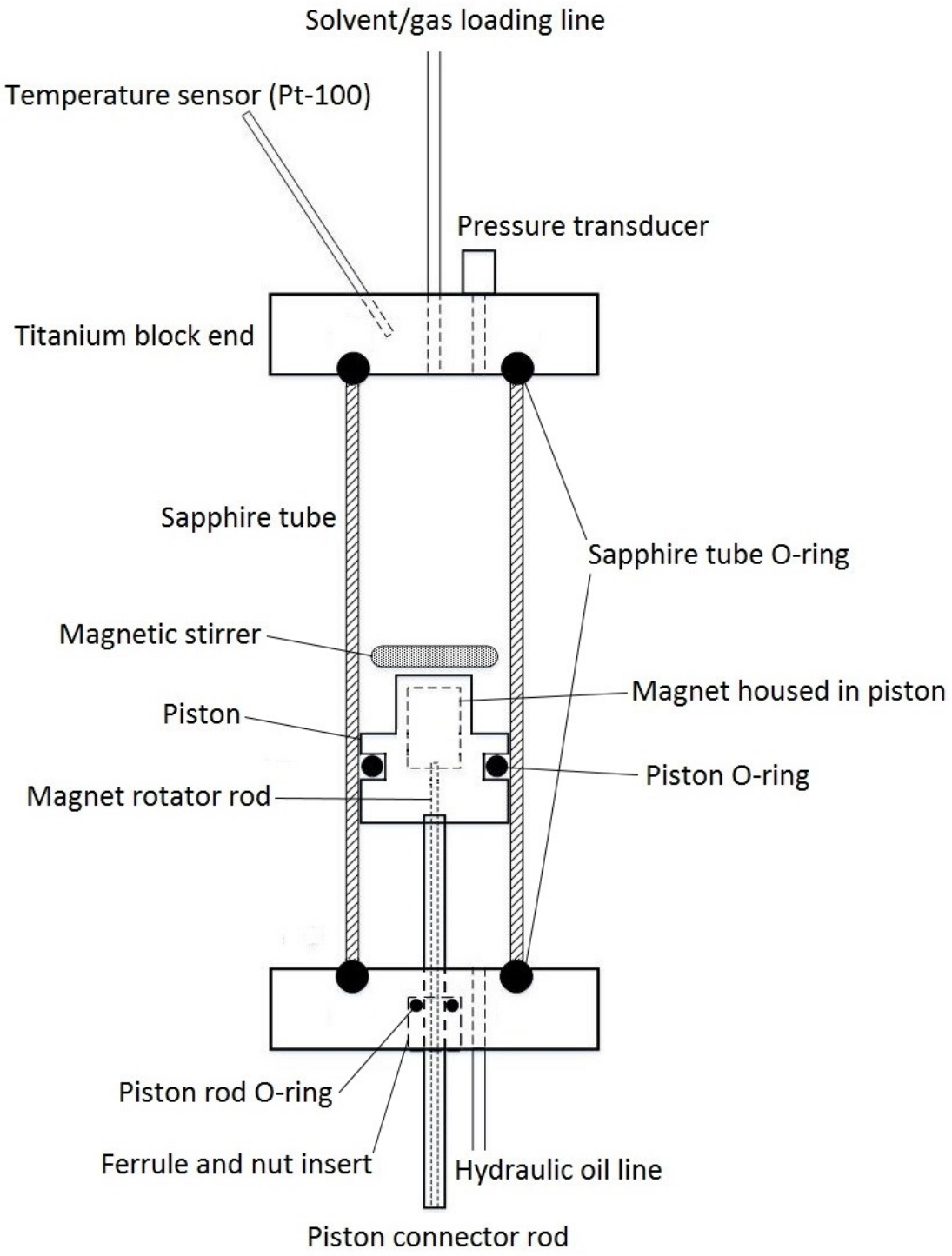


***Figure 43 Schematic of the variable volume cell used in the experiments.***

stirrer inside the cell. The magnet housing is connected to an electric motor (Bevi motor with Invertek Drives IP66 inverter) with a thin steel rod, which is housed inside a hollow steel rod connected to the piston, in order not to have rotation of the piston while operating the magnetic stirrer. The piston is sealed with an O-ring to separate

the pressurizing part of the cell below the piston from the actual sample part of the cell located above the piston. The connection of the steel rod through the bottom titanium end of the cell is also sealed with an O-ring setup, where the O-ring is kept in its groove around the rod with a special metallic ferrule and a nut. In addition to the stirrer/piston rod inlet, the bottom titanium end has an inlet with a valve for the pressurizing medium. Hydraulic oil was used as the pressurizing medium in this work. The maximum volume of the cell, when the piston is at its lowest position, is approximately 9,1 ml.

In addition to the cell, the experimental setup consisted of cell loading and pressurizing equipment, shown in Figure 44. The cell is housed inside a temperature controlled oven with an observation window, while other components are located outside the oven at room temperature. Pressure inside the cell during experiments is applied by moving the piston to change the volume, and hence the pressure, in a sealed system. The movement of the piston is controlled with hydraulic oil applied by a rotating hand pump with an oil reservoir, a pressure gauge, and a spring loaded safety valve (set to 100 bar). The top titanium end of the cell has an inlet with a needle valve for evacuation and solvent loading. The top end also has inserts for a temperature sensor (Pt-100) and a pressure transducer (Kulite Semiconductor XTEH). The transducer was calibrated using a MC2 Beamex calibration device that had been calibrated at the National Centre for Metrology and Accreditation in Finland (MIKES). Calibration data for the pressure transducer is provided in Appendix 1. The Pt-100 temperature sensor used in the experiments was also calibrated at MIKES. A vacuum pump is connected to both ends of the cell for evacuation. The equipment setup is very similar to that of Richon (2009), presented in Figure 42.

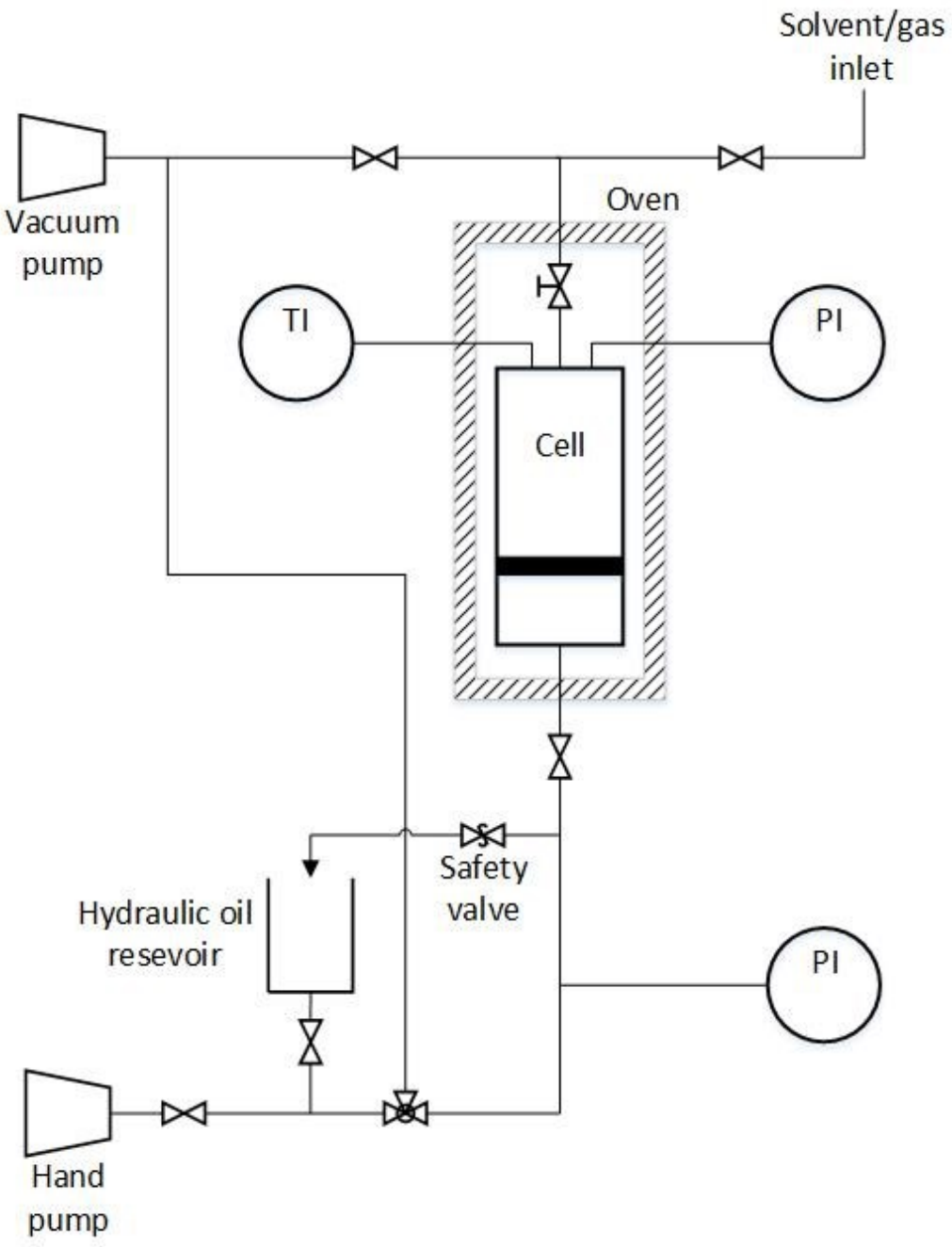


***Figure 44 Schematic of the equipment setup used in the experiments.***

## 6.3. Experimental procedure

Two types of systems were measured in the experiments. Binary systems were composed of polyethylene and n-hexane (purity > 99 %), and multicomponent systems contained the polymer, monomer (ethylene), co-monomer (1-octene or 1-

butene), and a solvent comprised of hexane isomers (mostly *n*-hexane) called hexane-cut or C6-cut. The loading of the sample mixture into the cell was done on the basis of mass fractions. Mass fractions presented in this work are simply the mass of the component divided by the total mass of the system. A Mettler Toledo XP2004S precision scale (accuracy 0.0001 g) was used for all mass measurements in this work.

Firstly, polymer pellets were weighed and inserted into the cell. Amounts of other components in the system were calculated on the basis of the polymer sample to achieve a certain overall composition with respect to mass fractions. Hexane-cut solvent along with other liquid components (1-octene, iso-octane), if included in the system to be investigated, were weighed and mixed in a round bottom flask in order to achieve the desired liquid mixture composition. The liquid mixture was degassed by ultrasound, and the flask was evacuated with a vacuum pump. The degassing and evacuation was performed in an ice bath in order to prevent the solvent mixture from evaporating. A sample of this liquid mixture was taken for analysis by gas chromatography to confirm the liquid mixture composition after degassing. The cell was sealed and evacuated with the vacuum pump. An appropriate amount of the liquid solvent mixture was weighed into the cell to achieve the desired overall composition. Lastly, calculated amounts of gas components, if included in the system to be investigated, were weighed into the cell through the top valve.

The cell was heated to the desired temperature under mixing, and left for at least 30 min to achieve thermodynamic equilibrium. Bubble point vapor pressure was usually recorded at this point, and all vapor pressures measured for the mixtures in this work are bubble point pressures. As some settling time was required for achieving thermodynamic equilibrium at each measurement, vapor pressures were not recorded at all the measurement points due to time constraints, and the system was desired to be kept in a liquid or liquid-liquid state throughout most of the measurements. After the initial vapor pressure measurement, the mixture was observed visually through a window in the oven. If only a single clear liquid phase was observed, the temperature was raised, and the mixture was again left for at least 30 min under mixing to achieve equilibrium. If the liquid was visually cloudy, implying a

second liquid phase, the pressure was raised until only a single homogeneous clear liquid phase again existed, and the mixture was again left for at least 30 min to achieve equilibrium. The pressure was then slowly lowered until the formation of a second liquid phase was visually observed as incipient and increasing turbidity in the liquid. The point where the first visually observable turbidity in the liquid appeared, was recorded as the cloud point. This observation was confirmed by further lowering the pressure, and observing increasing turbidity with decreasing pressure after this point. A new temperature was then set, and the measurement procedure was repeated. If possible, measurements were repeated for the same sample batch on consecutive days to ensure reproducibility of the results. All observations of phase changes in this work were done visually.

In some experiments a second, more abrupt change in the liquid was observed after the initial cloud point observation. Turbidity in the liquid would slowly increase with decreasing pressure after the observed cloud point, until a point where the liquid would abruptly start getting significantly more turbid. However, what exactly these points represent cannot be determined, as discussed by Klenin et al. (2013). These points, with sudden increases in turbidity formation, were recorded as secondary points, and can be found with the full results in Appendix 2.

Complete mixing of the system was determined to be imperative for achieving equilibrium in the system, as especially with higher polymer concentrations the mixture was quite viscous. To assure complete mixing the amount of sample was matched with the stirrer height. The height of the sample in the cell was calculated beforehand for every experiment from the overall system composition and component masses using approximate component densities and volume of the cell. The amount of sample was adjusted to match or just slightly exceed the height of the stirrer at the lowest temperature of the measurement range.

## 6.4. Challenges encountered in the experiments

Several challenges were encountered while conducting the experiments. Proper sealing of the cell during measurements proved to be a considerable issue, as pressure leakage due to O-ring failure was experienced several times during the experiments. Different O-ring compounds were experimented with, and finally Kalrez O-rings were used with the piston and shaft, while the top and bottom of the sapphire tube were sealed with measurement specifically machined graphite Teflon O-rings. These graphite Teflon O-rings were crushed upon sealing, and had to be replaced after one or two sets of measurements. The sealing of the piston rod was found to be most challenging, as the pressure and heat along with the movement of the rod forced the O-ring to extrude out of its groove and shear against the edge of the metal ferrule keeping it in place. The ferrule was redesigned to reduce shearing, and an expanding lead washer was added to keep the O-ring from extruding.

Another challenge during experiments was experienced with mixing. Proper mixing was considered essential for achieving thermodynamic equilibrium, and increasing viscosity in the systems caused the mixing to become less effective resulting in possible concentration gradients inside the cell. If the system was not completely mixed, a lower viscosity phase could start forming at the top of the cell, and this phase would be very hard to mix into the lower phase, as mass transfer at the phase interface was presumably very slow. The magnetic stirrer was redesigned several times to be more efficient, and achieve both radial and axial mixing throughout the sample mixture in the cell. The amount of sample mixture in the cell was calculated beforehand, and measured accordingly to roughly match the height of the stirrer at the lowest measurement temperature, in order to assure complete mixing of the system.

The biggest source of uncertainty in the measurements was observation accuracy of the cloud points, as observations were done purely visually. As pointed out by Klenin et al. (2013), visual observations can depend on the volume and shape of the vessel, the background color behind this vessel, and room illumination, along with human

errors made by the operator. The observation window and lighting of the cell were adjusted, as best seen fit under the circumstances of these experiments, and were kept the same throughout the experiments in order to keep measurement results coherent.

# 7. Experimental results

Measurements were conducted with six different types of industrial LLDPE, designated PE-1, PE-2, PE-3, PE-4, PE-5, and PE-6 in this work. PE-1 was used as a trial polymer, in order to investigate the different phenomena related to the experiments. Measurements were conducted in binary systems containing only the polymer and *n*-hexane, as well as more complex multicomponent systems. Experiments with PE-1 were conducted in binary mixtures with *n*-hexane, as well as multicomponent mixtures with the hexane-cut solvent, ethylene monomer, 1-octene comonomer, and iso-octane. PE-2 was investigated in binary mixtures with *n*-hexane, while PE-3, PE-4, PE-5, and PE-6 were investigated in multicomponent mixtures with the hexane-cut solvent, ethylene monomer, 1-butene comonomer, and butane. The multicomponent systems were measured to investigate phase behavior of simplified mixtures of solution polymerization, where the different compounds in the system were meant to emulate the different parts of the polymerization mixture.

Uncertainty in the experiments comes from mass measurements when loading the cell, temperature and pressure measurements, and visual observation accuracy of the cloud points. The accuracy of the scale used when loading the cell is 0.0001 g, but with such accuracy the scale measurements took some time to stabilize, and the final digit would often change slightly back and forth over a range of approximately 0.0005 – 0.0010 g. The uncertainty for the mass measurements could thus be evaluated as ± 0.001 g. Mass fraction uncertainty is presumably larger in the multicomponent systems, as more mass measurements needed to be made for these systems. Mass fraction uncertainty for a single experiment can be calculated by multiplying the mass

measurement uncertainty (0.001 g) by the number of components (number of mass measurements), and then dividing by the total mass of the system (the sum of masses of the components). Temperatures were recorded with 0.1 $^{o}$C accuracy. However, the temperature measurement probe is actually situated inside the top titanium end, and not in the cell itself. When warming the cell, temperature inside the cell lagged slightly behind the temperature of the titanium end shown in the measurement. This was another reason to let the cell properly stabilize in the measurement temperature in order to eliminate possible temperature differences between the inside of the cell and the titanium end measured by the sensor. Temperature measurement uncertainty was estimated to be approximately ± 0.5 $^{o}$C. Pressure measurements were recorded at 0.01 bar accuracy. Some uncertainty results from having to apply a correction to the pressure measurement dependent on the measurement temperature. Pressure measurement uncertainty was estimated to be approximately ± 0.05 bar. The biggest source of uncertainty in the measurements was the observation accuracy of the cloud points. The clarity of cloud point observations varied between experiments, and was usually approximately ± 1 - 1.5 bar. The maximum uncertainty of observations was evaluated to be approximately ± 2 bar, and this value was regarded as the uncertainty estimate. These uncertainties apply to all measurements. Error bars for measurement uncertainties are given in P-X diagrams presented below, but not in P-T diagrams, as the resolution in P-T diagrams is large in relation to the magnitude of uncertainties of P and T measurements.

The gathered data was examined for abnormal behavior by observing the trends in the measurement results. Any non-reproducible, irregular, or otherwise clearly erroneous data were regarded as unreliable, and omitted from the results analysis. Also all results from failed measurements, such as pressure leakage from the cell or clearly apparent contaminants in the system, were also disregarded when examining results. This section will cover results from successfully conducted experiments. All measured values are given with measurement accuracy. Full measurement results with tables and figures for each successful measurement instance are available in a supplementary file Appendix 2.

## 7.1. Mixing time experiments

Different mixing times were investigated using polymer PE-1 in binary systems with *n*-hexane. These measurements were done to investigate how long it takes for the system to achieve thermodynamic equilibrium, and if longer mixing times at constant temperature would have an impact on the cloud point measurement. Bubble point vapor pressures and cloud points were first measured normally after 30 min mixing times, and the system was then left under mixing at the same temperature in a homogeneous state (high pressure). The next cloud point measurements were done after 4 hours of mixing. In a following experiment, measurements were taken after 4 hours and an additional 6 hours (10 hours total time), and in a final measurement the system was left under mixing for 12 hours without interruption.

The first two measurements with 4 hours mixing time were conducted with the same batch, and the latter two measurements with 10 hours and 12 hours mixing time were done with a similar batch. The measurement results are given in Tables 1, 2, 3, and 4.

***Table 1 Results for the first mixing time measurements in a binary PE-1 + n-hexane system containing 20.8 m-% polymer.***

| mixing time | T (°C) | p,vapor (bar) | p,cloud (bar) |
|---|---|---|---|
| 0.5 h | 186.7 | 14.35 | 34.35 |
| 4 h | 186.7 | | 34.24 |

***Table 2 Results for the second mixing time measurements in a binary PE-1 + n-hexane system containing 20.8 m-% polymer.***

| mixing time | T (°C) | p, vapor (bar) | p,cloud (bar) |
|---|---|---|---|
| 0.5 h | 186.7 | 14.44 | 35.35 |
| 4 h | 186.7 | | 35.23 |

***Table 3 Results for the third mixing time measurements in a binary PE-1 + n-hexane system containing 19.7 m-% polymer.***

| mixing time | T (°C) | p, vapor (bar) | p,cloud (bar) |
|---|---|---|---|
| 0,5 h | 186.0 | 16.50 | 37.26 |
| 4 h | 186.0 | | 37.18 |
| 10 (4+6) h | 186.0 | | 37.41 |

***Table 4 Results for the fourth mixing time measurements in a binary PE-1 + n-hexane system containing 19.7 m-% polymer.***

| mixing time | T (°C) | p,cloud (bar) |
|---|---|---|
| 0,5 h | 186.0 | 36.40 |
| 12 h | 186.0 | 36.63 |

When observing the results from the first batch, it can be seen in both measurements that cloud point pressures after 4 h mixing time are within 0.12 bar from the pressures measured after 0.5 h mixing time. Pressures observed in the second measurement also match the pressures observed in the first measurement. The third and fourth measurements, with up to 12 h mixing time, show the same trend, as the cloud point pressure observed after 12 h of mixing differs only 0.23 bar from the pressure measured after 0.5 h of mixing. This would suggest that 0.5 h of mixing time is sufficient in the experiments, and longer mixing times are not needed. The composition of the batches was slightly different, but taking this into account, measurements from both batches are roughly equivalent, and measurements for this experiment were well reproducible.

## 7.2. Measurements in binary systems

### 7.2.1. Measurements with PE-1

Cloud point measurements were carried out for several batches of binary PE-1 + *n*-hexane systems at 10.2 m-% and 19.7 m-% polymer concentration. Two sets of

these measurements are presented below in Table 5 and 6, and Figure 45. The full measurement results can be found in Appendix 2.

***Table 5 Measurement results for the binary PE-1 + n-hexane system containing 10.2 m-% polymer.***

| T (°C) | p, vapor (bar) | p,cloud (bar) |
|---|---|---|
| 170.8 | 11.12 | 25.23 |
| 186.8 | 14.65 | 46.98 |
| 191.9 | | 53.08 |
| 196.9 | | 60.34 |
| 200.8 | | 65.46 |
| 211.8 | | 79.12 |
| 221.8 | | 90.38 |
| 229.9 | | 99.04 |

***Table 6 Measurement results for the binary PE-1 + n-hexane system containing 19.7 m-% polymer.***

| T (°C) | p, vapor (bar) | p,cloud (bar) |
|---|---|---|
| 171.0 | 13.40 | |
| 181.0 | | 26.97 |
| 191.2 | | 42.27 |
| 201.2 | | 53.54 |
| 211.0 | | 67.44 |
| 221.3 | | 78.98 |

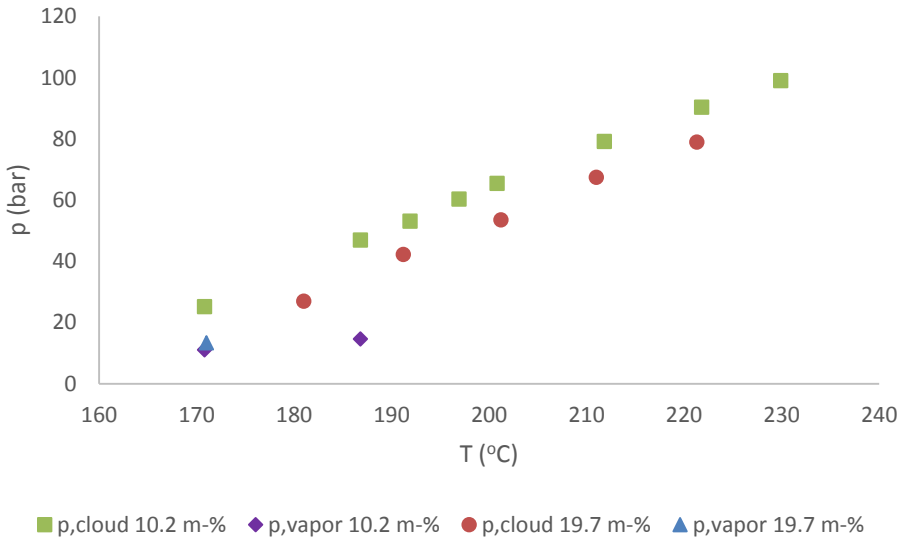


***Figure 45 Measured vapor pressures and cloud points for the 10.2 m-% and 19.7 m-% PE-1 + n-hexane systems.***

LCST type phase behavior can be observed in the binary PE-1 + *n*-hexane mixtures in the measured temperature range. Increasing polymer concentration shifts cloud points to lower pressures and higher temperatures. A very slight increase is seen in the vapor pressure for the higher polymer concentration. Comparison of measurements was also done by gathering results by temperature. Cases for such measurements at approximately 190 °C and 210 °C are presented in Tables 7 and 8, and Figure 46. The rest of the results can be found in Appendix 2.

***Table 7 Vapor pressure and cloud point measurements for binary PE-1 + n-hexane systems at approximately 190 °C. Uncertainties for pressure p(u) = ±2 bar, and polymer mass fraction c(u) = ±0.00103.***

| T (°C) | p, vapor (bar) | p,cloud (bar) | PE-1 mass fraction |
|---|---|---|---|
| 190 | 15.66 | 40.20 | 0.2127 |
| 189.5 | | 38.57 | 0.2011 |
| 191.7 | | 52.69 | 0.1000 |
| 191.9 | | 53.30 | 0.1000 |
| 191.9 | | 53.08 | 0.1023 |
| 190.2 | | 51.53 | 0.1023 |
| 190.3 | | 39.03 | 0.1952 |
| 191.2 | | 42.27 | 0.1969 |
| 190.6 | | 42.17 | 0.1969 |

***Table 8 Vapor pressure and cloud point measurements for binary PE-1 + n-hexane systems at approximately 210 °C. Uncertainties for pressure measurements p(u) = ±2 bar, and polymer mass fractions c(u) = ±0.001032.***

| T (°C) | p, vapor (bar) | p,cloud (bar) | PE-1 mass fraction |
|---|---|---|---|
| 211.0 | 22.52 | 68.32 | 0.2131 |
| 211.0 | 21.93 | 66.49 | 0.2127 |
| 210.3 | | 66.82 | 0.2011 |
| 211.7 | 21.62 | 77.37 | 0.1000 |
| 211.8 | 21.69 | 77.46 | 0.1000 |
| 211.8 | | 79.12 | 0.1023 |
| 210.2 | | 76.55 | 0.1023 |
| 211.0 | | 67.44 | 0.1969 |
| 210.5 | | 67.49 | 0.1969 |

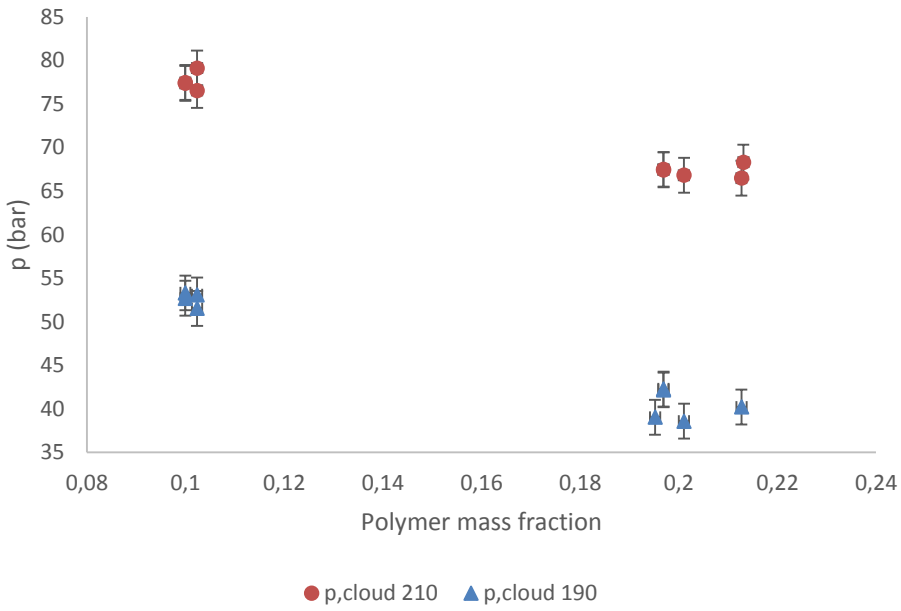


***Figure 46 Cloud point measurements for binary PE-1 + n-hexane systems at approximately 190 °C and 210 °C.***

Some variance can be seen in these results. Some of this is caused by slight temperature differences in the measurements, as actual measurement temperatures are not exactly equal. Part of the variance is also inevitably caused by measurement and observation inaccuracy. Polymer mass fraction uncertainties were calculated as described at the beginning of part 7. However, measurements of cloud point

pressures for both temperatures and concentrations are still closely grouped within 4 bar of each other even with slight measurement temperature differences, and decreasing cloud point pressure with increasing polymer concentration is clearly evident. Within experimental uncertainty and taking into account the slight temperature differences, the results appear coherent and well reproducible.

### 7.2.2. Measurements with PE-2

Larger polymer concentrations, and effects of increased viscosity of the mixture were measured in binary systems of PE-2 + *n*-hexane. Polymer concentrations of 19.7 m-% and 36.6 m-% were used in the experiments. Results for example instances of these measurements are presented in Table 9 and 10 and Figure 47. Full measurement results can be found in Appendix 2.

***Table 9 Measurement results for the binary PE-2 + n-hexane system containing 19.7 m-% polymer.***

| T (°C) | p, vapor (bar) | p,cloud (bar) |
|---|---|---|
| 181.1 | 13.57 | 21.68 |
| 191.1 | 15.74 | 36.18 |
| 201.1 | 18.41 | 49.59 |
| 211.1 | 21.42 | 61.97 |
| 221.2 | 24.81 | 73.73 |

***Table 10 Measurement results for the binary PE-2 + n-hexane system containing 36.6 m-% polymer.***

| T (°C) | p, vapor (bar) | p,cloud (bar) |
|---|---|---|
| 220.4 | 25.08 | 45.18 |
| 210.6 | | 31.74 |
| 200.6 | 18.53 | 19.67 |

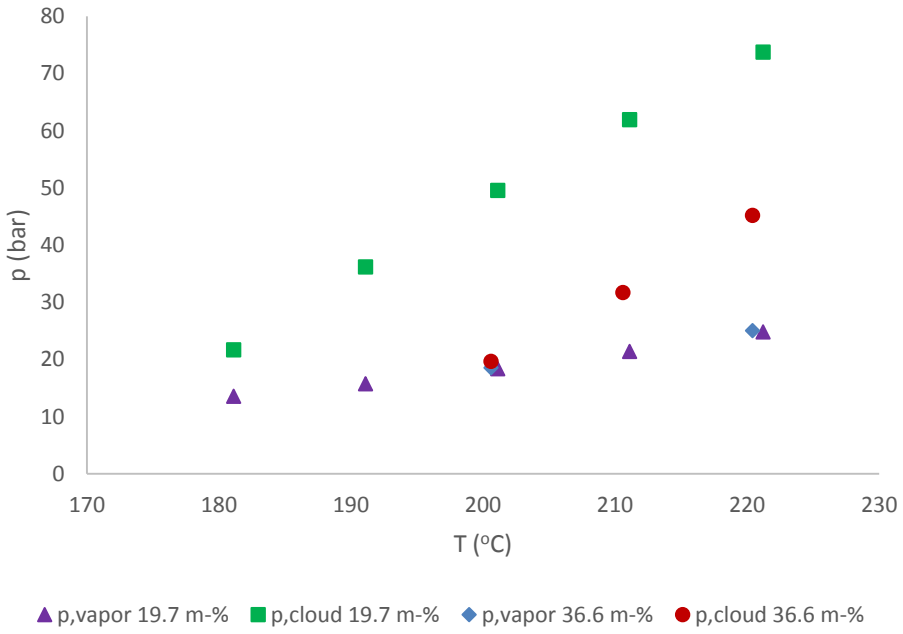


***Figure 47 Measured vapor pressures and cloud points for the 19.7 m-% and 36.6 m-% PE-2 + n-hexane systems.***

The same observations can be made here as for the binary mixtures with PE-1. The system has LCST type behavior, and cloud point pressures decrease with increasing polymer concentration. The 19.7 m-% systems of PE-1 and PE-2 (measurements in Table 6 and 9 respectively) can also be compared, which is presented in Figure 48.

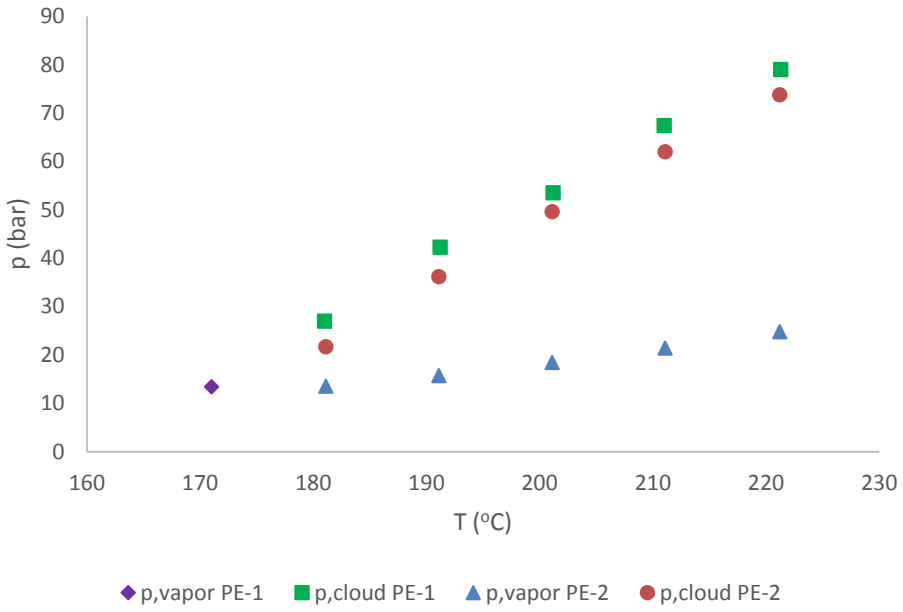


***Figure 48 Measured vapor pressures and cloud points for the 19.7 m-% PE-1 + n-hexane and PE-2 + n-hexane systems.***

By comparing the two LLDPE polymer types it can be seen that cloud point pressures for PE-1 are slightly higher than cloud point pressures for PE-2. This would suggest some difference between the polymers, such as slightly higher molar mass or density for PE-1, which would affect cloud point pressures.

Measurements for binary PE-2 + *n*-hexane systems were also gathered by measurement temperature. Measurement results for two example instances at approximately 200 °C and 220 °C are presented in Tables 11 and 12, and Figure 49.

***Table 11 Vapor pressure and cloud point measurements for binary PE-2 + n-hexane systems at approximately 200 °C. Uncertainties for pressure p(u) = ±2 bar, and polymer mass fraction c(u) = ±0.000928.***

| T (°C) | p, vapor (bar) | p,cloud (bar) | PE-2 mass fraction |
|---|---|---|---|
| 200.4 | 18.45 | 21.55 | 0.3663 |
| 200.6 | 18.53 | 19.67 | 0.3663 |
| 201.2 | 18.69 | 20.70 | 0.3831 |
| 201.1 | 18.39 | 25.78 | 0.3652 |
| 201.1 | | 50.99 | 0.1966 |
| 201.1 | 18.41 | 49.59 | 0.1966 |

***Table 12 Vapor pressure and cloud point measurements for binary PE-2 + n-hexane systems at approximately 220 °C. Uncertainties for pressure p(u) = ± 2bar, and polymer mass fraction c(u) = ±0.000938.***

| T (°C) | p, vapor (bar) | p,cloud (bar) | PE-2 mass fraction |
|---|---|---|---|
| 220.4 | 24.70 | 46.97 | 0.3663 |
| 220.4 | 25.08 | 45.18 | 0.3663 |
| 221.2 | 24.77 | 42.64 | 0.3831 |
| 221.2 | 24.74 | 75.11 | 0.1966 |
| 221.2 | 24.81 | 73.73 | 0.1966 |

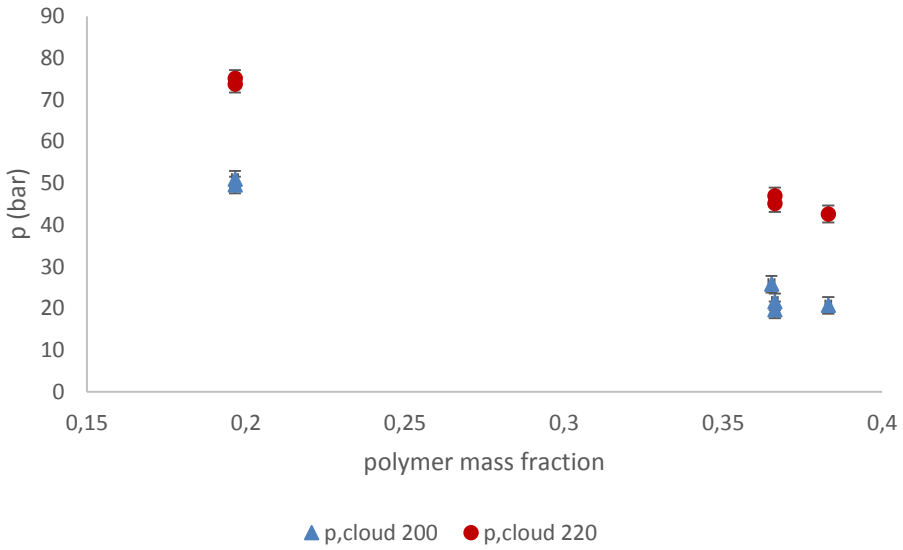


***Figure 49 Cloud point measurements for binary PE-2 + n-hexane systems at approximately 200 °C and 220 °C.***

Slight variance in measurement temperatures again affects the measurement results. Additionally, cloud points for the higher polymer concentrations measured in these experiments were hard to detect. Unlike systems with lower polymer concentrations, the mixture seemed to be initially slightly turbid already in the single phase region, and was never fully transparent. Because of this, the first changes in turbidity were difficult to observe. This difference was apparent even between the 19.7 m-% and 36.6 m-% systems presented here. Observation accuracy is assumed to be a large cause of measurement variance in these particular measurements. However, taking into account the slight temperature differences and measurement inaccuracies, the results appear coherent and reproducible, as measured cloud points for both temperatures and concentrations are closely grouped within 5 bar of each other.

As the properties of the polymers are unknown, accurate quantitative comparison to literature data cannot be done. However, measurement results of both polymers PE-1 and PE-2 are in qualitative agreement with binary PE + hexane systems (Chen et al., 2004; Haruki et al., 2008; Nagy et al., 2006) presented in the literature review part.

## 7.3. Measurements in multicomponent systems

### 7.3.1. Measurements with PE-1

Measurements were carried out with the polymer PE-1 in multicomponent systems containing the hexane-cut solvent, ethylene monomer, 1-octene comonomer, and iso-octane. The mixture was meant to emulate properties of a solution polymerization mixture. In a final experiment a small amount of nitrogen was added to the mixture to investigate its impact on the system. The amount of nitrogen was measured as a difference in the mass of the cell before and after the addition of nitrogen. Polymer mass fractions from approximately 15 m-% to 23 m-% were considered. Measurement results for example instances are presented in Tables 13 and 14, and Figure 50. Full measurement results can be found in Appendix 2.

***Table 13 Measurement results for the PE-1 multicomponent system containing 15.6 m-% polymer and 0.8 m-% ethylene.***

| T (°C) | p, vapor (bar) | p,cloud (bar) |
|---|---|---|
| 190.6 | | 33.75 |
| 200.9 | 20.83 | 46.38 |
| 210.9 | | 59.63 |
| 221.1 | | 70.25 |
| 230.1 | 28.62 | 79.64 |

***Table 14 Measurement results for the PE-1 multicomponent system containing 23.2 m-% polymer and 0.8 m-% ethylene.***

| T (°C) | p, vapor (bar) | p,cloud (bar) |
|---|---|---|
| 190.6 | 16.58 | 27.16 |
| 200.2 | | 39.44 |
| 210.8 | | 51.85 |
| 220.6 | | 63.17 |
| 230.9 | 29.92 | |

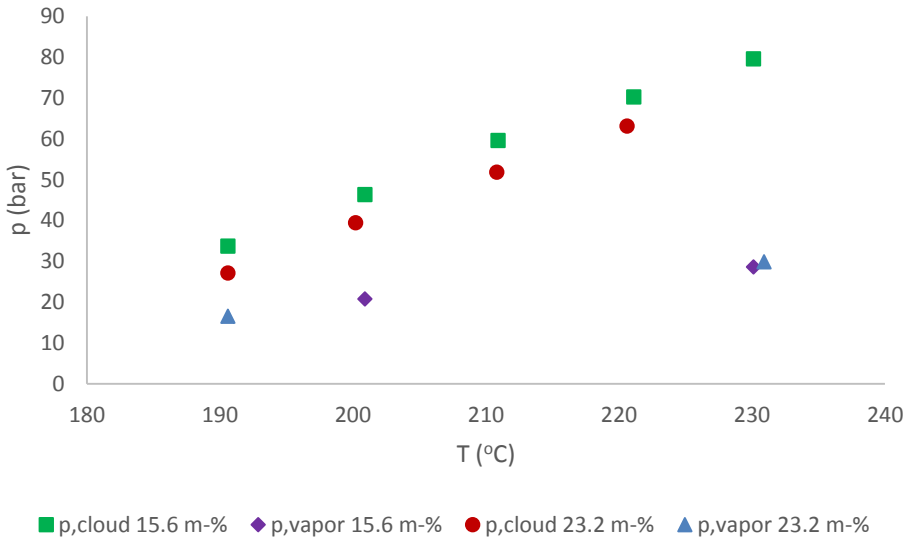


***Figure 50 Measured vapor pressures and cloud points for the 15.6 m-% and 23.2 m-% PE-1 multicomponent systems.***

LCST type behavior was also observed in the multicomponent system in the measured temperature range, and cloud point pressures decrease with increasing polymer concentration. The composition of the 15.6 m-% system is close to the composition of the system containing nitrogen, and the systems can be compared to investigate the impact of nitrogen. The measurement results for the nitrogen containing system are presented in Table 15, and comparison of the systems is presented in Figure 51.

***Table 15 Measurement results for the PE-1 multicomponent system containing 16.1 m-% polymer, 0.6 m-% ethylene, and 0.2 m-% nitrogen.***

| T (°C) | p, vapor (bar) | p,cloud (bar) |
|---|---|---|
| 171.9 | 16.62 | |
| 186.0 | 20.94 | |
| 191.1 | | 40.21 |
| 201.0 | | 53.70 |
| 211.0 | | 66.20 |
| 221.0 | 29.61 | 77.15 |

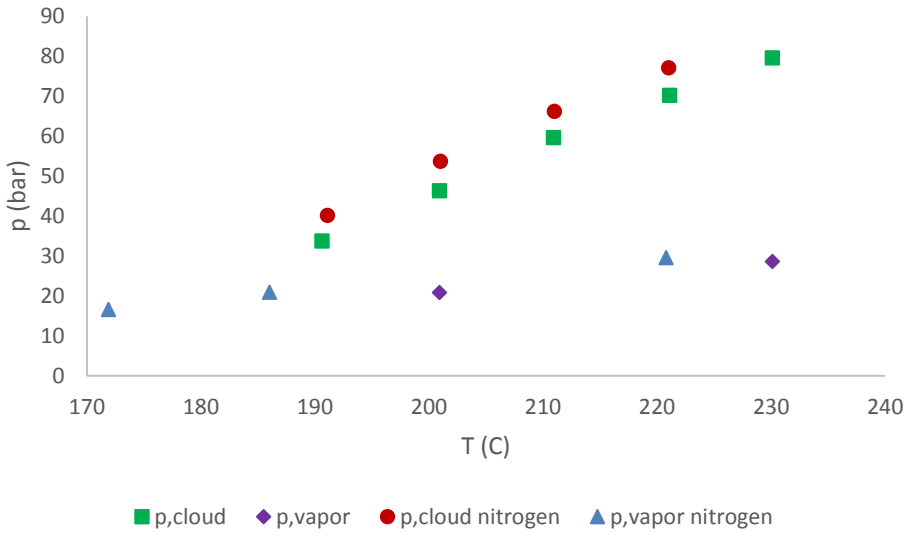


***Figure 51 Measured vapor pressures and cloud points for the approximately 16 m-% PE-1 multicomponent systems with and without nitrogen.***

It can be observed from the measurement results, that adding nitrogen to the system increases both cloud point pressures and vapor pressures. This is in agreement with the observations made by Dörr et al. (2001) and ter Horst et al. (2002) regarding the addition of nitrogen or other inert low solubility compounds to polymer – solvent systems.

Measurements for multicomponent systems with varying polymer concentrations were also gathered by measurement temperature. Measurements from the system containing nitrogen were not considered here, as the system and its behavior is somewhat different, and not exactly comparable to the other PE-1 multicomponent systems in terms of pressure and polymer concentration alone. Measurements at approximately 210 °C and 220 °C are presented in Tables 16 and 17, and Figure 52.

***Table 16 Vapor pressure and cloud point measurements for PE-1 multicomponent systems at approximately 210 °C. Uncertainties for pressure p(u) = ±2 bar, and polymer mass fraction c(u) = ±0.003956.***

| T (°C) | p, vapor (bar) | p,cloud (bar) | PE-1 mass fraction |
|---|---|---|---|
| 210.5 | | 56.23 | 0.1909 |
| 210.5 | 24.68 | 55.16 | 0.1909 |
| 211.3 | | 58.27 | 0.1557 |
| 210.9 | 23.29 | 59.63 | 0.1557 |
| 210.8 | | 51.85 | 0.2321 |

***Table 17 Vapor pressure and cloud point measurements for PE-1 multicomponent systems at approximately 220 °C. Uncertainties for pressure p(u) = ±2 bar, and polymer mass fraction c(u) = ±0.003956.***

| T (°C) | p, vapor (bar) | p,cloud (bar) | PE-1 mass fraction |
|---|---|---|---|
| 220.8 | | 68.48 | 0.1909 |
| 220.9 | | 67.46 | 0.1909 |
| 221.4 | 25.50 | 70.02 | 0.1557 |
| 221.1 | | 70.25 | 0.1557 |
| 220.6 | | 63.17 | 0.2321 |

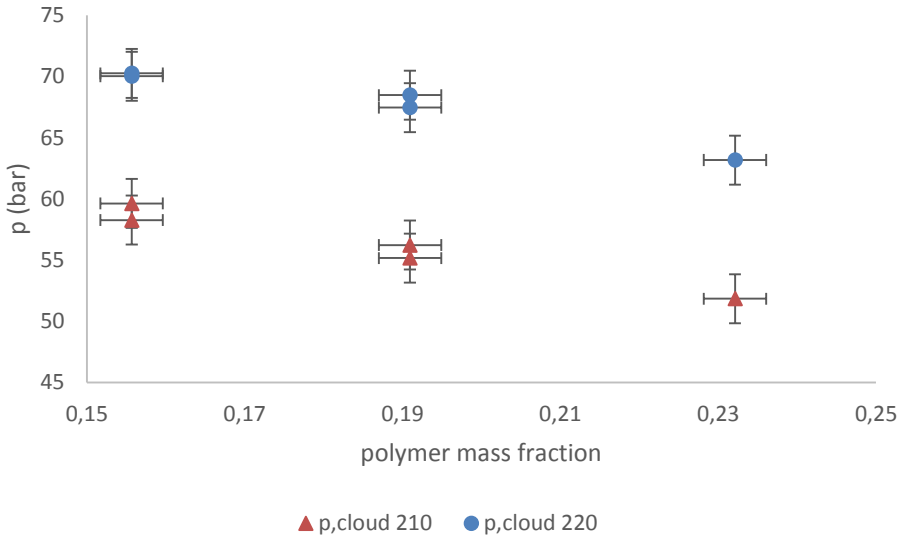


***Figure 52 Cloud point measurements for PE-1 multicomponent systems at approximately 210 °C and 220 °C.***

The results exhibit slight variance similarly as corresponding results from binary systems. This could again be caused by the reasons explained before, such as temperature variation and measurement inaccuracies, but with multicomponent systems also the composition of the mixtures (aside from the polymer) is not identical in all measurements. This variation of mixture composition affects the properties and phase behavior of the systems, and thus makes exact comparison of cloud point pressures at a given temperature difficult. Also composition uncertainty is larger for multicomponent systems, resulting from mass measurement uncertainties when weighing components into the cell. Clear trends can, however, be again seen in Figure 52, which are consistent with the behavior of such polymer – solvent systems. The

results appear coherent and reproducible, as measured pressures for similar system compositions are within 2 bar of each other.

### 7.3.2. Measurements with PE-3

Two measurements were performed for polymer PE-3 in multicomponent systems with approximately 17.7 m-% and 17.4 m-% polymer concentrations. Measurements were not collected by temperature, as there are only two measurement instances for PE-3. Measurement results for the two systems are presented in Tables 18 and 19, and Figure 53.

***Table 18 Measurement results for PE-3 multicomponent system containing 17.7 m-% polymer and 2.3 m-% ethylene.***

| T (°C) | p, vapor (bar) | p,cloud (bar) |
|---|---|---|
| 170.8 | 31.53 | 49.39 |
| 180.7 | | 64.32 |
| 190.6 | | 78.08 |
| 200.6 | 36.32 | 91.68 |

***Table 19 Measurement results for PE-3 multicomponent system containing 17.4 m-% polymer and 3.5 m-% ethylene.***

| T (°C) | p, vapor (bar) | p,cloud (bar) |
|---|---|---|
| 130.4 | | 46.80 |
| 140.3 | | 60.35 |
| 150.4 | 25.32 | 71.11 |
| 160.6 | | 81.19 |
| 170.5 | | 94.51 |

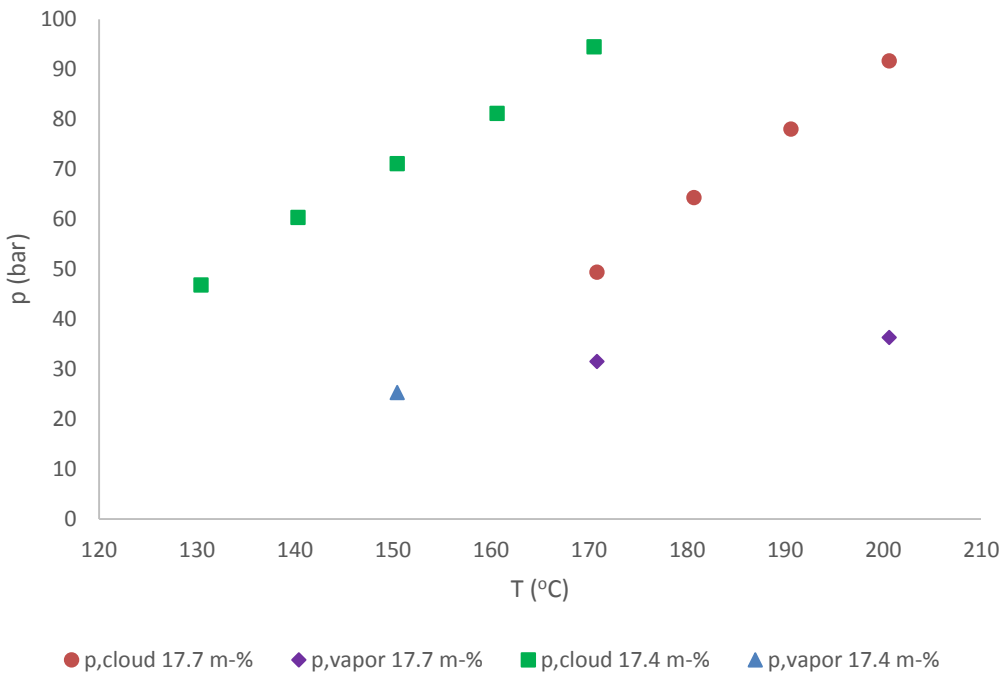


***Figure 53 Measured vapor pressures and cloud points for the 17.7 m-% and 17.4 m-% PE-3 multicomponent systems.***

Measurement results clearly show a considerable difference in cloud point pressures between the measurements, even though the polymer concentration in both is roughly the same. This could be due to a difference in the overall composition of the systems, as system the 17.4 m-% system has a larger concentration of ethylene. This results in an increased difference in size and density between the polymer and solvent mixture, and reduces solubility of the polymer shifting cloud points to higher pressures and lower temperatures. The large difference in cloud points could also be due to an unknown contaminant in the cell affecting the measurements. Vapor pressures of both the systems, however, are consistent with each other and vapor pressures of similar systems.

### 7.3.3. Measurements with PE-4

Two separate batches were measured with polymer PE-4 in multicomponent systems considering polymer concentrations 17.9 m-% and 18.9 m-%. Measurement results for the systems are presented in Tables 20 and 21, and Figure 54.

***Table 20 Measurement results for the PE-4 multicomponent system containing 18.9 m-% polymer and 2.3 m-% ethylene.***

| T (°C) | p,vapor | p,cloud |
|---|---|---|
| 130.2 | | 58.69 |
| 140.2 | | 68.55 |
| 150.2 | | 80.98 |
| 160.1 | 57.71 | 93.27 |

***Table 21 Measurement results for the PE-4 multicomponent system containing 17.9 m-% polymer and 3.6 m-% ethylene.***

| T (°C) | p,vapor | p,cloud |
|---|---|---|
| 171.0 | | 91.13 |
| 161.0 | 31.53 | 82.54 |
| 150.9 | | 68.39 |
| 140.9 | | 53.07 |
| 130.8 | 23.03 | 36.71 |

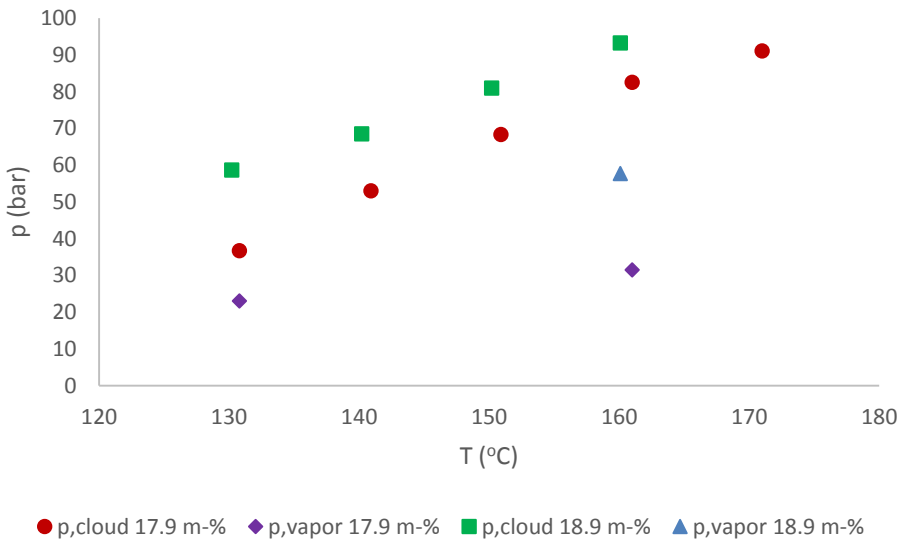


***Figure 54 Measured vapor pressures and cloud points for the 17.9 m-% and 18.9 m-% PE-4 multicomponent systems.***

A significant difference in vapor pressure can be seen between the systems. Also cloud point pressures increase with increasing polymer concentration, which is opposite behavior to previous measurements in this work. This could possibly be due to differing compositions of the solvent mixture in the systems, as the 17.9 m-% system has a larger ethylene, and increasing ethylene content should result in

increased cloud point pressures. The 17.9 m-% mixture, however, has lower cloud point pressures than the 18.9 m-% system, which points to the differing measurements possibly resulting from measurement error. However, measured cloud points from different measurement instances for the same 17.9 m-% system were within the 2 bar uncertainty to the cloud point measurements presented in Table 21, so the behavior of this particular system appears systematic. Therefore, a probable cause for the differing phase behavior could be the presence of unknown contaminants in the cell, which could affect the measurement. When comparing vapor pressures to values measured from similar solvent compositions, it is found that the vapor pressures measured for the 18.9 m-% system are much closer to those values than the vapor pressure measured for the 17.9 m-% system. In this case, measurements from the 17.9 m-% system appear abnormal, and should be regarded as unreliable and erroneous data.

### 7.3.4. Measurements with PE-5

A single measurement was performed for polymer PE-5 in the multicomponent system with a polymer concentration of 18.3 m-%. The measurement results for this system are presented in Table 22 and Figure 55.

***Table 22 Measurement results for the PE-5 multicomponent system containing 18.3 m-% polymer and 2.5 m-% ethylene.***

| T (°C) | p,cloud (bar) |
|---|---|
| 160.4 | 37.42 |
| 170.3 | 50.10 |
| 180.3 | 62.85 |
| 190.3 | 77.26 |
| 200.3 | 91.53 |
| 210.3 | 100.96 |

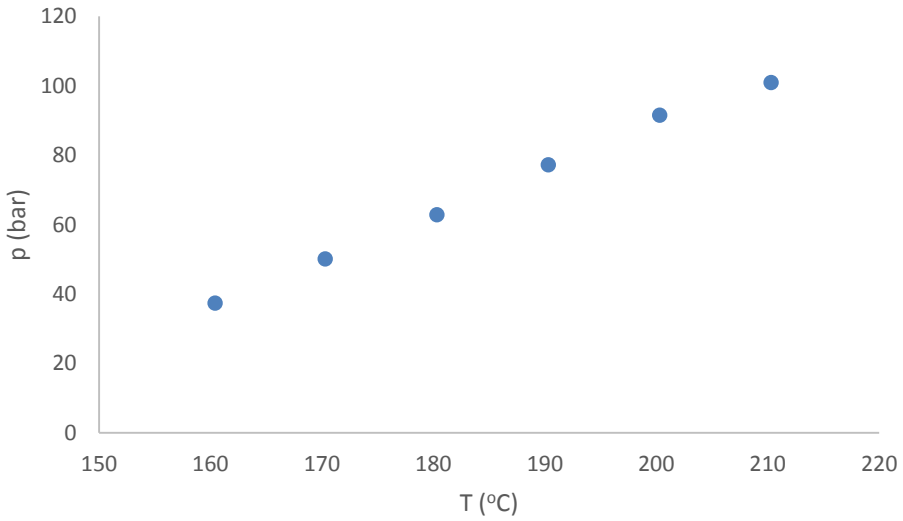


***Figure 55 Measured cloud points for the 18.3 m-% PE-5 multicomponent system.***

### 7.3.5. Measurements with PE-6

A single measurement was performed for polymer PE-6 in the multicomponent system with a polymer concentration of 18.9 m-%. The measurement results for this system are presented in Table 23 and Figure 56.

***Table 23 Measurement results for the PE-6 multicomponent system containing 18.9 m-% polymer and 2.4 m-% ethylene.***

| T (°C) | p,vapor (bar) | p,cloud (bar) |
|---|---|---|
| 151.6 | 21.68 | |
| 161.0 | 23.95 | 33.83 |
| 170.9 | | 48.34 |
| 181.0 | | 62.07 |
| 191.1 | | 73.40 |
| 201.0 | | 85.29 |
| 210.9 | | 96.94 |

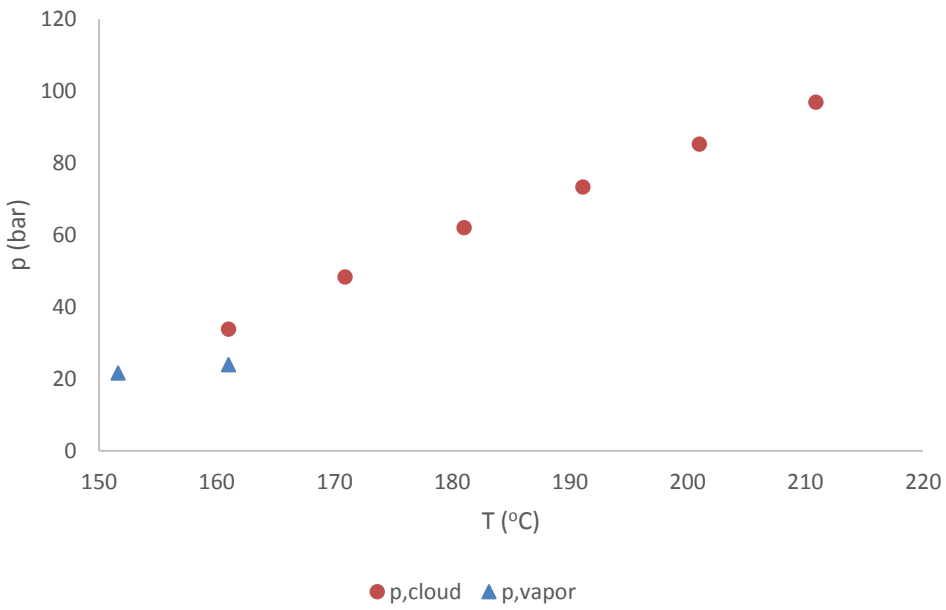


***Figure 56 Measured vapor pressures and cloud points for the 18.9 m-% PE-6 multicomponent system.***

### 7.3.6. Comparison of multicomponent systems

Since the properties of the polymers used in these experiments are unkown, quantitative comparison to data found in literature cannot be done. Additionally, the mixture used in the multicomponent systems is comprised of many components, and no data on mixtures of this type is readily available. The measured systems are more less in qualitative agreement with the behavior of such polymer solvent systems. The multicomponent systems can, however, be compared with each other. Measurements with PE-3, PE-4, PE-5, and PE-6 were all done in a system with the same components, and with polymer concentrations near each other (17-19 m-%). Overall mixture concentrations vary slightly, but are roughly equivalent in all the systems. This is also a way to analyze measurements done with PE-5 and PE-6, since only a single measurement for each was done. A measurement of PE-1 with similar polymer concentration is also compared for interest, even though the multicomponent system for PE-1 is different, including 1-octene and iso-octane instead of 1-butene and butane. Measured cloud points for the systems are presented in Figure 57, and measured vapor pressures are presented in Figure 58.

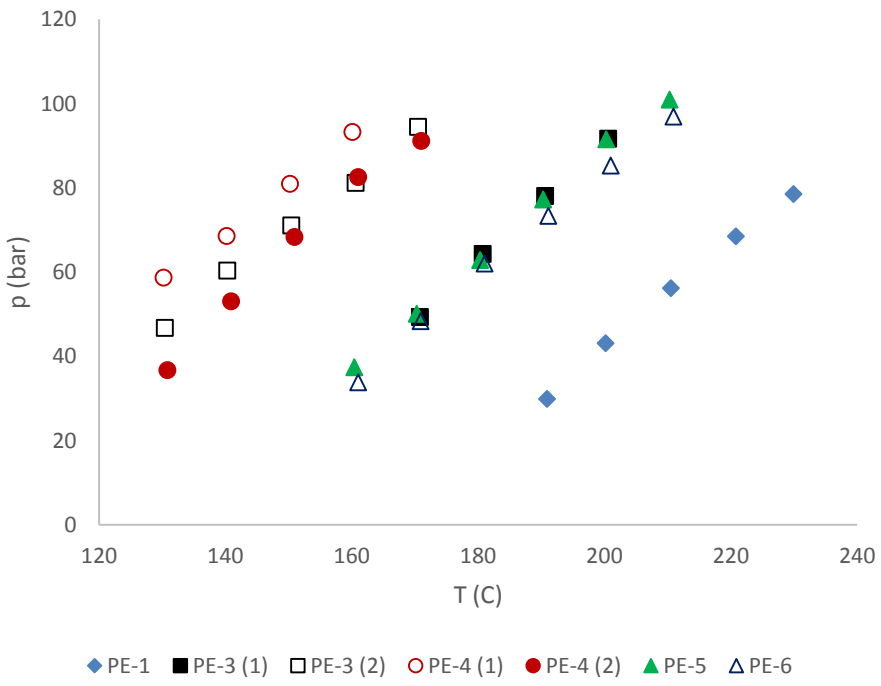


***Figure 57 Measured cloud points for the multicomponent systems with 17-19 m-% polymer concentration.***

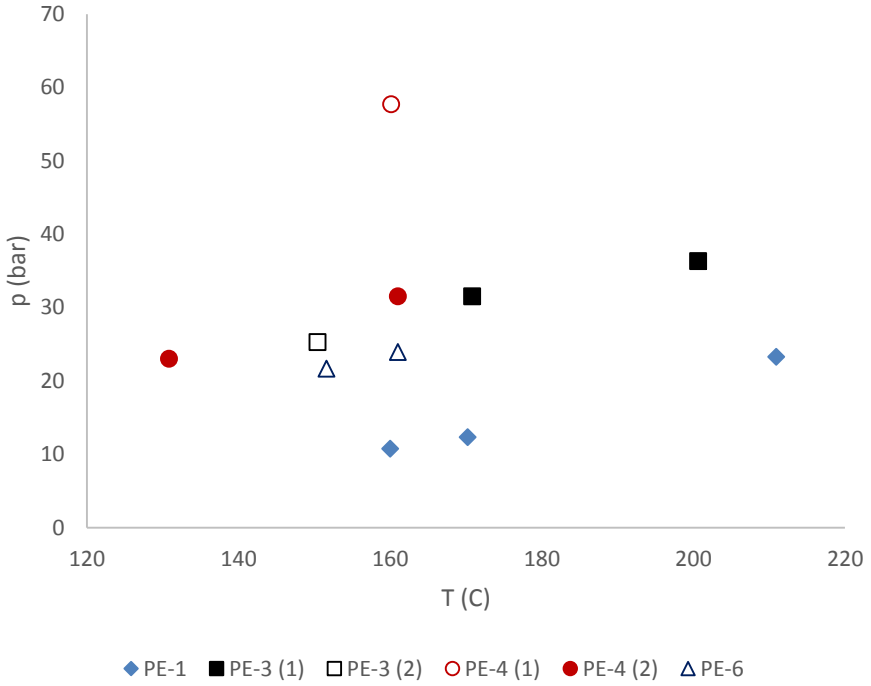


***Figure 58 Measured vapor pressures for the multicomponent systems with 17-19 m-% polymer concentration.***

As can be seen from Figure 57 and Figure 58, the PE-1 system has both the lowest vapor and cloud point pressures. This is to be expected, as it contains 8-carbon compounds 1-octene and iso-octane instead of 4-carbon compounds 1-butene and butane in the other systems. 1-butene and butane are more volatile than 1-octene and iso-octane, and increase the solvent vapor pressure. Compared to 1-octene and iso-octane, 1-butene and butane are lighter compounds, and also increase the size and density difference between the polymer and solvent resulting in decreased polymer solubility and higher cloud point pressures.

The general cloud point behavior is very similar in all the systems, as seen in Figure 57. The highest and third highest cloud point pressures were measured in the system containing PE-4, with a considerable difference between the measurements. This could possibly be partially due to differences in overall compositions between systems, but could also result from a systematic error, such as contaminants in the system, as discussed earlier. When examining the vapor pressures in Figure 58, the measured vapor pressures for all the systems with PE-3, PE-4, PE-5, and PE-6 are situated more less near an imaginary vapor pressure curve, except for the first measurement containing PE-4, which has considerably higher vapor pressure than the other similar systems. The first measurement set with PE-4 was already earlier presumed to be erroneous and unreliable, as it differs so significantly from the other similar systems.

There is also a considerable gap between the measurements with PE-3. However, the vapor pressures of this system are consistent with other measurements, so this could be explained by the differences in overall compositions of the systems and measurement inaccuracy. Of the systems compared here, the PE-3 (2) system with higher cloud point pressures has the lowest polymer concentration and highest overall concentration of 1-butene, butane, and ethylene, resulting in the observed elevated cloud point pressures.

The measurements with PE-5, and PE-6, along with the first measurement with PE-3 (1) have quite similar cloud point pressures, with PE-6 having the lowest pressures of the three. This could result from PE-6 being most similar of the polymers with the

solvent system in properties affecting the solubility of the polymer, such as density, polarity or molar mass. The polymers can thus be arranged by increasing differences in these properties with the solvent mixture in the order PE-6 < PE-5 < PE-3 < PE-4.

## 7.4. Comparison of vapor pressures

The reliability and reproducibility of the measurement results was assessed by analyzing the vapor pressures measured during experiments. As vapor pressures of polymer – solvent systems are very close to vapor pressures of the pure solvent, vapor pressures measured during experiments were evaluated against calculated pressures (bubble-point pressures) for the pure solvents using Aspen Plus v. 8.8. Evaluation was done for the binary solvent, *n*-hexane, as well as the multicomponent solvent using the Soave-Redlich-Kwong (SRK) equation of state. This EOS was selected, as it is suitable for non-polar hydrocarbon systems. Evaluation was done by examining pressure residuals (i.e. differences) between measured values and values calculated by Aspen. Alternately, measured hexane vapor pressures could have been compared to experimental hexane vapor pressures obtained from a databank. Evaluation of measured hexane pressures against values calculated by Aspen is shown in Table 24, and evaluation of measured multicomponent solvent pressures against values calculated by Aspen is shown in Table 26. The “N” column in these tables corresponds to the number of the measurement instance found in Appendix 2. Some instances of unsuccessful measurements were included to investigate whether they show larger differences between measured and calculated vapor pressures, and are presented in Table 25 for binary systems and Table 27 for multicomponent systems. Unsuccessful experiments include instances of pressure leakage as well as suspected instances of contaminants in the system, for example the unreliable measurement for polymer PE-4 discussed before in section 7.3.3. Standard deviation values of 1 % for composition measurements, and 0.01 % for temperature measurements were used in Aspen, when evaluating the data. The calculated pressure residuals are also examined in Figure 59 - 64.

***Table 24 Evaluation of measured hexane vapor pressures from successful experiments against values calculated by Aspen. In the table N is the number of the experiment, PMF is the polymer mass fraction, p,exp is the experimental pressure, p,calc is the calculated pressure, diff is the pressure residual (difference between the calculated and experimental pressure), and % diff is the relative error between the measured and calculated pressures in percentage.***

| N | Polymer | T (°C) | PMF | p,exp (bar) | p,calc (bar) | diff (bar) | % diff |
|---|---|---|---|---|---|---|---|
| 1 | PE-1 | 186.7 | 0.2081 | 14.35 | 14.77 | 0.42 | 2.9 |
| 2 | PE-1 | 179.7 | 0.1023 | 14.44 | 14.77 | 0.34 | 2.3 |
| 3 | PE-1 | 186.0 | 0.1969 | 16.50 | 14.48 | -2.02 | -12.3 |
| 5 | PE-1 | 196.0 | 0.2131 | 17.95 | 17.16 | -0.79 | -4.4 |
| 5 | PE-1 | 211.0 | 0.2131 | 22.52 | 21.60 | -0.91 | -4.1 |
| 6 | PE-1 | 184.0 | 0.2127 | 15.05 | 14.10 | -0.94 | -6.3 |
| 6 | PE-1 | 190.0 | 0.2127 | 15.66 | 15.60 | -0.06 | -0.4 |
| 6 | PE-1 | 196.0 | 0.2127 | 17.16 | 17.18 | 0.02 | 0.1 |
| 6 | PE-1 | 211.0 | 0.2127 | 21.93 | 21.65 | -0.28 | -1.3 |
| 6 | PE-1 | 220.0 | 0.2127 | 24.65 | 24.71 | 0.06 | 0.2 |
| 7 | PE-1 | 171.0 | 0.2011 | 11.18 | 11.29 | 0.10 | 0.9 |
| 7 | PE-1 | 185.0 | 0.2011 | 14.62 | 14.36 | -0.25 | -1.7 |
| 8 | PE-1 | 187.6 | 0.1000 | 14.87 | 15.00 | 0.13 | 0.8 |
| 8 | PE-1 | 211.7 | 0.1000 | 21.62 | 21.87 | 0.25 | 1.2 |
| 9 | PE-1 | 211.8 | 0.1000 | 21.69 | 21.91 | 0.22 | 1.0 |
| 9 | PE-1 | 179.8 | 0.1000 | 13.21 | 13.16 | -0.06 | -0.4 |
| 10 | PE-1 | 170.8 | 0.1023 | 11.12 | 11.25 | 0.13 | 1.1 |
| 10 | PE-1 | 186.8 | 0.1023 | 14.65 | 14.80 | 0.16 | 1.1 |
| 11 | PE-1 | 171.2 | 0.1023 | 11.39 | 11.33 | -0.06 | -0.5 |
| 11 | PE-1 | 230.0 | 0.1023 | 28.12 | 28.45 | 0.33 | 1.2 |
| 11 | PE-1 | 186.6 | 0.1023 | 14.65 | 14.75 | 0.11 | 0.7 |
| 12 | PE-1 | 171.6 | 0.1952 | 11.66 | 11.41 | -0.25 | -2.1 |
| 13 | PE-1 | 171.0 | 0.1969 | 13.40 | 11.16 | -2.24 | -16.7 |
| 21 | PE-2 | 200.4 | 0.3663 | 18.45 | 18.42 | -0.03 | -0.2 |
| 21 | PE-2 | 220.4 | 0.3663 | 24.70 | 24.85 | 0.15 | 0.6 |
| 22 | PE-2 | 220.4 | 0.3663 | 25.08 | 24.84 | -0.23 | -0.9 |
| 22 | PE-2 | 200.6 | 0.3663 | 18.53 | 18.47 | -0.06 | -0.3 |
| 23 | PE-2 | 201.2 | 0.3831 | 18.69 | 18.65 | -0.05 | -0.3 |
| 23 | PE-2 | 201.2 | 0.3482 | 24.77 | 25.13 | 0.35 | 1.4 |
| 24 | PE-2 | 201.1 | 0.3652 | 18.39 | 18.62 | 0.22 | 1.2 |
| 24 | PE-2 | 180.8 | 0.3652 | 13.05 | 13.38 | 0.34 | 2.6 |
| 24 | PE-2 | 191.1 | 0.3721 | 15.66 | 15.88 | 0.22 | 1.4 |
| 25 | PE-2 | 221.1 | 0.1966 | 24.74 | 25.09 | 0.35 | 1.4 |
| 26 | PE-2 | 181.1 | 0.1966 | 13.57 | 13.45 | -0.12 | -0.9 |
| 26 | PE-2 | 191.2 | 0.1966 | 15.74 | 15.91 | 0.17 | 1.1 |
| 26 | PE-2 | 201.3 | 0.1966 | 18.41 | 18.67 | 0.26 | 1.4 |
| 26 | PE-2 | 211.3 | 0.1966 | 21.42 | 21.74 | 0.33 | 1.5 |
| 26 | PE-2 | 221.2 | 0.1966 | 24.81 | 25.13 | 0.31 | 1.3 |

***Table 25 Evaluation of measured hexane vapor pressures from unsuccessful experiments against values calculated by Aspen. In the table, PMF is the polymer mass fraction, p,exp is the experimental pressure, p,calc is the calculated pressure, diff is the pressure residual (difference between the calculated and experimental pressure), and % diff is the relative error between the measured and calculated pressures in percentage.***

| Polymer | T (°C) | PMF | p,exp (bar) | p,calc (bar) | diff (bar) | % diff | Problem |
|---|---|---|---|---|---|---|---|
| PE-1 | 186.7 | 0.2081 | 13.25 | 13.14 | -0.12 | -0.9 | Mixing fail, pressure leak |
| PE-2 | 221.2 | 0.3831 | 19.41 | 18.62 | -0.79 | -4.1 | Pressure leak |
| PE-2 | 191.1 | 0.3652 | 18.15 | 18.64 | 0.48 | 2.7 | Mixing fail |
| PE-2 | 201.2 | 0.3721 | 13.21 | 13.45 | 0.24 | 1.8 | Mixing fail |
| PE-2 | 181.1 | 0.3721 | 15.44 | 15.88 | 0.44 | 2.8 | Mixing fail |

The "Problem" column in the tables for unsuccessful experiments lists what was wrong with each unsuccessful experiment presented here. Mixing fail means that the system could not be properly mixed into a single homogeneous phase at any point due to problems with the magnetic stirrer. This hinders the achieving of thermodynamic equilibrium in the system. Pressure leak means that pressure could not be maintained in the cell due to failure of a pressure seal (O-ring). Contaminant, listed in Table 27, means that hydraulic oil was leaking into the sample part of the cell, or the presence of some other suspected contaminant while loading the cell.

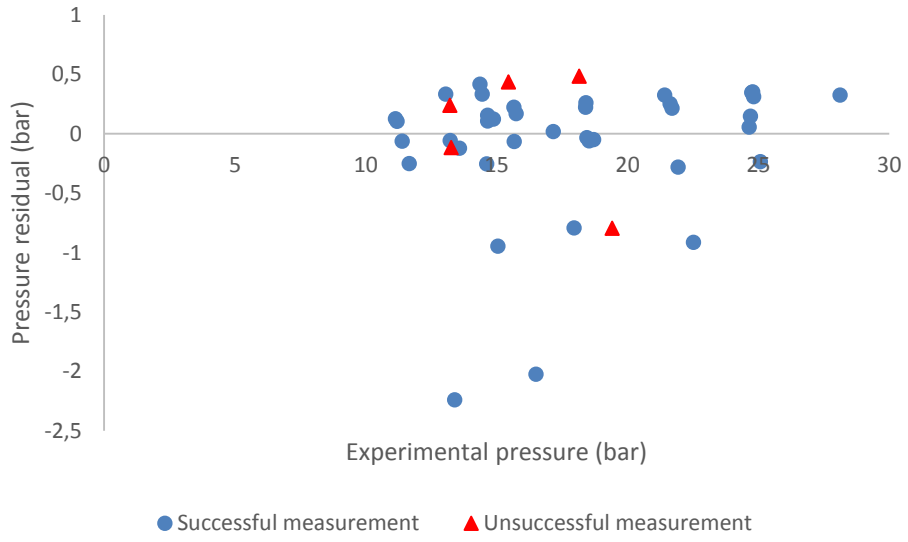


***Figure 59 Pressure residuals (p,exp – p,calc) for hexane vapor pressures as a function of measured hexane vapor pressures.***

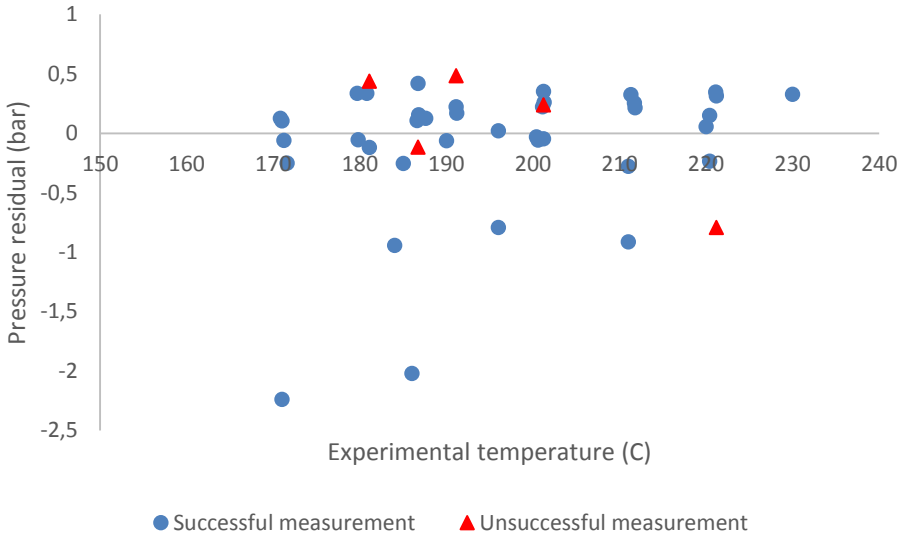


***Figure 60 Pressure residuals (p,exp – p,calc) for hexane vapor pressures as a function of measurement temperatures.***

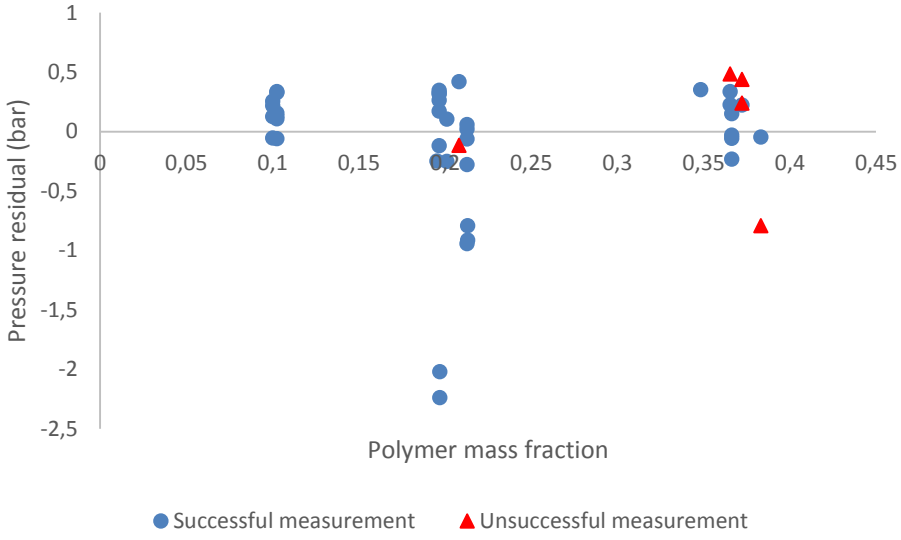


***Figure 61 Pressure residuals (p,exp – p,calc) for hexane vapor pressures as a function of polymer mass fraction.***

***Table 26 Evaluation of measured multicomponent vapor pressures from successful experiments against values calculated by Aspen. In the table N is the number of the experiment, PMF is the polymer mass fraction, p,exp is the experimental pressure, p,calc is the calculated pressure, diff is the pressure residual (difference between the calculated and experimental pressure), and % diff is the relative error between the measured and calculated pressures in percentage.***

| N | Polymer | T (°C) | PMF | p,exp (bar) | p,calc (bar) | diff (bar) | % diff |
|---|---|---|---|---|---|---|---|
| 15 | PE-1 | 160.0 | 0.1909 | 10.78 | 12.29 | 1.51 | 14.0 |
| 15 | PE-1 | 170.2 | 0.1909 | 12.32 | 14.19 | 1.87 | 15.2 |
| 15 | PE-1 | 210.9 | 0.1909 | 23.29 | 24.25 | 0.96 | 4.1 |
| 16 | PE-1 | 210.5 | 0.1909 | 24.68 | 24.17 | -0.52 | -2.1 |
| 17 | PE-1 | 171.0 | 0.1557 | 13.50 | 14.55 | 1.06 | 7.8 |
| 17 | PE-1 | 221.4 | 0.1557 | 25.50 | 27.57 | 2.08 | 8.1 |
| 18 | PE-1 | 200.9 | 0.1557 | 20.83 | 21.56 | 0.73 | 3.5 |
| 18 | PE-1 | 230.1 | 0.1557 | 28.62 | 30.40 | 1.78 | 6.2 |
| 19 | PE-1 | 190.6 | 0.2321 | 16.58 | 19.48 | 2.90 | 17.5 |
| 19 | PE-1 | 230.9 | 0.2321 | 29.92 | 31.25 | 1.33 | 4.4 |
| 20 | PE-1 | 171.9 | 0.1608 | 16.62 | 16.62 | 0.00 | 0.0 |
| 20 | PE-1 | 186.0 | 0.1608 | 20.94 | 20.92 | -0.02 | -0.1 |
| 20 | PE-1 | 220.8 | 0.1608 | 29.61 | 29.55 | -0.06 | -0.2 |
| 27 | PE-4 | 170.8 | 0.1770 | 31.53 | 28.38 | -3.15 | -10.0 |
| 27 | PE-4 | 200.6 | 0.1770 | 36.32 | 36.23 | -0.09 | -0.2 |
| 28 | PE-3 | 150.4 | 0.1736 | 25.32 | 28.04 | 2.71 | 10.7 |
| 29 | PE-4 | 130.9 | 0.1791 | 22.98 | 23.72 | 0.73 | 3.2 |
| 30 | PE-4 | 161.0 | 0.1791 | 31.53 | 31.53 | 0.00 | 0.0 |
| 30 | PE-4 | 130.8 | 0.1791 | 23.03 | 23.71 | 0.68 | 3.0 |
| 32 | PE-6 | 161.0 | 0.1892 | 23.95 | 24.08 | 0.12 | 0.5 |
| 32 | PE-6 | 151.6 | 0.1892 | 21.68 | 21.89 | 0.21 | 1.0 |

***Table 27 Evaluation of measured multicomponent vapor pressures from unsuccessful experiments against values calculated by Aspen. In the table PMF is the polymer mass fraction, p,exp is the experimental pressure, p,calc is the calculated pressure, diff is the pressure residual (difference between the calculated and experimental pressure), and % diff is the relative error between the measured and calculated pressures in percentage.***

| Polymer | T (°C) | PMF | p,exp (bar) | p,calc (bar) | diff (bar) | % diff | Problem |
|---|---|---|---|---|---|---|---|
| PE-3 | 170.1 | 0.1770 | 25.25 | 27.27 | 2.02 | 8.0 | Contaminant |
| PE-3 | 210.2 | 0.1770 | 34.57 | 38.79 | 4.22 | 12.2 | Contaminant |
| PE-3 | 151.0 | 0.1736 | 25.04 | 28.09 | 3.06 | 12.2 | Contaminant |
| PE-3 | 130.8 | 0.1736 | 18.25 | 22.29 | 4.03 | 22.1 | Contaminant |
| PE-4 | 160.1 | 0.1889 | 57.71 | 53.90 | -3.81 | -6.6 | Contaminant |

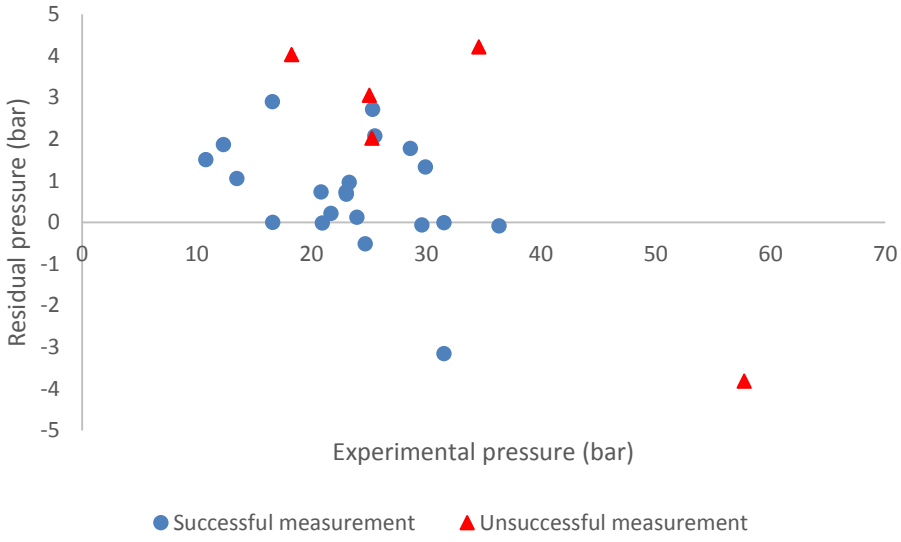


***Figure 62 Pressure residuals (p,exp – p,calc) for multicomponent vapor pressures as a function of measured multicomponent vapor pressures.***

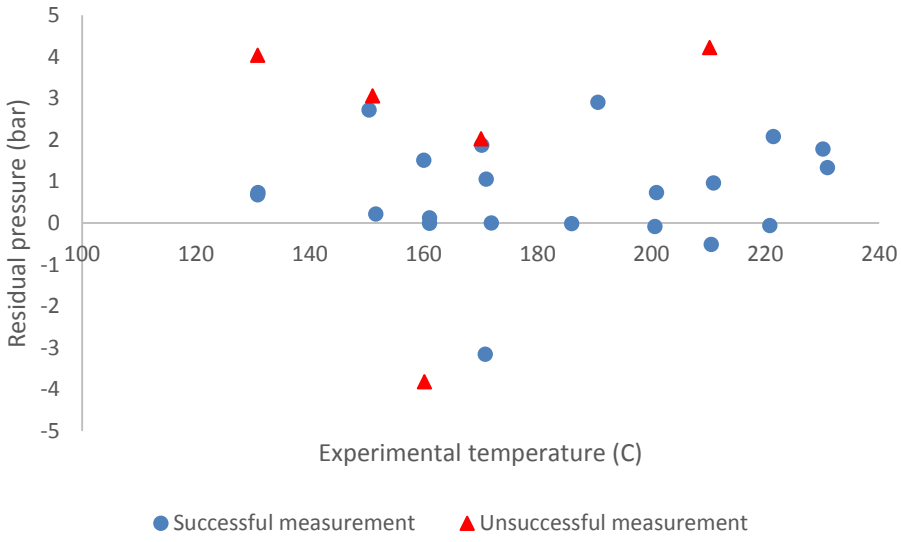


***Figure 63 Pressure residuals (p,exp – p,calc) for multicomponent vapor pressures as a function of measurement temperatures.***

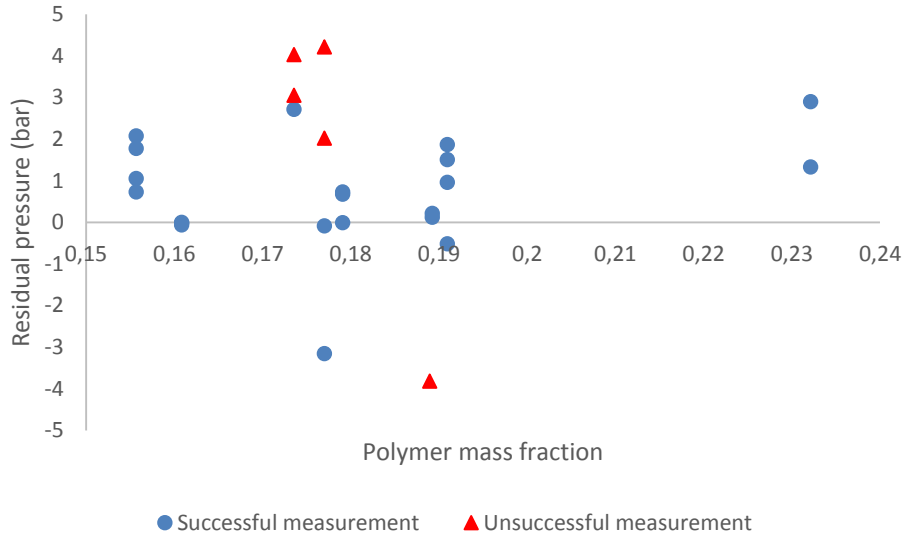


***Figure 64 Pressure residuals (p,exp – p,calc) for multicomponent vapor pressures as a function of polymer mass fraction.***

Pressure residuals calculated with Aspen were evaluated in terms of the measured pressure, temperature, and polymer concentration of the experimental mixtures. Evaluation especially with hexane showed little difference for the most part between the measured vapor pressures and the calculated pure hexane vapor pressures. Only two measurements for hexane vapor pressures had residuals over 1 bar, while the vast majority of measurements have calculated residuals of under 0.5 bar. For very little or no difference in the evaluation, it can be assumed that no unknown contaminants affected the vapor pressure measurement during experiments, and results for measurements are reliable. The unsuccessful measurements for the hexane vapor pressures don't show any clear deviation from the successful measurements, and are all instances of either mixing failure or pressure leakage, in which case the vapor pressure measurement could still be close the actual vapor pressure. No systematic behavior of the pressure residuals in terms of measured pressure, temperature or polymer concentration could be observed for the binary systems.

The multicomponent evaluation shows a little more fluctuation in the data. Four instances of successful measurements, along with the unsuccessful measurements

show residuals above 2 bar. As the system has several components, some of this fluctuation may be slight inaccuracy due to the complexity of the calculation. Another reason undoubtedly is the observation accuracy during measurements. For the multicomponent system, unsuccessful experiments containing known or suspected contaminants were selected. These measurements clearly show generally larger pressure residuals between the measured and calculated pressures than the successful measurements, and can thus be confirmed to be unreliable. For example, the unreliable measurement for PE-3 discussed before has a difference of 3.81 bar to the value calculated by Aspen for that mixture composition. However, no systematic behavior of the pressure residuals in terms of measured pressure, temperature or polymer concentration could be observed for the multicomponent systems either. Successful measurements with residuals over 2 bar should also not be considered absolutely reliable without supporting measurement results. This type of supporting evidence could be logical behavior when compared to similar systems, or reproducibility in measurement results, as was attempted to do in this work.

# 8. Conclusions and outlook

Cloud point measurements for various linear low-density polyethylene – solvent systems was carried out in a variable volume cell. Cloud points were measured for binary systems with *n*-hexane, and multicomponent systems as a simplification of solution polymerization mixtures. The observation of cloud points was done visually, and results were investigated for abnormal behavior. Results were also evaluated by comparing measured vapor pressures to vapor pressures of the solvent systems calculated with Aspen. Erroneous data was omitted from the results, and the remaining measurements were in qualitative agreement with similar polymer – solvent systems found in literature.

LCST behavior was observed in the investigated temperature range. Increasing polymer concentration was found to increase the solubility of the polymer, meaning

the polymer concentrations investigated were larger than the critical polymer concentrations. In accordance with general findings from other studies, increasing differences between the polymer and solvent in properties such as molar mass and density was found to decrease polymer solubility. This was achieved by varying the concentrations of some components in the systems, for example increasing the concentration of lower molar mass components such as ethylene. However, phase behavior of polymer – solvent systems also depend on the properties of the polymer, such as molar mass and molar mass distribution, which were unknown in this study. It is important to keep in mind, that even though some generalizations can be made, the actual phase behavior is always specific for each unique system.

The commercial importance of polymers in general will undoubtedly continue to drive the research of polymer manufacturing. Phase equilibria knowledge is of the utmost importance when developing, improving, and implementing various techniques and processes for polymer manufacturing. For the experimental polymer systems in this work more experiments could be systematically conducted to obtain phase boundaries for a larger range of system compositions (e.g. polymer concentration) in the studied temperature and pressure range. The addition of ethylene and/or other components could also be systematically investigated for their impact on the phase boundary behavior. Modeling of the obtained data could also subsequently be attempted using a suitable equation of state. The equipment and procedures used in this work can certainly be used for phase equilibria measurements of a large variety of systems, even beyond polymer mixtures.

# 9. Bibliography


AHVENAINEN, A., SARANTILA, K., ANDTSJO, H., TAKAKARHU, J. and PALMROOS, A., 1994. *Multi-stage process for producing polyethylene,* Patent No. WO1992012182 A1

BAE, Y., LAMBERT, S., SOANE, D. and PRAUSNITZ, J., 1991. Cloud-point curves of polymer solutions from thermooptical measurements. *Macromolecules,* **24**(15), pp. 4403-4407.

BULKATOV, A., 2008. Comparative analysis of various polyethylene production technologies. *Chemical and Petroleum Engineering,* **44**(7-8), pp. 429-432.

CHAN, A.K.C., ADIDHARMA, H. and RADOSZ, M., 2000. Fluid-liquid transitions of poly (ethylene-co-octene-1) in supercritical ethylene solutions. *Industrial & Engineering Chemistry Research,* **39**(11), pp. 4370-4375.

CHAN, A.K.C., RUSSO, P.S. and RADOSZ, M., 2000. Fluid–liquid equilibria in poly (ethylene-co-hexene-1) propane: a light-scattering probe of cloud-point pressure and critical polymer concentration. *Fluid Phase Equilibria,* **173**(1), pp. 149-158.

CHEN, A. and RADOSZ, M., 1999. Phase equilibria of dilute poly (ethylene-co-1-butene) solutions in ethylene, 1-butene, and 1-butene ethylene. *Journal of Chemical & Engineering Data,* **44**(4), pp. 854-859.

CHEN, S.J., ECONOMOU, I.G. and RADOSZ, M., 1992. Density-tuned polyolefin phase equilibria. 2. Multicomponent solutions of alternating poly (ethylene-propylene) in subcritical and supercritical olefins. Experiment and SAFT model. *Macromolecules,* **25**(19), pp. 4987-4995.

CHEN, S.J. and RADOSZ, M., 1992. Density-tuned polyolefin phase equilibria. 1. Binary solutions of alternating poly (ethylene-propylene) in subcritical and supercritical propylene, 1-butene, and 1-hexene. Experiment and Flory-Patterson model. *Macromolecules,* **25**(12), pp. 3089-3096.

CHEN, X., YASUDA, K., SATO, Y., TAKISHIMA, S. and MASUOKA, H., 2004. Measurement and correlation of phase equilibria of ethylene n-hexane metallocene polyethylene at temperatures between 373 and 473K and at pressures up to 20MPa. *Fluid Phase Equilibria,* **215**(1), pp. 105-115.

DE LOOS, T.W., DE GRAAF, L. and DE SWAAN ARONS, J., 1996. Liquid-liquid phase separation in linear low density polyethylene-solvent systems. *Fluid Phase Equilibria,* **117**(1), pp. 40-47.

DE LOOS, T.W., LICHTENTHALER, R. and DIEPEN, G., 1983. Fluid phase equilibriums in the system polyethylene ethylene. 2. Calculation of cloud curves for systems of linear polyethylene ethylene. *Macromolecules,* **16**(1), pp. 117-121.

DE LOOS, T.W., POOT, W. and LICHTENTHALER, R., 1995. The influence of branching on high-pressure vapor-liquid equilibria in systems of ethylene and polyethylene. *The Journal of Supercritical Fluids,* **8**(4), pp. 282-286.

DE LOOS, T.W., NAGY, I., KRENZ, R.A. and HEIDEMANN, R.A., 2004. The Influence of the Addition of Supercritical Ethylene on the High Pressure Phase Behaviour of the System Linear Low Density Polyethylene + n-Hexane: Experimental Results and Modelling with the Sanchez-Lacombe EOS, *Proceedings of the 9th Meeting on Supercritical Fluids* 2004.

DE LOOS, T.W., POOT, W. and DIEPEN, G., 1983. Fluid phase equilibriums in the system polyethylene ethylene. 1. Systems of linear polyethylene ethylene at high pressure. *Macromolecules,* **16**(1), pp. 111-117.

DE LOOS, T.W., VAN DER KOOI, HEDZER J and OTT, P.L., 1986. Vapor-liquid critical curve of the system ethane 2-methylpropane. *Journal of Chemical and Engineering Data,* **31**(2), pp. 166-168.

DÖRR, H., KINZL, M. and LUFT, G., 2001. The influence of inert gases on the high-pressure phase equilibria of EH-copolymer/1-hexene/ethylene-mixtures. *Fluid Phase Equilibria,* **178**(1), pp. 191-201.

FLORY, P.J., 1942. Thermodynamics of high polymer solutions. *The Journal of chemical physics,* **10**(1), pp. 51-61.

FOLIE, B. and RADOSZ, M., 1995. Phase equilibria in high-pressure polyethylene technology. *Industrial & Engineering Chemistry Research,* **34**(5), pp. 1501-1516.

GREGG, C.J., STEIN, F.P., MORGAN, C.K. and RADOSZ, M., 1994. A variable-volume optical pressure-volume-temperature cell for high-pressure cloud points, densities, and infrared spectra, applicable to supercritical fluid solutions of polymers up to 2 kbar. *Journal of Chemical and Engineering Data,* **39**(2), pp. 219-224.

GREGG, C., CHEN, S., STEIN, F. and RADOSZ, M., 1993. Phase behavior of binary ethylene-propylene copolymer solutions in sub-and supercritical ethylene and propylene. *Fluid Phase Equilibria,* **83**, pp. 375-382.

HARPER, C.A., 2000. *Modern Plastics Handbook.* New York: McGraw-Hill, pp. 40-45.

HARUKI, M., MANO, S., KOGA, Y., KIHARA, S. and TAKISHIMA, S., 2010. Phase behaviors for the supercritical ethylene 1-hexene hexane polyethylene systems at elevated temperatures and pressures. *Fluid Phase Equilibria,* **295**(1), pp. 137-147.

HARUKI, M., SATO, K., KIHARA, S. and TAKISHIMA, S., 2009. High pressure phase behavior for the supercritical ethylene cyclohexane hexane polyethylene systems. *The Journal of Supercritical Fluids,* **49**(2), pp. 125-134.

HARUKI, M., TAKAKURA, Y., SUGIURA, H., KIHARA, S. and TAKISHIMA, S., 2008. Phase behavior for the supercritical ethylene hexane polyethylene systems. *The Journal of Supercritical Fluids,* **44**(3), pp. 284-293.

HASCH, B.M., MEILCHEN, M.A., LEE, S. and MCHUGH, M.A., 1992. High-Pressure phase behavior of mixtures of poly (ethylene-co-methyl acrylate) with low-molecular weight hydrocarbons. *Journal of Polymer Science Part B: Polymer Physics,* **30**(12), pp. 1365-1373.

HIGGINS, J.S., LIPSON, J.E. and WHITE, R.P., 2010. A simple approach to polymer mixture miscibility. *Philosophical transactions.Series A, Mathematical, physical, and engineering sciences,* **368**(1914), pp. 1009-1025.

HORST, R., WOLF, B., KINZL, M., LUFT, G. and FOLIE, B., 1998. Shear influences on the solubility of LDPE in ethene. *The Journal of supercritical fluids,* **14**(1), pp. 49-54.

HUGGINS, M.L., 1941. Solutions of long chain compounds. *The Journal of chemical physics,* **9**(5), pp. 440-440.

JEREMIC, D., 2014. Polyethylene. *Ullmann's Encyclopedia of Industrial Chemistry.* Wiley-VCH Verlag GmbH & Co. KGaA, .

KINZL, M., LUFT, G. and UNGAR, C., 2001. The influence of inert gases on the high-pressure phase equilibria of EVA-copolymer/vinyl acetate/ethylene mixtures. *Fluid Phase Equilibria,* **178**(1), pp. 179-189.

KLENIN, V. and SHMAKOV, S., 2013. Features of Phase Separation in Polymeric Systems: Cloud-Point Curves (Discussion). *Universal Journal of Materials Science,* **1**(2), pp. 39-45.

KOAK, N., VISSER, R. and DE LOOS, T.W., 1999. High-pressure phase behavior of the systems polyethylene ethylene and polybutene 1-butene. *Fluid Phase Equilibria,* **158**, pp. 835-846.

KONINGSVELD, R. and KLEINTJENS, L., 1971. Liquid-liquid phase separation in multicomponent polymer systems. X. Concentration dependence of the pair-interaction parameter in the system cyclohexane-polystyrene. *Macromolecules,* **4**(5), pp. 637-641.

KRENZ, R., HEIDEMANN, R. and DE LOOS, T.W., 2005. Three and four phase predictions for polyethylene hydrocarbon systems. *Fluid Phase Equilibria,* **228**, pp. 427-437.

LEE, S., 2005. Phase behavior of binary and ternary mixtures of poly (ethylene-co-octene)–hydrocarbons. *Journal of Applied Polymer Science,* **95**(1), pp. 161-165.

LIU, K. and KIRAN, E., 2001. Pressure-induced phase separation in polymer solutions: Kinetics of phase separation and crossover from nucleation and growth to

spinodal decomposition in solutions of polyethylene in n-pentane. *Macromolecules,* **34**(9), pp. 3060-3068.

NAGY, I., DE LOOS, T.W., KRENZ, R. and HEIDEMANN, R., 2006. High pressure phase equilibria in the systems linear low density polyethylene n-hexane and linear low density polyethylene n-hexane ethylene: Experimental results and modelling with the Sanchez-Lacombe equation of state. *The Journal of supercritical fluids,* **37**(1), pp. 115-124.

NAGY, I., KRENZ, R.A., HEIDEMANN, R.A. and DE LOOS, T.W., 2007. High-pressure phase equilibria in the system linear low density polyethylene isohexane: Experimental results and modelling. *The Journal of supercritical fluids,* **40**(1), pp. 125-133.

NAIDOO, P., 2013. *A comparative analysis of the chemical composition of linear low density polyethylene polymers synthesised with 1-hexene comonomer under different catalytic conditions.,* .

PAN, C. and RADOSZ, M., 1999. Phase Behavior of Poly (ethylene-co-hexene-1) Solutions in Isobutane and Propane. *Industrial & Engineering Chemistry Research,* **38**(7), pp. 2842-2848.

RADOSZ, M., 1987. Multiphase behavior of supercritical fluid systems: oil solutions in light hydrocarbon solvents. *Industrial & Engineering Chemistry Research,* **26**(10), pp. 2134-2139.

RICHON, D., 2009. Experimental techniques for the determination of thermophysical properties to enhance chemical processes. *Pure and Applied Chemistry,* **81**(10), pp. 1769-1782.

SCHNELL, M., STRYUK, S. and WOLF, B.A., 2004. Liquid/Liquid demixing in the system n-hexane/narrowly distributed linear polyethylene. *Industrial & Engineering Chemistry Research,* **43**(11), pp. 2852-2859.

TER HORST, M., BEHME, S., SADOWSKI, G. and DE LOOS, T.W., 2002. The influence of supercritical gases on the phase behavior of polystyrene–cyclohexane and polyethylene–cyclohexane systems: experimental results and modeling with the SAFT-equation of state. *The Journal of supercritical fluids,* **23**(3), pp. 181-194.

TRUMPI, H., DE LOOS, T.W., KRENZ, R. and HEIDEMANN, R., 2003. High pressure phase equilibria in the system linear low density polyethylene ethylene: experimental results and modelling. *The Journal of supercritical fluids,* **27**(2), pp. 205-214.

XIONG, Y. and KIRAN, E., 1998. High-pressure light scattering apparatus to study pressure-induced phase separation in polymer solutions. *Review of scientific instruments,* **69**(3), pp. 1463-1471.

# Appendix 1. Calibration of the Kulite Semiconductor XTEH pressure transducer

The pressure transducer used in the experiments (Kulite Semiconductor XTEH) was temperature sensitive, and thus had to be calibrated to obtain pressure corrections by temperature. The calibration was done by pressurizing the cell with nitrogen, and comparing the pressure given by the transducer to the pressure given by a MC2 Beamex calibration device, which had been calibrated at the National Centre for Metrology and Accreditation in Finland (MIKES). The values of the calibrator represent the true actual pressure in the system. Zero and gain on the pressure signal transmitter for the Kulite transducer were adjusted for the pressure scale to roughly equal an intermediate temperature (about 200 $^{o}$C), and pressure differences were recorded by measuring pressures in the pressure range of the experiments in several temperatures within the temperature range in the experiments. A linear dependence was noticed between the transducer measurement and the calibrator measurement, and the measurements at each temperature were correlated linearly, by calculating slopes, intercepts, and r-squared values (RSQ) for each measurement series. The RSQ value can be interpreted as the extent of a linear relationship between the data points, i.e. how well the linear approximation depicts the data. Corrections were calculated from these linear correlations between the transducer and calibration device measurements. The correlated slopes and intercept points were gathered for all temperatures. The pressure transducer calibration data in the measurement range of 150 – 200 $^{o}$C is presented in the following Tables and Figures.

***Table 28 Pressure calibration measurements at 150.3 °C.***

| T (°C) | 150.3 | |
|---|---|---|
| | | |
| p,transducer (bar) | p,calbrator (bar) | error |
| 2.59 | 1.08 | 1.51 |
| 10.74 | 9.24 | 1.50 |
| 20.41 | 18.93 | 1.48 |
| 30.37 | 28.91 | 1.46 |
| 40.43 | 39.00 | 1.43 |
| 50.64 | 49.22 | 1.42 |
| 60.10 | 58.70 | 1.40 |
| 70.26 | 68.88 | 1.38 |
| 80.30 | 78.93 | 1.37 |
| 90.10 | 88.75 | 1.35 |
| 100.00 | 98.67 | 1.33 |

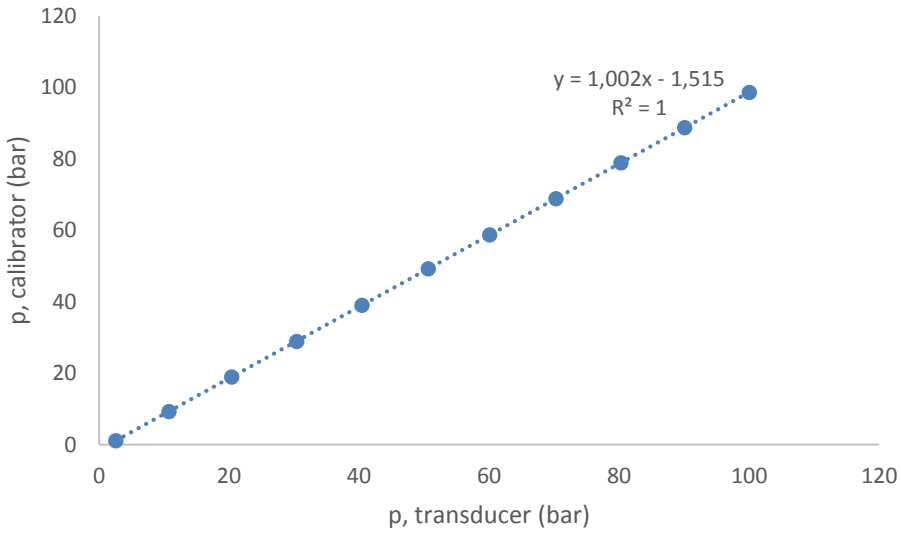


***Figure 65 Pressure calibration measurement correlation at 150.3 °C.***

***Table 29 Pressure calibration measurement correlation parameters at 150.3 °C.***

| | |
|---|---|
| slope | 1.002 |
| itercept | -1.515 |
| RSQ | 1.000 |

***Table 30 Pressure calibration measurements at 175.5 °C.***

| T (°C) | 175.5 | |
|---|---|---|
| | | |
| p,transducer (bar) | p,calbrator (bar) | error |
| 2.36 | 1.34 | 1.02 |
| 11.96 | 10.92 | 1.04 |
| 20.32 | 19.29 | 1.03 |
| 30.30 | 29.27 | 1.03 |
| 40.23 | 39.20 | 1.03 |
| 50.43 | 49.40 | 1.03 |
| 61.83 | 60.80 | 1.03 |
| 70.31 | 69.29 | 1.02 |
| 80.05 | 79.03 | 1.02 |
| 90.62 | 89.60 | 1.02 |
| 100.20 | 99.18 | 1.02 |

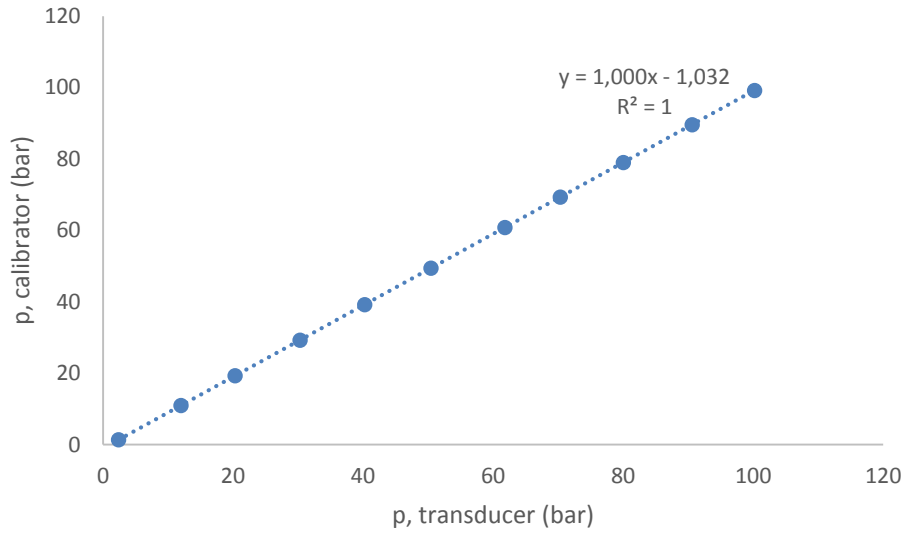


***Figure 66 Pressure calibration measurement correlation at 175.5 °C.***

***Table 31 Pressure calibration measurement correlation parameters at 175.5 °C.***

| slope | 1.000 |
|---|---|
| itercept | -1.032 |
| RSQ | 1.000 |

***Table 32 Pressure calibration measurements at 200.6 °C.***

| T (°C) | 200.6 | |
|---|---|---|
| | | |
| p,transducer (bar) | p,calbrator (bar) | error |
| 1.73 | 1.25 | 0.48 |
| 10.40 | 9.91 | 0.49 |
| 20.16 | 19.67 | 0.49 |
| 30.26 | 29.77 | 0.49 |
| 40.13 | 39.63 | 0.50 |
| 50.14 | 49.65 | 0.49 |
| 60.20 | 59.70 | 0.50 |
| 70.29 | 69.80 | 0.49 |
| 80.33 | 79.83 | 0.50 |
| 90.43 | 89.93 | 0.50 |
| 100.00 | 99.50 | 0.50 |

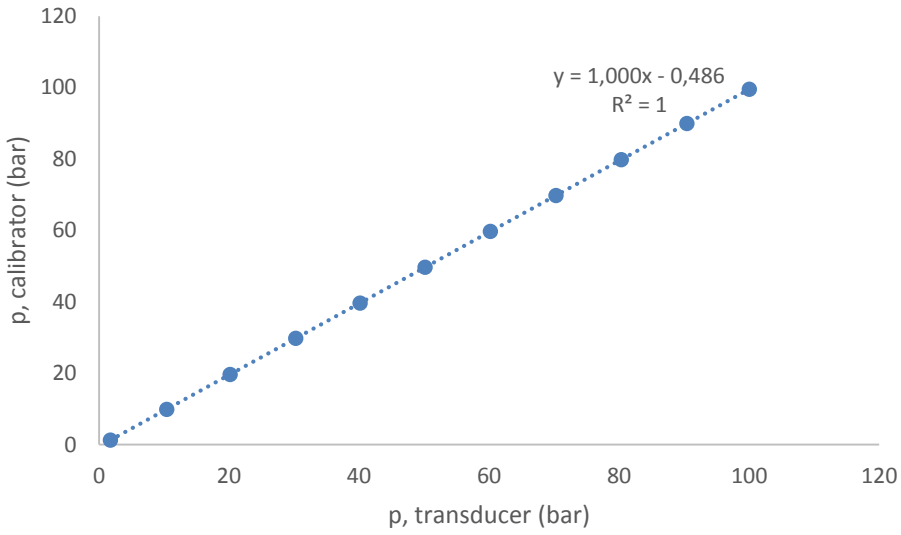


***Figure 67 Pressure calibration measurement correlation at 200.6 °C.***

***Table 33 Pressure calibration measurement correlation parameters at 200.6 °C.***

| slope | 1.000 |
|---|---|
| itercept | -0.486 |
| RSQ | 1.000 |

***Table 34 Pressure calibration measurements at 225.6 °C.***

| T (°C) | 225.6 | |
|---|---|---|
| | | |
| p,transducer (bar) | p,calbrator (bar) | error |
| 1.08 | 1.25 | -0.17 |
| 10.20 | 10.36 | -0.16 |
| 20.33 | 20.49 | -0.16 |
| 30.20 | 30.37 | -0.17 |
| 40.32 | 40.50 | -0.18 |
| 50.20 | 50.38 | -0.18 |
| 59.77 | 59.97 | -0.20 |
| 70.19 | 70.39 | -0.20 |
| 80.14 | 80.36 | -0.22 |
| 90.19 | 90.42 | -0.23 |
| 99.70 | 99.94 | -0.24 |

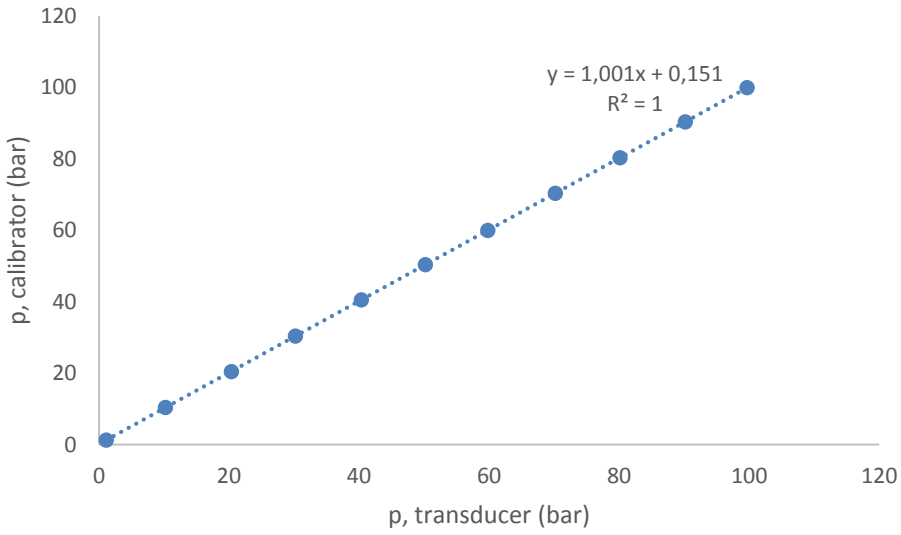


***Figure 68 Pressure calibration measurement correlation at 225.6 °C.***

***Table 35 Pressure calibration measurement correlation parameters at 225.6 °C.***

| slope | 1.001 |
|---|---|
| itercept | 0.151 |
| RSQ | 1.000 |

***Table 36 Pressure calibration measurements at 250.5 °C.***

| T (°C) | 250.5 | |
|---|---|---|
| | | |
| p,transducer (bar) | p,calbrator (bar) | error |
| 0.47 | 1.35 | -0.88 |
| 11.87 | 12.77 | -0.90 |
| 20.20 | 21.12 | -0.92 |
| 30.26 | 31.21 | -0.95 |
| 40.18 | 41.16 | -0.98 |
| 50.20 | 51.20 | -1.00 |
| 60.23 | 61.27 | -1.04 |
| 70.07 | 71.14 | -1.07 |
| 80.49 | 81.59 | -1.10 |
| 90.57 | 91.70 | -1.13 |
| 100.07 | 101.24 | -1.17 |

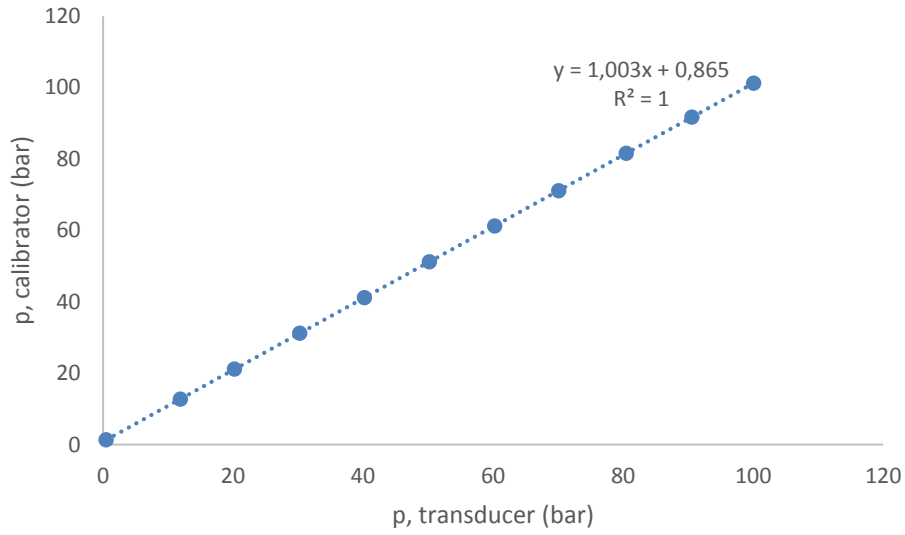


***Figure 69 Pressure calibration measurement correlation at 250.5 °C.***

***Table 37 Pressure calibration measurement correlation parameters at 250.5 °C.***

| slope | 1.003 |
|---|---|
| itercept | 0.865 |
| RSQ | 1.000 |

***Table 38 Pressure calibration measurement correlation parameters.***

| T (°C) | slope | intercept |
|---|---|---|
| 150.3 | 1.002 | -1.515 |
| 175.5 | 1.000 | -1.032 |
| 200.6 | 1.000 | -0.486 |
| 225.6 | 1.001 | 0.151 |
| 250.5 | 1.003 | 0.865 |

As can be seen, the slope for all the measurement correlations is essentially 1, meaning the gain of the transducer was adjusted well for the measured temperature range. The slopes were thus assumed to be 1, and the intercept terms were correlated with respect to temperatures, presented in the figure below.

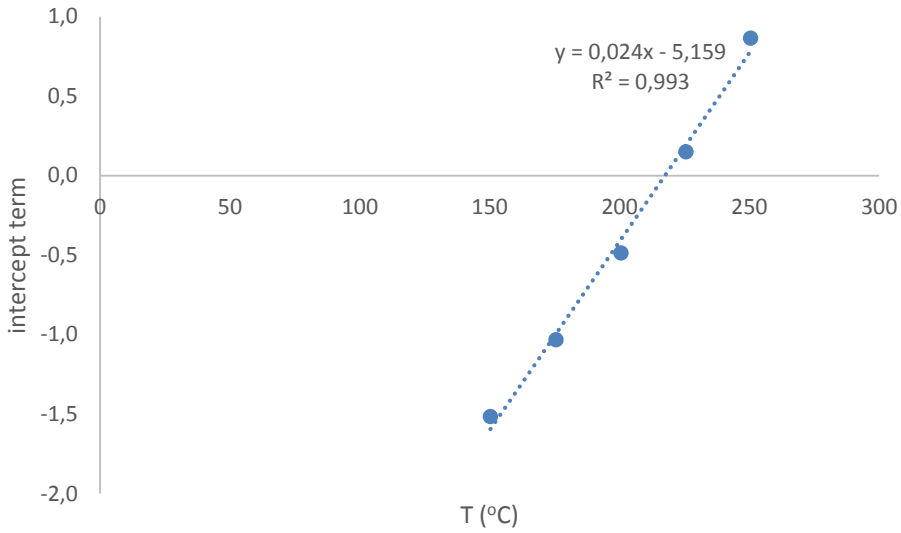


***Figure 70 Correlation of the intercept term for pressure measurement correction function.***

***Table 39 Intercept term correlation parameters for pressure measurement correction function.***

| | |
|---|---|
| slope | 0.024 |
| intercept | -5.159 |
| RSQ | 0.993 |

Assuming all slopes to be 1, and using the correlated values in Table 39 to calculate intercept points for any given temperature, temperature corrections for the pressure measurements could be obtained at any temperature within the measurement range of 150 – 250 °C. Actual pressures were calculated from the measurement values using the following correction formula:

$$p_{actual} = 1 * p_{measured} + c$$

where

$$c = 0.024 * \frac{T}{^{o}C} - 5.159$$

*c* is the correction term gotten by temperature from the intercept term correlation, and *T* is the measured temperature in degrees Celsius.

# Appendix 2. Vapor pressure and cloud point measurement data

Measurement data from all successful vapor pressure and cloud point measurements are available in a supplementary file at the Aalto University Aaltodoc publication archive (https://aaltodoc.aalto.fi/).